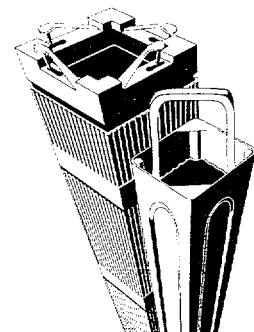


# SIEMENS

EMF-2158(NP)(A)  
Revision 0

## Siemens Power Corporation Methodology for Boiling Water Reactors: Evaluation and Validation of CASMO-4/MICROBURN-B2

October 1999



---

Siemens Power Corporation  
Nuclear Division

Siemens Power Corporation – Nuclear Division

ISSUED IN SFORD ON-LINE  
DOCUMENT SYSTEM

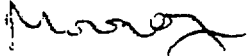
DATE: 12/29/98

EMF – 2158(NP)  
Revision 0

Issue Date:

**Siemens Power Corporation Methodology for Boiling Water Reactors: Evaluation and  
Validation of CASMO – 4/MICROBURN – B2**

Prepared by:

 12/21/98  
\_\_\_\_\_  
H. Moon, Ph. D., Senior Engineer  
Neutronics Analysis Method

December 1998

/hm

**NUCLEAR REGULATORY COMMISSION  
REPORT DISCLAIMER**

**IMPORTANT NOTICE REGARDING CONTENTS AND USE OF THIS DOCUMENT**

**PLEASE READ CAREFULLY**

This technical report was derived through research and development programs sponsored by Siemens Power Corporation. It is being submitted by Siemens Power Corporation to the U.S. Nuclear Regulatory Commission as part of a technical contribution to facilitate safety analyses by licensees of the U.S. Nuclear Regulatory Commission which utilize Siemens Power Corporation-fabricated reload fuel or other technical services provided by Siemens Power Corporation for light water power reactors and it is true and correct to the best of Siemens Power Corporation's knowledge, information, and belief. The information contained herein may be used by the U.S. Nuclear Regulatory Commission in its review of this report, and under the terms of the respective agreements, by licensees or applicants before the U.S. Nuclear Regulatory Commission which are customers of Siemens Power Corporation in their demonstration of compliance with the U.S. Nuclear Regulatory Commission's regulations.

Siemens Power Corporation's warranties and representations concerning the subject matter of this document are those set forth in the agreement between Siemens Power Corporation and the customer to which this document is issued. Accordingly, except as otherwise expressly provided in such agreement, neither Siemens Power Corporation nor any person acting on its behalf:

- A. Makes any warranty, or representation, express or implied, with respect to the accuracy, completeness, or usefulness of the information contained in this document, or that the use of any information, apparatus, method, or process disclosed in this document will not infringe privately owned rights, or
  
- B. Assumes any liabilities with respect to the use of, or for damages resulting from the use of, any information, apparatus, method, or process disclosed in this document.



UNITED STATES  
NUCLEAR REGULATORY COMMISSION  
WASHINGTON, D.C. 20555-0001

October 18, 1999

Mr. James F. Mallay  
Director, Regulatory Affairs  
Siemens Power Corporation  
2101 Horn Rapids Road  
Richland, Washington 99352-0130

SUBJECT: ACCEPTANCE FOR REFERENCING OF LICENSING TOPICAL REPORT  
EMF-2158(P), REVISION 0, "SIEMENS POWER CORPORATION  
METHODOLOGY FOR BOILING WATER REACTORS: EVALUATION AND  
VALIDATION OF CASMO-4/MICROBURN-B2" (TAC NO. MA4592)

Dear Mr. Mallay:

We have completed our review of the subject topical report submitted by the Siemens Power Corporation (SPC) on December 30, 1998. The report is acceptable for referencing in licensing applications to the extent specified and under the limitations delineated in the report and in the associated NRC safety evaluation, which is enclosed. The safety evaluation defines the basis for NRC acceptance of the report.

We do not intend to repeat our review and acceptance of the matters described in the report when the report appears as a reference in license applications, except to assure that the material presented is applicable to the specific plant involved. Our acceptance applies only to the matters described in the report.

In accordance with procedures established in NUREG-0390, it is requested that SPC publish accepted versions of this report, proprietary and non-proprietary, within 3 months of receipt of this letter. The accepted versions shall incorporate this letter and the enclosed evaluation between the title page and the abstract. The accepted versions shall include an "A" (designating accepted) following the report identification symbol.

If our criteria or regulations change so that our conclusions about acceptability of the report are invalidated, SPC and the licensees referencing the topical report will be expected to revise and resubmit their respective documentation, or to submit justification for the continued effective applicability of the topical reports without revision of their respective documentation.

Sincerely,

  
Stephen Dembek, Chief, Section 2  
Project Directorate IV & Decommissioning  
Division of Licensing Project Management  
Office of Nuclear Reactor Regulation

Project No. 702

Enclosure: Safety Evaluation



UNITED STATES  
NUCLEAR REGULATORY COMMISSION  
WASHINGTON, D.C. 20555-0001

SAFETY EVALUATION BY THE OFFICE OF NUCLEAR REACTOR REGULATION

RELATING TO TOPICAL REPORT EMF-2158(P), REVISION 0,

"SIEMENS POWER CORPORATION METHODOLOGY FOR BOILING WATER REACTORS:

EVALUATION AND VALIDATION OF CASMO-4/MICROBURN-B2"

1.0 BACKGROUND

Topical Report EMF-2158(P), Revision 0, describes the methodology behind the application of the Siemens Power Corporation's (SPC's) boiling water reactor (BWR) neutronics design code system (Reference 1). The code system consists of two codes: the lattice spectrum/depletion code (CASMO-4), and the steady-state reactor core simulator code (MICROBURN-B2). Together these two codes are used to perform initial and reload core design, calculate parameters for safety analyses, and perform off-line and on-line core monitoring functions. CASMO-4 and MICROBURN-B2 have received benchmark approval for use in commercial reactor applications. The new code system replaces the existing neutron codes used for the current SPC BWR neutron design and safety methodology (Reference 2).

The new SPC code system incorporates advanced model features that are essential for today's new core design. One of these features is the inclusion of the pin power reconstruction method.

This report establishes a methodology evaluation and validation criteria by which a new neutronics design code or code system would be assessed for application to BWR neutronics design. These criteria are established to address the need for more accurate modeling for current and future reactor core/fuel lattice designs and operations. This report contains the results of the application of these criteria to assess the calculational results of CASMO-4 and MICROBURN-B2 to SPC. The evaluation and validation of the SPC code system is benchmarked with data from a variety of operating reactor core/fuel lattice designs.

2.0 TECHNICAL EVALUATION

The upgraded SPC BWR neutronics design code system consists of the CASMO-4 lattice spectrum/depletion code and the MICROBURN-B2 steady-state reactor core simulator code. The CASMO-4 code, was developed by Studvik of America, and the MICROBURN-B2 code was developed by Siemens. MICROBURN-B2 has been applied to European BWR core designs, and benchmarked against European BWRs.

The CASMO-4 code determines a multi-group heterogeneous medium neutron spectrum in a fuel lattice consisting of fuel rods, burnable poison rods, water rod/channels, and structural components. CASMO-4 homogenizes the heterogeneous lattice spectrum into a neutronically equivalent homogeneous medium, determines the pin power distributions, and depletes

nuclides in fuel and burnable poison pins. CASMO-4 uses a variety of nuclear data libraries, ranging from BNL-84, JEF-1, JEF-2.1, END/B-V, END/B-III, END/B-IV, and END/B-V.

The main data output from CASMO-4 is a set of the following two neutron energy group data (1) a microscopic and macroscopic cross-section for a spatially homogenized lattice, and (2) pinwise power distribution, exposure distribution, and energy deposition in various components of a fuel lattice. The output data from CASMO-4 is processed by an auxiliary code into a lattice neutronic data library for the MICROBURN-B2 core simulator code.

The MICROBURN-B2 code determines core-wide nodal exposure and nuclide density distributions, channel inlet flow distribution, and fuel thermal performance parameters such as linear heat generation rate, axial planer linear heat generation rate (APLHGR), and critical power ratio. These predicted results are used to design fuel cycles, to assess safety limit margins, and to monitor operating reactor cores.

The local pin power distributions calculated by the MICROBURN-B2 code are validated by comparison with results from higher order methods and pin gamma scan measurements. A substantial colorset of geometries were simulated and the resulting pin power distributions were simulated; the resulting pin power distributions were compared with the predicted values of MICROBURN-B2 and CASMO-3/CASMO-4. Comparisons were also made with Quad Cities Unit 1 and KWU-S gamma scan measurements, to determine the uncertainties of predicted local pin power distributions.

The SPC core monitoring system utilizes the Transverse-Incore-Probes (TIPs) to determine (measured) incore power distribution. Although the core simulator model uses the MICROBURN-B2 code to calculate (predict) incore power distribution, the TIP obtained measured power has associated with it a statistical uncertainty. To determine the magnitude of this uncertainty, a statistical analysis is performed of the predicted-versus-measured TIP distributions and local pin power distributions using NRC-approved statistical methods (Reference 2).

### 3.0 STATISTICAL ASPECTS OF CASMO-4/MICROBURN-B2

The statistical aspects of CASMO-4 and MICROBURN-B2 consist of applying appropriate statistical techniques (Reference 2) to the CASMO-4/MICROBURN-B2 code system database. The statistical analysis procedure in this approved reference is employed to determine the uncertainties in the measured power distribution of the CASMO-4/MICROBURN-B2 code system.

The procedure consists of determining the measured nodal power distribution and the measured maximum pin power distribution in a node with their associated uncertainties. Similarly, the measured bundle power and the measured maximum pin power in a bundle, with their associated uncertainties, are also determined. The staff reviewed the methodology for determining these uncertainties in an earlier submittal (Reference 2).

SPC compared the calculated power distribution and the measured power distribution. SPC then used these comparisons to verify the results of the evaluation of the calculated power

distribution uncertainty from the calculated TIP distribution uncertainty. The data base used for verifying these uncertainties consisted of full-core measurements from C-lattice and D-lattice reactors. Detailed information on the data base is in Table 9.1 of Topical Report EMF-2158(P).

Comparison of the measured power distribution uncertainties for the new CASMO-4/MICROBURN-B2 code system, and the associated criteria reported in Section 5.3 of Topical Report EMF-2158(P), are in Table 9.9 of the topical report. The comparisons show that the measured power distribution uncertainties of the new code system are less than the acceptance criteria as specified in Section 5.3 of the topical report. The staff agrees with these results.

#### 4.0 EVALUATION OF THE CASMO-4/MICROBURN-B2 METHODOLOGY

##### 4.1 CASMO-4

The CASMO-4 code is capable of generating heterogeneous medium multi-group neutron spectrum and calculating burnup chain equation solutions for heavy nuclides, fission product nuclides, and poison nuclides in each fuel pin. CASMO-4 uses deterministic transport methods. At the pin cell level, it exclusively uses the collision probability method to collapse the 40/70 group nuclear data into multi-group data. At the lattice level, it uses a characteristics method for the neutron transport equation solution. One improvement of CASMO-4 over its predecessor CASMO-3 is that CASMO-4 does not need to perform any pin cell spatial homogenization to perform a 2-D lattice-wide transport calculation, a highly desired feature when dealing with burnable poison rods with high gadolinia concentration (Reference 3).

The primary use of CASMO-4 within the SPC neutronics method is to determine two groups of homogenized microscopic and macroscopic cross section data as well as pin power and burnup distributions for fuel lattices.

##### 4.2 MICROBURN-B2

MICROBURN-B2 is an improved version of the NRC-approved MICROBURN-B simulator code. MICROBURN-B2 solves the two-group neutron diffusion equation based on the interface current method. It is capable of calculating the burnup chain equation solutions for heavy nuclides and burnable poison nuclides. It is also capable of determining the nodal power, bundle flow, and void distribution, as well as of determining pin power distributions and thermal margins to technical specification limits. MICROBURN-B2 incorporates several new and advanced features, such as the advanced nodal expansion method solution of diffusion equation, nodal burnup and spectral history gradient model, and a pin power reconstruction model. All these features enable MICROBURN-B2 to obtain more accurate nodal and pin power distributions (Reference 4).

Analysis conducted by SPC shows that the application of MICROBURN-B2 to BWR core designs would not necessitate changes to the SPC's approved safety analysis methodology. MICROBURN-B2 is compatible with the approved safety analysis codes and is consistent with the approved neutronics safety methodologies of SPC presented in Reference 2.

## 5.0 VALIDATION OF CASMO-4/MICROBURN-B2 METHODOLOGY

The validation of the CASMO-4 code is based on critical experiments, such as those conducted at KRITZ (Reference 5) and those conducted by Babcock and Wilcox (B&W) (Reference 6). These experiments provided critical K-effective and pin-by-pin fission rate measurements. Additional validation data included Doppler resonance measurements, and isotopic inventory measurements, such as those from Yankee Rowe, which provides what is considered to be acceptable measured data within the industry (Reference 7).

In addition to these measurements, comparisons with results from Monte Carlo simulation codes (such as MCNP, Reference 8), which are generally accepted by the industry, were also performed to further validate the overall methodology of the CASMO-4 code. Gamma scan measurements data of pin power distribution was also utilized in the validation process of CASMO-4 and MICROBURN-B2. The analysis showed that the CASMO-4 lattice spectrum/depletion code produces a level of accuracy acceptable for SPC BWR fuel bundle and core design. SPC chose six operating BWR reactors to validate the CASMO-4/MICROBURN-B2 code system. SPC conducted analyses on hot operating conditions critical K-effective measurements, TIP measurements, and cold critical measurements for a very large number of fuel cycles. These fuel cycles were specifically chosen to contain various types of fuel mechanical designs from different vendors throughout the world. The results of the analysis indicated that the CASMO-4/MICROBURN-B2 code system accurately predicts core physics parameters. Analysis of the predicted accuracy was found to be independent of core loading patterns, fuel assembly types, and core operating modes. A tabulation of these physics parameters (validation criteria) appear in Tables 5.1, 5.2, and 5.3, along with the tabulated results of the analysis, in Chapter 7 of Reference 1. The staff agrees with these results.

## 6.0 CONCLUSION

The staff has reviewed the analyses in Topical Report EMF-2158(P), Revision 0, "Siemens Power Corporation Methodology for Boiling Water Reactors: Evaluation and Validation of CASMO-4/MICROBURN-B2," and concludes that on the basis of its findings, Topical Report EMF-2158(P), Revision 0, is acceptable for licensing evaluations of BWR neutronics designs and applications in accordance with SPC's agreement (Reference 9), subject to the following conditions:

1. The CASMO-4/MICROBURN-B2 code system shall be applied in a manner that predicted results are within the range of the validation criteria (Tables 2.1 and 2.2) and measurement uncertainties (Table 2.3) presented in EMF-2158(P).
2. The CASMO-4/MICROBURN-B2 code system shall be validated for analyses of any new fuel design which departs from current orthogonal lattice designs and/or exceed gadolinia and U-235 enrichment limits.
3. The CASMO-4/MICROBURN-B2 code system shall only be used for BWR licensing analyses and BWR core monitoring applications.
4. The review of the CASMO-4/MICROBURN-B2 code system should not be construed as a generic review of the CASMO-4 or MICROBURN-B2 computer codes.

5. The CASMO-4/MICROBURN-B2 code system is approved as a replacement for the CASMO-3/MICROBURN-B code system used in NRC-approved SPC BWR licensing methodology and in SPC BWR core monitoring applications. Such replacements shall be evaluated to ensure that each affected methodology continues to comply with its SER restrictions and/or conditions.
6. SPC shall notify any customer who proposes to use the CASMO-4/MICROBURN-B2 code system independent of any SPC fuel contract that conditions 1 through 4 above must be met. SPC's notification shall provide positive evidence to the NRC that each customer has been informed by SPC of the applicable conditions for using the code system.

#### 7.0 REFERENCES

1. Letter from James F. Mallay (SPC) to the U.S. Nuclear Regulatory Commission, submitting Topical Report EMF-2158(P), Revision 0, "Siemens Power Corporation Methodology for Boiling Water Reactors: Evaluation and Validation of CASMO-4/MICROBURN-B2," December 30, 1998.
2. Exxon Nuclear Methodology for Boiling Water Reactors-Neutronic Methods for Design and Analysis," XN-NF-80-19 (A), Vol. 1 (March 1983), Supplements 1 and 2, and "Benchmark Results for the CASMO-3G/MICROBURN-B Calculation Methodology," XN-NF-80-19(P)(A), Vol. 1, Supplements 3 and 4 (November 1990).
3. D. Knott, B.H. Forssen, and M. Edenius, "CASMO-4, A Fuel Assembly Burnup Program, Methodology," STUDSVIK/SOA-95/2, Studsvik Proprietary (September 1995).
4. H. Moon, "MICROBURN-B2: Steady State BWR Core Physics Method," EMF-1833(P), Rev. 2, Siemens Power Corporation (September 1998).
5. R. Person, E. Blomsjo, and M. Edenius, "High-Temperature Critical Experiments with H<sub>2</sub>O-Moderated Fuel Assemblies in KRITS," Technical Mtg. No. 2/11, NUCLEX 72 (1972).
6. L.W. Newman, "Urania-Gadolinia: Nuclear Model Development and Critical Experiment Benchmark," BAW-1810, B&W Company (April 1984).
7. R.J. Nodvik, et al., "Evaluation of Mass Spectrometric and Radiochemical Analysis of Yankee Core 1 Spent Fuel," WCAP-6068 (1966).
8. J. Briesmeister, "MCNP-A General Monte Carlo Code for Neutron and Photon Transport, Version 3 A," LA-7396-M Revision 2 (1992).
9. Letter from James F. Mallay (SPC) to the U.S. Nuclear Regulatory Commission, "SER Conditions for CASMO-4/MICROBURN-B2," September 9, 1999.

Principal Contributor: A. Attard

Date: October 18, 1999



UNITED STATES  
NUCLEAR REGULATORY COMMISSION

WASHINGTON, D.C. 20555-0001

February 29, 2000

Mr. James F. Mallay  
Director, Nuclear Regulatory Affairs  
Siemens Power Corporation  
2101 Horn Rapids Road  
Richland, WA 99352

SUBJECT: ACCEPTANCE OF CLARIFICATIONS ON TOPICAL REPORT EMF-2158(P)  
REVISION 0, "SIEMENS POWER CORPORATION METHODOLOGY FOR  
BOILING WATER REACTORS: EVALUATION AND VALIDATION OF  
CASMO-4/MICROBURN-B2" (TAC NO. MA4592)

Dear Mr. Mallay:

The staff has completed its review of the clarifications of the subject topical report submitted by Siemens Power Corporation (SPC) by letter dated December 20, 1999. On the basis of our review, the staff finds the clarifications to be acceptable for referencing in the topical report to the extent specified, and under the limitations delineated, and in the safety evaluation (SE) sent on October 18, 1999. The SE defines the basis for NRC acceptance of the report.

The staff will not repeat its review of the matters described in the report, and found acceptable when the report appears as a reference in license applications, except to ensure that the material presented is applicable to the specific plant involved. Our acceptance applies only to the matters described in the report.

In accordance with procedures established in NUREG-0390, the NRC requests that SPC publish accepted versions of this report, including the safety evaluation, and this letter of concurrence in proprietary and non-proprietary versions within 3 months of receipt of this letter. The accepted versions shall incorporate this letter and the SE contained in our October 18, 1999, letter between the title page and the abstract. The accepted versions shall include an "A" (designating accepted) following the report identification symbol. The accepted versions shall also incorporate all communications between SPC and the staff during this review.

Should our criteria or regulations change so that our conclusions as to the acceptability of the report are no longer valid, SPC and the licensees referencing the topical report will be expected to revise and resubmit their respective documentation, or to submit justification for the

Mr. James F. Mallay

- 2 -

February 29, 2000

continued effective applicability of the topical report without revision of their respective documentation.

Sincerely,

A handwritten signature in black ink, appearing to read "S. Richards", with a large, sweeping flourish extending to the right.

Stuart A. Richards, Director  
Project Directorate IV and Decommissioning  
Division of Licensing Project Management  
Office of Nuclear Reactor Regulation

Project No. 702

# SIEMENS

December 20, 1999  
NRC:99:050

Document Control Desk  
ATTN: Chief, Planning, Program and Management Support Branch  
U.S. Nuclear Regulatory Commission  
Washington, D.C. 20555-0001

## **EMF-2158(P) Revision 0, "Siemens Power Corporation Methodology for Boiling Water Reactors: Evaluation and Validation of CASMO-4/MICROBURN-B2"**

- Ref.: 1. Letter, Stephen Dembek (NRC) to James F. Mallay (SPC), "Acceptance for Referencing of Licensing Topical Report EMF-2158(P) Revision 0, 'Siemens Power Corporation Methodology for Boiling Water Reactors: Evaluation and Validation of CASMO-4/MICROBURN-B2' (TAC No. MA4592)," October 18, 1999.
- Ref.: 2. Letter, James F. Mallay (SPC) to Document Control Desk, "SER Conditions for CASMO-4/MICROBURN-B2," NRC:98:038, September 9, 1999.
- Ref.: 3. Letter, James F. Mallay (SPC) to Document Control Desk, "Request for Copies of Reports Referenced in EMF-2158(P) Revision 0, 'Siemens Power Corporation Methodology for Boiling Water Reactors: Evaluation and Validation of CASMO-4/MICROBURN-B2,'" NRC:99:016, April 28, 1999.

Siemens Power Corporation conducts a formal review of all new SERs to determine whether any of its restrictions need to be clarified. If clarifications are needed, they are incorporated into the approved version of the topical report. The initial review of the SER contained in Reference 1 confirmed that it corresponds to the proposed conditions in Reference 2. However, a more detailed evaluation revealed two instances where clarification appears necessary.

SPC requests the NRC's concurrence with the following points of clarification regarding Conclusions 1 and 5 in the Reference 2 SER. We will appreciate a reply by January 31, 2000 so that the approved version of the topical report can be distributed in a timely way.

### Conclusion 1

"The CASMO-4/MICROBURN-B2 code system shall be applied in a manner that predicted results are within the range of the validation criteria (Tables 2.1 and 2.2) and measurement uncertainties (Table 2.3) presented in EMF-2158(P)."

### Clarification 1

There are selectable constitutive models, which make up the thermal-hydraulic model of the MICROBURN-B2 code described in EMF-1833(P) Revision 2, "MICROBURN-B2: Steady State BWR Core Physics Method." The selected set that produced the validation results in Tables 2.1 and 2.2

## **Siemens Power Corporation**

2101 Horn Rapids Road  
Richland, WA 99352

Tel: (509) 375-8100  
Fax: (509) 375-8402

and the uncertainties in Table 2.3 was not the set previously used in CASMO-3G/MICROBURN-B or the codes which interface with CASMO-4/MICROBURN-B2. Updates to, selection of, and new constitutive models are allowed as long as the conditions of the SER for CASMO-4/MICROBURN-B2 are met. (Note: EMF-1833 was provided to the NRC for information by Reference 3.)

#### Clarification 2

As noted in Section 3.0 Statistical Aspects of CASMO-4/MICROBURN-B2 of the SER for EMF-2158(P) "The statistical aspects of CASMO-4 and MICROBURN-B2 consist of applying appropriate statistical techniques (Reference 2 [XN-NF-80-19(P)(A) Vol.1, Supplement 3 and Supplement 4, 'Advanced Nuclear Fuels Methodology for Boiling Water Reactors, Benchmark Results for the CASMO-3G/MICROBURN-B Calculation Methodology,' November 1990]) to the CASMO-4/MICROBURN-B2 code system data base." The statistical analysis procedure in this approved reference has been employed to determine the uncertainties in the measured power distribution of the CASMO-4/MICROBURN-B2 code system and the current CASMO-3G/MICROBURN-B code system.

However, for CASMO-3G/MICROBURN-B there was an SER condition "The currently approved TIP asymmetry uncertainty value of 6.0 percent should be used in determining the radial power uncertainty." (Note: "...currently approved..." referred to a core simulator methodology, XTGBWR, approved in 1983 in XN-NF-80-19(P)(A) Volume 1 and Supplements 1 and 2, "EXXON Nuclear Methodology for Boiling Water Reactors - Neutronic Methods for Design and Analyses," March 1983.) Using the approved statistical analysis procedure and the CASMO-3G/MICROBURN-B data base, and applying the TIP asymmetry uncertainty of 6.0 percent, the calculated radial power uncertainties are 4.09% for C-Lattice reactors and 4.32% for D-Lattice reactors.

The comparable uncertainty values for CASMO-4/MICROBURN-B2 are 2.90% for C-Lattice reactors and 4.10% for D-Lattice reactors. These uncertainties, though calculated using the same statistical analysis procedure, are smaller than the CASMO-3G/MICROBURN-B uncertainties because the TIP asymmetry uncertainties applied were those derived from the CASMO-4/MICROBURN-B2 data base and not the 6% value previously applied to CASMO-3G/MICROBURN-B.

The uncertainties listed in Table 2.3 in EMF-2158(P) will be used by SPC when the CASMO-4/MICROBURN-B2 code system is fully implemented for BWR licensing and core monitoring applications. If the CASMO-4/MICROBURN-B2 code system is changed, new uncertainties will be calculated and used in subsequent licensing and core monitoring applications.

#### Conclusion 5

"The CASMO-4/MICROBURN-B2 code system is approved as a replacement for the CASMO-3/MICROBURN-B code system used in NRC-approved SPC BWR licensing methodology and in SPC BWR core monitoring applications. Such replacements shall be evaluated to ensure that each affected methodology continues to comply with its SER restrictions and/or conditions."

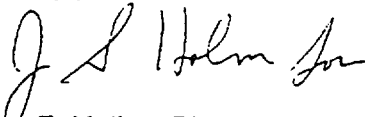
#### Clarification 1

The modifications, upgrades, and applications of the code system discussed in reference to Conclusion 1 must also satisfy the conditions of Conclusion 5.

In Conclusion 5 it is stated that the "...code system is approved as a replacement for the CASMO-3/MICROBURN-B code system..." It is recognized that MICROBURN-B2 cannot be executed without CASMO-4 input. Hence, the use of MICROBURN-B2 is part of a "code system." However, SPC routinely uses CASMO-3 to calculate numerous parameters such as fuel lattice kinetic parameters (e.g., Doppler, void and moderator reactivity coefficients, neutron lifetimes, and delayed neutron fractions), fuel actinide concentrations, and others. SPC intends to use CASMO-4 in a comparable manner.

If the above clarifications of the SER conclusions are found to be acceptable, SPC requests that the NRC concur. This letter of concurrence will be included in the approved version of the topical report.

Very truly yours,



James F. Mallay, Director  
Regulatory Affairs

/arn

cc: A. C. Attard  
N. Kalyanam  
J. S. Wermiel  
Project No. 702

# SIEMENS

September 9, 1999  
NRC:99:038

Document Control Desk  
ATTN: Chief, Planning, Program and Management Support Branch  
U.S. Nuclear Regulatory Commission  
Washington, D.C. 20555-0001

## SER Conditions for CASMO-4/MICROBURN-B2

Ref.: 1. Letter, James F. Mallay (SPC) to Document Control Desk, "Request for Review of EMF-2158(P) Revision 0, 'Siemens Power Corporation Methodology for Boiling Water Reactors: Evaluation and Validation of CASMO-4/MICROBURN-B2,'" NRC:98:087, December 30, 1998.

The attachment to this letter provides a list of conditions proposed for the approved application of CASMO-4/MICROBURN-B2 methodology described in the topical report submitted to the NRC by Reference 1. Siemens Power Corporation finds these conditions acceptable and appropriate.

Very truly yours,



✓ James F. Mallay, Director  
Regulatory Affairs

/am

Attachment

cc: Mr. A. C. Attard (w/attachment)  
Mr. N. Kalyanam (w/attachment)  
Project No. 702

**Siemens Power Corporation**

2101 Horn Rapids Road  
Richland, WA 99352

Tel: (509) 375-8100  
Fax: (509) 375-8402

**Proposed SER Conditions for CASMO-4/MICROBURN-B2**

1. The CASMO-4/MICROBURN-B2 code system shall be applied in a manner that predicted results are within the range of the validation criteria (Tables 2.1 and 2.2) and measurement uncertainties (Table 2.3) presented in EMF-2158(P).
2. The CASMO-4/MICROBURN-B2 code system shall be validated for analyses of any new fuel design which departs from current orthogonal lattice designs and/or exceed gadolinia and U-235 enrichment limits.
3. The CASMO-4/MICROBURN-B2 code system shall only be used for BWR licensing analyses and BWR core monitoring applications.
4. The review of the CASMO-4/MICROBURN-B2 code system should not be construed as a generic review of the CASMO-4 or MICROBURN-B2 computer codes.
5. The CASMO-4/MICROBURN-B2 code system is approved as a replacement for the CASMO-3/MICROBURN-B code system used in NRC-approved SPC BWR licensing methodology and in SPC BWR core monitoring applications. Such replacements shall be evaluated to ensure that each affected methodology continues to comply with its SER restrictions and/or conditions.
6. SPC shall notify any customer who proposes to use the CASMO-4/MICROBURN-B2 code system independent of any SPC fuel contract that conditions 1 through 4 above must be met. SPC's notification shall provide positive evidence to the NRC that each customer has been informed by SPC of the applicable conditions for using the code system.

# SIEMENS

June 18, 1999  
NRC:99:027

Document Control Desk  
ATTN: Chief, Planning, Program and Management Support Branch  
U.S. Nuclear Regulatory Commission  
Washington, D.C. 20555-0001

## Validation Requirements for CASMO-4/MICROBURN-B2

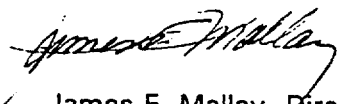
Ref.: 1. Letter, James F. Mallay (SPC) to Document Control Desk, "Request for Review of EMF-2158(P) Revision 0 'Siemens Power Corporation Methodology for Boiling Water Reactors: Evaluation and Validation of CASMO-4/MICROBURN-B2,'" NRC:98:087, December 30, 1998.

The attachment to this letter provides additional explanation for the code validation requirements and clarification of the statistical equations used in the CASMO-4/MICROBURN-B2 topical report submitted to the NRC by Reference 1.

As noted in the attachment, typographical errors were found in Table 2.1 and Table 5.1. These tables will be corrected in the published A-version of the topical report.

Some of the information contained in the attachment is considered to be proprietary to Siemens Power Corporation. The information considered to be proprietary has been enclosed in brackets. The affidavit originally submitted for the review of the topical report satisfies the requirements of 10 CFR 2.790(b) to support the withholding of this information from public disclosure.

Very truly yours,



James F. Mallay, Director  
Regulatory Affairs

/arn

Attachment

cc: Mr. A. C. Attard  
Mr. E. Y. Wang  
Mr. J. L. Wermiel  
Project No. 702

## Siemens Power Corporation

2101 Horn Rapids Road  
Richland, WA 99352

Tel: (509) 375-8100  
Fax: (509) 375-8402

### Validation Requirements for CASMO-4/MICROBURN-B2

This attachment provides an explanation for the code validation requirements mentioned in Section 3 of the CASMO-4/MICROBURN-B2 topical report (Reference 1) and a clarification on a few statistical equations used in Section 9 of the report. The actual validation requirements are specified in Tables 5.1, 5.2, and 5.3 of the report. These tables show the acceptance criteria for the accuracy of k-effectives, TIP predictions, pin-by-pin power distributions, and measured power distribution uncertainty to be determined by SPC's BWR neutronics methodology.

#### Background for Acceptance Criteria

SPC has accumulated considerable BWR core reload design experiences since the early 1970s, which has been documented in two licensing submittals of XFYRE/XTGBWR (Reference 2) and of CASMO-3/MICROBURN-B (Reference 3). Numerous fuel cycle design reports issued in support of licensing reload fuel cycles contain results of BWR core follow analyses performed using these licensed methodologies. These results and available critical core and gamma scan measurements constitute a large data base for establishing a set of acceptance criteria for a BWR neutronic design methodology. The acceptance criteria are designed to show the soundness of a BWR core physics method. The criteria are expressed as maximum acceptable deviations on four key measured parameters: the hot critical k-effective, the cold critical k-effective, the detector reaction rate, and the pin-by-pin gamma scan comparison. A BWR neutronic design methodology that satisfies the accuracy requirements specified in Tables 5.1, 5.2, and 5.3 is acceptable for application to SPC's BWR reload design.

#### SPC BWR Fuel Lattice Spectrum/Depletion Code Validation Requirements

The requirements specified in Table 5.1 were established based on the following considerations:

1. Average of predicted k-effectives within  $1.0 \pm [ \quad ]$  --- The measurement uncertainty of criticality in a critical core depends on the measurement technique used. Post-measurement analysis of a critical core must use measured or reported parameters for modeling. Considering these variables, a k-effective deviation less than  $[ \quad ]$  is an indication of the high quality of a lattice physics method. This criterion demonstrates that there is no inherent bias in the lattice physics method.
2. Variation of predicted k-effective  $< [ \quad ]$  --- This criterion represents the  $1 \sigma$  standard deviation of calculated critical k-effectives. The measured critical core parameters include uncertainties in moderator temperatures and boron concentrations. Reference 4 states that the measured boron concentration uncertainty was 200 pcm of reactivity. Hence, the criterion of  $[ \quad ] \Delta k$  was chosen. This criterion, in combination with the average k-effective criterion, is significantly more restrictive than the criteria used in the NRC-approved methodology (Reference 5) for PWR analysis, namely,  $[ \quad ]$

]

3. Fission rate distribution RMS deviation < [ ] % --- The fission rate measurement uncertainty of [ ] is given in Reference 6. This uncertainty represents a measurement uncertainty associated with a pin-by-pin gamma scan. Therefore, the [ ] RMS deviation for a lattice physics code is reasonable.
4. Average deviation of U-235, U-236, Pu-239, Pu-240, Pu-241, Pu-242 densities from measurements < 10% --- These nuclides are key contributors to a lattice reactivity change during fuel burnup. The measurement uncertainty of atom densities based on mass spectrometry and alpha spectrometry is large (~ 10%). In addition, the reactor operating conditions for the samples loaded in Yankee Rowe are not well known. Due to these variables, it is reasonable to allow a [ ] deviation in the calculated values.
5. Fission rate distribution RMS deviation (compared to a Monte Carlo calculation) < [ ] --- A typical Monte Carlo simulation of a BWR lattice produces about [ ] of statistical uncertainty in fission rate distribution. In addition, a difference in base cross-section libraries (ENDF-B/IV, ENDF-B/V, or JEF2.2, etc.) can add an additional [ ] of variation. For this reason, a maximum difference of [ ] in [ ] RMS between a lattice physics code based on a transport method and a Monte Carlo code is reasonable.
6. Control rod worth deviation (compared to a Monte Carlo calculation) < [ ] --- Because a BWR control blade is located at one corner of a fuel lattice, the overall lattice reactivity is heavily dependent on the neutron flux distribution on the opposite corner. This creates an increased uncertainty for both the Monte Carlo method and the transport method. Also, the control rod worth or the lattice reactivity in general is sensitive to the base cross section library used. Reference 7 shows that the MCNP Monte Carlo code can make a reactivity bias of [ ] for a critical core. This amounts to about [ ] uncertainty in the worth of a typical control rod (total worth  $\equiv$  [ ]). Hence, it is reasonable to set the maximum difference in control rod worth between a Monte Carlo calculation and a lattice code at [ ]. The actual operation of a BWR is protected by a conservative criterion on startup critical measurements (see Item 3 below).

#### SPC BWR Core Simulator Code Validation Requirements

The requirements specified in Table 5.2 were established based on the following considerations:

1. Standard deviation of in-cycle hot critical k-effectives < [ ] --- BWR core simulators generally exhibit certain variations in critical k-effectives during the course of tracking a cycle. The variations are in part due to the uncertainty of measured parameters (core flow, power, inlet subcooling, pressure, etc.) input to the core simulator. The uncertainty of core simulator methodology (neutronic and hydraulic)

contributes to the remaining k-effective variation. The equivalent criterion used and approved for PWR analysis is [ ]. This worth ([ ]) is approximately [ ]  $\Delta k$ . Experiences have shown that the in-cycle hot critical k-effectives calculated using SPC's core simulators are usually well within the 1  $\sigma$  deviation of [ ]  $\Delta k$ . The largest impact of a k-effective variation is on the fuel cycle energy requirement and such a deviation is acceptable.

2. Cycle-to-cycle average hot critical k-effective change < [ ] --- This criterion was established for the same reason stated in Item 1. This is a different way of qualifying the hot critical k-effective prediction of a core simulator.
3. BOC cold critical k-effective variation < [ ] --- Operators of BWRs are required to perform a startup cold critical measurement of one or more critical cores depending on plant-specific technical specification. When several critical cores are measured and subsequently simulated, a variation in critical k-effectives often appears. This variation is due to the measurement uncertainty and the calculation uncertainty. The design cold shutdown margin requirement is generally 1% or more in reactivity. The technical specification limit is typically about 0.4%. Thus, a core simulator prediction uncertainty may not exceed [ ]. SPC's approved core simulator MICROBURN-B has shown a scattering well below this criterion.
4. Cycle-to-cycle BOC average cold critical k-effective change < [ ] --- This criterion was established using the basis discussed in Item 3. This is a different way of qualifying the cold critical k-effective prediction of a core simulator.
5. Cycle average 2-D radial TIP relative standard deviation including limited measurement uncertainty --- The SPC BWR neutronic design practice requires a routine performance of core follow analyses. The purpose of this analysis is to verify that the cycle operation follows the projection and that the measured TIP data agrees with the predicted TIP data within the approved uncertainty limit. Past analyses show that the 2-D radial TIP, 1  $\sigma$  deviation is between [ ] for C-lattice reactors and between [ ] for D-lattice reactors. Any deviation beyond these ranges would indicate an anomaly in either the measurement or the calculation. If the problem is found in SPC's core simulator, then the design thermal margin would be increased for the future cycle design. For the actual cycle operation, the thermal margin is protected by the design of the core monitoring system and the measured power uncertainty.
6. Cycle average 3-D radial TIP relative standard deviation including limited measurement uncertainty --- This criterion was established using the same reasoning as provided in Item 5. This is another component needed to qualify the TIP prediction of a core simulator.
7. Net calculation uncertainty of pin-by-pin gamma scan < [ ]% --- This criterion was established using the uncertainty of the approved lattice code CASMO-3 in its benchmark of the Quad Cities gamma scan measurement (Reference 3).

SPC BWR Core Simulator Code Measured Power Distribution Uncertainty Limit

The criteria shown in Table 5.3 are various components of the uncertainty shown for the currently approved methodology CASMO-3/MICROBURN-B (Reference 3).

Clarification of Statistical Equations

The statistical method used in the current submittal is identical to the previously approved statistical method in Reference 3. The following discussion clarifies three of the statistical equations used in the current submittal.

**Equation (9-9):** This equation is derived on Page 151 of Reference 3. Eq. (5-32) of Reference 3 is simplified to Eq. (5-33), which is Eq. (9-9) in the current CASMO-4/MICROBURN-B2 submittal, by setting all bundle power ( $B_k$  and  $B_j$ ) to an average bundle power ( $\bar{B}$ ).



Canceling out the bundle power results:



From this simplified equation, the term  $\delta_B$  is defined as shown in Eq. (5-33) of Reference 3.

**Equation (9-10):** A correlation coefficient between two independent variables ( $x$  and  $y$ ) is defined using the variance of the two variables ( $\sigma_x$  and  $\sigma_y$ ). A correlation found in a standard statistical method textbook (e.g., A. H. Bowker and G. J. Lieberman, "Engineering Statistics," 2d ed., pp. 362-363) is:

$$\rho = \frac{\sigma_{xy}}{\sigma_x \sigma_y}$$

where  $\sigma_{xy} = \text{covariance} = \sum_{n=1}^k dx_n dy_n$

$\sigma_x, \sigma_y = \text{variance} = \sqrt{k-1} S$ , where

$S =$  standard deviation of differences between calculated and measured powers for neighboring bundles or nodes.

$dx_n, dy_n$  = differences between calculated and measured powers for neighboring bundles or nodes.

Hence,

$$\rho = \frac{1}{(k-1)S^2} \sum_{n=1}^k dx_n dy_n$$

**Equation (9-2):** This equation is derived based on the condition that the mean values of  $L_{ijk}$  and  $P_{ijk}^n$  are 1 because they are normalized to an average value of 1.

References:

1. EMF-2158(P) Revision 0, "Siemens Power Corporation Methodology for Boiling Water Reactors: Evaluation and Validation of CASMO-4/MICROBURN-B2," Siemens Power Corporation, December 1998.
2. XN-NF-80-19(P)(A) Volume 1 and Supplements 1 and 2, "Exxon Nuclear Methodology for Boiling Water Reactors - Neutronic Methods for Design and Analysis," Exxon Nuclear Company, March 1983.
3. XN-NF-80-19(P)(A) Volume 1 Supplement 3, Supplement 3 Appendix F, and Supplement 4, "Advanced Nuclear Fuels Methodology for Boiling Water Reactors: Benchmark Results for the CASMO-3G/MICROBURN-B Calculation Methodology," Advanced Nuclear Fuels Corporation, November 1990.
4. STUDSVIK/SOA-94/13, "CASMO-4 Benchmark Against Critical Experiments," STUDSVIK Proprietary, December 1995.
5. EMF-96-029(P)(A) Volumes 1 and 2, "Reactor Analysis Systems for PWRs Volume 1 – Methodology Description, Volume 2 – Benchmarking Results," Siemens Power Corporation, January 1997.
6. EPRI NP-214, "Gamma Scan Measurements at Quad Cities Nuclear Power Station Unit 1 Following Cycle 2," Electric Power Research Institute, July 1976.
7. R. D. Mosteller, "ENDF/B-V and ENDF/B-VI Results for UO<sub>2</sub> Lattice Benchmark Problems Using MCNP," International Conference on the Physics of Nuclear Science and Technology, 1998, Vol. 2, p. 1282.

# SIEMENS

May 7, 1999  
NRC:99:021

Document Control Desk  
ATTN: Chief, Planning, Program and Management Support Branch  
U.S. Nuclear Regulatory Commission  
Washington, D.C. 20555-0001

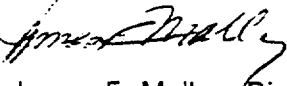
## Request for a Copy of EMF-2147(P), "MICROBURN-B2 User's Manual"

Ref.: 1. Letter, James F. Mallay (SPC) to Document Control Desk, "Request for Review of EMF-2158(P) Revision 0 'Siemens Power Corporation Methodology for Boiling Water Reactors: Evaluation and Validation of CASMO-4/MICROBURN-B2'," NRC:98:087. December 30, 1998.

One copy of the MICROBURN-B2 User's Manual has been sent to Mr. E. Y. Wang. This report is complementary to the topical report submitted to the NRC by Reference 1. The reviewer has indicated that having this report will facilitate his evaluation of the topical report.

Some of the information contained in this report is considered to be proprietary to Siemens Power Corporation. The affidavit originally submitted for the review of the topical report by Reference 2 satisfies the requirements of 10 CFR 2.790(b) to support the withholding of this information from public disclosure.

Very truly yours,



James F. Mallay, Director  
Regulatory Affairs

/arn

cc: Mr. E. Y. Wang (1 proprietary report)  
Mr. J. L. Wermiel  
Project No. 702

## Siemens Power Corporation

2101 Horn Rapids Road  
Richland, WA 99352

Tel: (509) 375-8100  
Fax: (509) 375-8402

# Studsvik Scandpower, Inc.

April 30, 1999

Document Control Desk  
ATTN: Chief, Planning, Program and Management Support Branch  
U.S. Nuclear Regulatory Commission  
Washington, D.C. 20555-0001

**Subject: Transmittal of Copies of CASMO-4 Benchmark Reports Relevant to EMF-2158(P) Revision 0 "Siemens Power Corporation Methodology for Boiling Water Reactors: Evaluation and Validation of CASMO-4/MICBROBURN-B2"**

#### References:

- 1 CASMO-4 Benchmark Against MCNP, SOA-94/12
- 2 CASMO-4 Benchmark Against Critical Experiments, SOA-94/13
- 3 CASMO-4 Benchmark against Yankee Rowe Isotopic Measurements, Studsvik/SCOAB-96/5
- 4 Letter, James F. Mallay (SPC) to Document Control Desk, "Request for Review of EMF-2158(P) Revision 0 'Siemens Power Corporation Methodology for Boiling Water Reactors: Evaluation and Validation of CASMO-4/MICROBURN-B2'," NRC:98:087, December, 1998.

One copy each of the reports in References 1,2, and 3 have been sent to Mr. E. Y. Wang. These reports are relevant to the topical report submitted to the NRC by Reference 4. The reviewer has indicated that having such reports will facilitate his evaluation of the topical report.

Some of the information contained in each of the reports is considered to be proprietary to Studsvik Scandpower, Inc. The affidavit originally submitted for the review of the topical report by Reference 4 satisfies the requirements of 10CFR 2.790(b) to support the withholding of this information from public disclosure.

---

Studsvik Scandpower, Inc.  
1087 Beacon Street, Suite 301  
Newton, MA 02459-1700

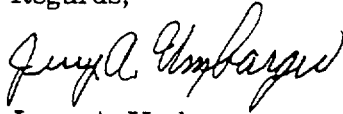
Telephone  
617-965-7450

Telefax  
617-965-7549

# Studsvik Scandpower, Inc.

If you have any questions or if I can be of further assistance, please call me at 617-965-7451.

Regards,



Jerry A. Umbarger

U.S. Business Manager

cc: Mr. E. Y. Wang (USNRC) (3 proprietary reports)  
Mr. J. L. Wermiel (USNRC)  
Project No. 702

# SIEMENS

April 28, 1999  
NRC:99:016

Document Control Desk  
ATTN: Chief, Planning, Program and Management Support Branch  
U.S. Nuclear Regulatory Commission  
Washington, D.C. 20555-0001

bc: (via e-mail)  
H. D. Curet *HD*  
D. J. Denver  
R. G. Grummer  
J. S. Holm  
H. Moon  
File/LB

## Request for Copies of Reports Referenced in EMF-2158(P) Revision 0, "Siemens Power Corporation Methodology for Boiling Water Reactors: Evaluation and Validation of CASMO-4/MICROBURN-B2"

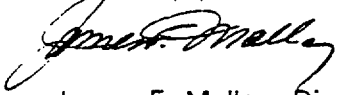
- Ref.: 1. STUDSVIK/SOA-95/2, "CASMO-4, A Fuel Assembly Burnup Program Methodology," Studsvik Proprietary, September 1995.
- Ref.: 2. EMF-1833(P) Revision 2, "MICROBURN-B2: Steady State BWR Core Physics Method," Siemens Power Corporation, September 1998.
- Ref.: 3. Letter, James F. Mallay (SPC) to Document Control Desk, "Request for Review of EMF-2158(P) Revision 0 'Siemens Power Corporation Methodology for Boiling Water Reactors: Evaluation and Validation of CASMO-4/MICROBURN-B2'," NRC:98:087, December 30, 1998.

One copy each of the reports in References 1 and 2 have been sent to Mr. E. Y. Wang as requested by Dr. A. C. Attard. These reports are referenced in the topical report submitted to the NRC by Reference 3. Dr. Attard has indicated that having these two reports will facilitate his evaluation of the topical report.

Some of the information contained in References 1 and 2 is considered to be proprietary to Studsvik and to Siemens Power Corporation, respectively. The affidavit originally submitted for the review of the topical report by Reference 3 satisfies the requirements of 10 CFR 2.790(b) to support the withholding of this information from public disclosure.

If you have any questions or if I can be of further assistance, please call me at (509)375-8757.

Very truly yours,



James F. Mallay, Director  
Regulatory Affairs

/arn

cc: Mr. E. Y. Wang (2 proprietary reports)  
Mr. J. L. Wermiel

Project No. 702

### Siemens Power Corporation

2101 Horn Rapids Road  
Richland, WA 99352

Tel: (509) 375-8100  
Fax: (509) 375-8402

# SIEMENS

April 7, 1999  
NRC:99:012

Document Control Desk  
ATTN: Chief, Planning, Program and Management Support Branch  
U.S. Nuclear Regulatory Commission  
Washington, D.C. 20555-0001

## **Request for Copies of Topical Reports Referenced in EMF-2158(P) Revision 0 "Siemens Power Corporation Methodology for Boiling Water Reactors: Evaluation and Validation of CASMO-4/MICROBURN-B2"**

- Ref.: 1. XN-NF-80-19(P)(A) Volume 1 Supplement 3, Supplement 3 Appendix F, and Supplement 4, "Advanced Nuclear Fuels Methodology for Boiling Water Reactors: Benchmark Results for the CASMO-3G/MICROBURN-B Calculation Methodology," Advanced Nuclear Fuels Corporation, November 1990.
- Ref.: 2. XN-NF-80-19(P)(A) Volume 1 and Supplements 1 and 2. "Exxon Nuclear Methodology for Boiling Water Reactors - Neutronic Methods for Design and Analysis," Exxon Nuclear Company, March 1983.
- Ref.: 3. Letter, James F. Mallay (SPC) to Document Control Desk, "Request for Review of EMF-2158(P) Revision 0 'Siemens Power Corporation Methodology for Boiling Water Reactors: Evaluation and Validation of CASMO-4/MICROBURN-B2'," NRC:98:087, December 30, 1998.

One copy each of the reports in References 1 and 2 have been sent to Mr. E. Y. Wang in response to his request made during a telecon with H. D. Curet on April 6, 1999. These reports are referenced in the topical report submitted to the NRC by Reference 3. The reviewer has indicated that having these two reports will facilitate his evaluation of the topical report.

Some of the information contained in each of the reports is considered to be proprietary to Siemens Power Corporation. The affidavit originally submitted for the review of the topical report by Reference 3 satisfies the requirements of 10 CFR 2.790(b) to support the withholding of this information from public disclosure.

## **Siemens Power Corporation**

2101 Horn Rapids Road  
Richland, WA 99352

Tel: (509) 375-8100  
Fax: (509) 375-8402

If you have any questions or if I can be of further assistance, please call me at (509) 375-8757.

Very truly yours,



James F. Mallay, Director  
Regulatory Affairs

jak

cc: Mr. E. Y. Wang (USNRC) (2 proprietary reports)  
Mr. J. L. Wermiel (USNRC)  
Project No. 702

# SIEMENS

December 30, 1998  
NRC:98:087

Document Control Desk  
ATTN: Chief, Planning, Program and Management Support Branch  
U.S. Nuclear Regulatory Commission  
Washington, D.C. 20555-0001

**Request for Review of EMF-2158(P) Revision 0 "Siemens Power Corporation Methodology for Boiling Water Reactors: Evaluation and Validation of CASMO-4/MICROBURN-B2"**

Ref.: 1. XN-NF-80-19(P)(A) Volume 1 Supplement 3, Supplement 3 Appendix F, and Supplement 4, "Advanced Nuclear Fuels Methodology for Boiling Water Reactors: Benchmark Results for the CASMO-3G/MICROBURN-B Calculation Methodology," Advanced Nuclear Fuels Corporation, November 1990.

Ref.: 2. Letter, James F. Mallay (SPC) to T. E. Collins (NRC), "Revised Schedule for the Submittal of Topical Reports," NRC:98:080, December 9, 1998.

Enclosed are 15 copies of the proprietary and 12 copies of the non-proprietary version of EMF-2158(P) Revision 0, "Siemens Power Corporation Methodology for Boiling Water Reactors: Evaluation and Validation of CASMO-4/MICROBURN-B2." (NOTE: Three proprietary copies and one non-proprietary copy have been forwarded to Mr. Egan Wang). This topical report describes an upgraded BWR neutronics design code system which includes a lattice spectrum/depletion code and steady-state reactor core simulator code. The benchmark results for the current neutronics design code methodology were provided to the NRC almost 10 years ago in March 1989 (Reference 1). The NRC is requested to review this report for an upgraded neutronics code system to support neutronic design analyses performed by Siemens for its BWR customers. This report is one of the topical reports listed in Reference 2 that Siemens informed the NRC would be submitted in FY 98/99.

Some of the information contained in the enclosed topical report is considered to be proprietary to Siemens Power Corporation. As required by 10 CFR 2.790(b), an affidavit is enclosed to support the withholding of this information from public disclosure.

## Siemens Power Corporation

2101 Horn Rapids Road  
Richland, WA 99352

Tel: (509) 375-8100  
Fax: (509) 375-8402

Chief, Planning, Program and Management Support Branch  
December 30, 1998

NRC:98:087  
Page 2

If you have any questions or if I can be of further assistance, please call me at (509) 375-8757.

Very truly yours,

  
James F. Mallay, Director  
Regulatory Affairs

cc: Mr. T. E. Collins (USNRC)  
Mr. E. Y. Wang (USNRC) (3 proprietary copies/1 non-proprietary)  
Mr. J. E. Lyons (USNRC)  
Project No. 702 (12 proprietary/11 non-proprietary copies)

bc: (via e-mail)  
O. C. Brown  
R. E. Collingham  
H. D. Curet *File*  
D. J. Denver  
R. L. Feuerbacher  
D. E. Garber  
M. E. Garrett  
R. G. Grummer  
L. E. Hansen  
ALB Ho  
J. S. Holm  
H. Moon  
C. M. Powers  
D. W. Pruitt  
R. S. Reynolds  
K. V. Walters  
T. A. Wells  
File/LB

EMF – 2158(NP)  
Revision 0

Siemens Power Corporation Methodology for  
Boiling Water Reactors: Evaluation and  
Validation of CASMO – 4/MICROBURN – B2

December 1998

## Table of Contents

<b>1.</b>	<b>Introduction .....</b>	<b>1-1</b>
<b>2.</b>	<b>Summary .....</b>	<b>2-1</b>
<b>3.</b>	<b>Overview .....</b>	<b>3-1</b>
<b>4.</b>	<b>Methodology Requirements .....</b>	<b>4-1</b>
4.1	Lattice Spectrum/Depletion Code Methodology .....	4-1
4.1.1	Nuclear Data Library .....	4-1
4.1.2	Lattice Spectrum/Depletion Code .....	4-1
4.2	Reactor Core Simulator Code .....	4-2
4.2.1	Code Capabilities .....	4-2
4.2.2	Compatibility and Consistency with Safety Analysis Methodology .....	4-3
<b>5.</b>	<b>Validation Requirements .....</b>	<b>5-1</b>
5.1	Critical Experiments and Isotopic Measurements .....	5-1
5.2	Measurements from Commercial Reactors .....	5-2
5.2.1	Selection of Reactors .....	5-2
5.2.2	Hot Operating Condition Measurements .....	5-2
5.2.3	Cold Shutdown Condition Measurements .....	5-4
5.2.4	Hot Operating Condition Local Pin Power Measurements .....	5-4
5.3	Verification of Measured Power Distribution Uncertainty .....	5-5
<b>6.</b>	<b>Evaluation of CASMO-4/MICROBURN-B2 Methodology .....</b>	<b>6-1</b>
6.1	CASMO-4 Lattice Spectrum/Depletion Code Methodology .....	6-1
6.2	Core Simulator Code Methodology .....	6-1
6.3	Compatibility and Consistency with Safety Analysis Methodology .....	6-2
<b>7.</b>	<b>Validation of CASMO-4/MICROBURN-B2 Methodology .....</b>	<b>7-1</b>
7.1	Critical Experiments and Isotopic Measurements .....	7-1
7.2	Validation against Commercial Reactors .....	7-2
7.2.1	Hot Operating Condition Critical K-effectives .....	7-3
7.2.2	Cold Critical K-effectives .....	7-5
7.2.3	Detector Reaction Rate Comparison .....	7-6
7.3	Independent Validation of MICROBURN-B2 Methodology .....	7-8
7.4	Summary of CASMO-3/MICROBURN-B2 Validation .....	7-9
<b>8.</b>	<b>Validation of CASMO-4/MICROBURN-B2 BWR Pin Power Methodology ...</b>	<b>8-1</b>
8.1	Validation Against Higher Order Method .....	8-1
8.2	Validation Against Measurements .....	8-3
8.2.1	Quad Cities Unit 1 Measurement .....	8-3
8.2.2	KWU-S Measurement .....	8-4
<b>9.</b>	<b>Verification of CASMO-4/MICROBURN-B2 Measured Power Distribution Uncertainty .....</b>	<b>9-1</b>
9.1	Statistical Analysis of Measured Power Distribution Uncertainty .....	9-1

## Table of Contents

9.2	Data Base for Verification of Measured Power Distribution Uncertainty ..	9-6
9.3	Verification of Predicted Local Pin Power Distribution Uncertainty .....	9-8
9.4	Verification of Calculated TIP Distribution Uncertainty .....	9-8
9.5	Verification of Synthesized TIP Distribution Uncertainty .....	9-9
9.6	Verification of Calculated Bundle Power Distribution Uncertainty .....	9-10
9.7	Verification of Measured Power Uncertainty .....	9-10
10.	References .....	10-1
APPENDIX A	Illustration of CASMO-4/MICROBURN-B2 Application to BWR Core Neutronic Designs .....	A-1

### List of Tables

Table 2.1	SPC BWR Fuel Lattice Spectrum/Depletion Code Validation Results .....	2-4
Table 2.2	SPC BWR Core Simulator Code Validation Results .....	2-5
Table 2.3	SPC BWR Core Simulator Code Measured Power Distribution Uncertainty Verification .....	2-6
Table 5.1	SPC BWR Fuel Lattice Spectrum/Depletion Code Validation Requirement ..	5-2
Table 5.2	SPC BWR Core Simulator Code Validation Requirement .....	5-3
Table 5.3	SPC BWR Core Simulator Code Measured Power Distribution Uncertainty Limit .....	5-6
Table 6.1	Sample Comparison of Neutronics Input Data for BWR Transient Analysis ..	6-3
Table 7.1	Selection of Commercial BWRs for Benchmark Analysis .....	7-2
Table 7.2	BWR-A Cycle Average Hot Critical K-effectives .....	7-12
Table 7.3	BWR-A Beginning of Cycle Average Cold Critical K-effectives .....	7-13
Table 7.4	BWR-B Cycle Average Hot Critical K-effectives .....	7-19
Table 7.5	BWR-B Beginning of Cycle Average Cold Critical K-effectives .....	7-20
Table 7.6	BWR-C Cycle Average Hot Critical K-effectives .....	7-26
Table 7.7	BWR-C Beginning of Cycle Average Cold Critical K-effectives .....	7-27
Table 7.8	BWR-D Cycle Average Hot Critical K-effectives .....	7-33
Table 7.9	KWU-S Cycle Average Hot Critical K-effectives .....	7-39
Table 7.10	KWU-S Beginning of Cycle Average Cold Critical K-effectives .....	7-40
Table 7.11	BWR-E Cycle Average Hot Critical K-effectives .....	7-46

### List of Tables

Table 7.12 BWR-E Beginning of Cycle Average Cold Critical K-effectives .....	7-47
Table 8.1 Colorset Geometries for Benchmark Against Higher Order Method .....	8-2
Table 8.2 Results of Benchmark Against Higher Order Method .....	8-3
Table 8.3 Summary of Quad Cities Unit 1 EOC 2 Pin Power Benchmark .....	8-6
Table 8.4 Summary of Quad Cities Unit 1 EOC 3 Pin Power Benchmark .....	8-7
Table 8.5 Summary of KWU-S EOC 13 Pin Power Benchmark .....	8-8
Table 8.6 Summary of KWU-S EOC 13 Axially Continuous Pin Power Benchmark .....	8-9
Table 9.1 Data Base for Verification of Measured Power Distribution .....	9-7
Table 9.2 BWR-A TIP Standard Deviation of Relative Differences .....	9-12
Table 9.3 BWR-B TIP Standard Deviation of Relative Differences .....	9-14
Table 9.4 BWR-E TIP Standard Deviation of Relative Differences .....	9-17
Table 9.5 KWU-S TIP Standard Deviation of Relative Differences .....	9-19
Table 9.6 BWR-C TIP Standard Deviation of Relative Differences .....	9-21
Table 9.7 BWR-D TIP Standard Deviation of Relative Differences .....	9-22
Table 9.8 Measured Power Distribution Uncertainty Components .....	9-25
Table 9.9 Measured Power Distribution Uncertainty .....	9-28

### List of Figures

Figure 2.1	SPC Standard BWR Neutronics Calculation Process .....	2-3
Figure 7.1	BWR-A Core Power/Flow and Inlet Subcooling/Core Pressure Drop Trend .	7-10
Figure 7.2	BWR-A Core Void/Control Density, and Axial Power/Exposure Tilt Trend ..	7-11
Figure 7.3	BWR-A Hot Critical K-effective Trend .....	7-12
Figure 7.4	BWR-A Cycle 1 to 7 Cold Critical K-effective Trend .....	7-13
Figure 7.5	BWR-A TIP 2-D Radial Relative Standard Deviations and Frequency Distribution of Relative Differences .....	7-14
Figure 7.6	BWR-A TIP 3-D Nodal Relative Standard Deviations and Frequency Distribution of Relative Differences .....	7-15
Figure 7.7	BWR-A TIP 3-D Planar Relative Standard Deviations and Frequency Distribution of Relative Differences .....	7-16
Figure 7.8	BWR-B Core Power/Flow and Inlet Subcooling/Core Pressure Drop Trend .	7-17
Figure 7.9	BWR-B Core Void/Control Density, and Axial Power/Exposure Tilt Trend ..	7-18
Figure 7.10	BWR-B Hot Critical K-effectives .....	7-19
Figure 7.11	BWR-B Cycle 1 to 9 Cold Critical K-effectives .....	7-20
Figure 7.12	BWR-B TIP 2-D Radial Relative Standard Deviations and Frequency Distribution of Relative Differences .....	7-21
Figure 7.13	BWR-B TIP 3-D Nodal Relative Standard Deviations and Frequency Distribution of Relative Differences .....	7-22
Figure 7.14	BWR-B TIP 3-D Planar Relative Standard Deviations and Frequency Distribution of Relative Differences .....	7-23
Figure 7.15	BWR-C Core Power/Flow and Inlet Subcooling/Core Pressure Drop Trend	7-24
Figure 7.16	BWR-C Core Void/Control Density, and Axial Power/Exposure Tilt Trend .	7-25

### List of Figures

Figure 7.17	BWR-C Hot Critical K-effectives .....	7-26
Figure 7.18	BWR-C Cycle 8 to 11 Cold Critical K-effectives .....	7-27
Figure 7.19	BWR-C TIP 2-D Radial Relative Standard Deviations and Frequency Distribution of Relative Differences .....	7-28
Figure 7.20	BWR-C TIP 3-D Nodal Relative Standard Deviations and Frequency Distribution of Relative Differences .....	7-29
Figure 7.21	BWR-C TIP 3-D Planar Relative Standard Deviations and Frequency Distribution of Relative Differences .....	7-30
Figure 7.22	BWR-D Core Power/Flow and Inlet Subcooling/Core Pressure Drop Trend	7-31
Figure 7.23	BWR-D Core Void/Control Density, and Axial Power/Exposure Tilt Trend .	7-32
Figure 7.24	BWR-D Hot Critical K-effectives .....	7-33
Figure 7.25	BWR-D TIP 2-D Radial Relative Standard Deviations and Frequency Distribution of Relative Differences .....	7-34
Figure 7.26	BWR-D TIP 3-D Nodal Relative Standard Deviations and Frequency Distribution of Relative Differences .....	7-35
Figure 7.27	BWR-D TIP 3-D Planar Relative Standard Deviations and Frequency Distribution of Relative Differences .....	7-36
Figure 7.28	KWU-S Core Power/Flow and Inlet Subcooling/Core Pressure Drop Trend	7-37
Figure 7.29	KWU-S Core Void/Control Density, and Axial Power/Exposure Tilt Trend .	7-38
Figure 7.30	KWU-S Hot Critical K-effectives .....	7-39
Figure 7.31	KWU-S Beginning of Cycle Cold Local Critical K-effectives .....	7-40
Figure 7.32	KWU-S TIP 2-D Radial Relative Standard Deviations and Frequency Distribution of Relative Differences .....	7-41

### List of Figures

Figure 7.33	KWU-S TIP 3-D Nodal Relative Standard Deviations and Frequency Distribution of Relative Differences .....	7-42
Figure 7.34	KWU-S TIP 3-D Planar Relative Standard Deviations and Frequency Distribution of Relative Differences .....	7-43
Figure 7.35	BWR-E Core Power/Flow and Inlet Subcooling/Core Pressure Drop Trend	7-44
Figure 7.36	BWR-E Core Void/Control Density, and Axial Power/Exposure Tilt Trend .	7-45
Figure 7.37	BWR-E Hot Critical K-effectives .....	7-46
Figure 7.38	BWR-E Cold Critical K-effectives .....	7-47
Figure 7.39	BWR-E TIP 2-D Radial Relative Standard Deviations and Frequency Distribution of Relative Differences .....	7-48
Figure 7.40	BWR-E TIP 3-D Nodal Relative Standard Deviations and Frequency Distribution of Relative Differences .....	7-49
Figure 7.41	BWR-E TIP 3-D Planar Relative Standard Deviations and Frequency Distribution of Relative Differences .....	7-50
Figure 8.1	Examples of Colorset Geometries .....	8-2
Figure 8.2	BWR-D EOC2 Bundle CX672 Pin Power Comparison for Axial Level 1 and 2 .....	8-10
Figure 8.3	Quad Cities Unit 1 EOC2 Bundle CX672 Pin Power Comparison for Axial Level 3 and 4 .....	8-11
Figure 8.4	Quad Cities Unit 1 EOC2 Bundle GEH02 Pin Power Comparison for Axial Level 1 and 2 .....	8-12
Figure 8.5	Quad Cities Unit 1 EOC2 Bundle GEH02 Pin Power Comparison for Axial Level 3 and 4 .....	8-13
Figure 8.6	Quad Cities Unit 1 EOC2 Bundle CX214 Pin Power Comparison for Axial Level 1 and 2 .....	8-14

### List of Figures

Figure 8.7	Quad Cities Unit 1 EOC2 Bundle CX214 Pin Power Comparison for Axial Level 3 and 4 .....	8-15
Figure 8.8	Quad Cities Unit 1 EOC2 Bundle GEB159 Pin Power Comparison for Axial Level 1 and 2 .....	8-16
Figure 8.9	Quad Cities Unit 1 EOC2 Bundle GEB159 Pin Power Comparison for Axial Level 3 and 4 .....	8-17
Figure 8.10	Quad Cities Unit 1 EOC3 Bundle L2593 Pin Power Comparison for Axial Level 1 and 2 .....	8-18
Figure 8.11	Quad Cities Unit 1 EOC3 Bundle L2593 Pin Power Comparison for Axial Level 3 and 4 .....	8-19
Figure 8.12	Quad Cities Unit 1 EOC3 Bundle GEB159 Pin Power Comparison for Axial Level 1 and 2 .....	8-20
Figure 8.13	Quad Cities Unit 1 EOC3 Bundle GEB159 Pin Power Comparison for Axial Level 3 and 4 .....	8-21
Figure 8.14	Quad Cities Unit 1 EOC3 Bundle GEH06 Pin Power Comparison for Axial Level 1 and 2 .....	8-22
Figure 8.15	Quad Cities Unit 1 EOC3 Bundle GEH06 Pin Power Comparison for Axial Level 3 and 4 .....	8-23
Figure 8.16	Quad Cities Unit 1 EOC3 Bundle L2532 Pin Power Comparison for Axial Level 1 and 2 .....	8-24
Figure 8.17	Quad Cities Unit 1 EOC3 Bundle L2532 Pin Power Comparison for Axial Level 3 and 4 .....	8-25
Figure 8.18	KWU-S EOC 13 Bundle B91427 Pin Power Comparison for Axial Level 1 and 2 .....	8-26
Figure 8.19	KWU-S EOC 13 Bundle B91427 Pin Power Comparison for Axial Level 3 and 4 .....	8-27
Figure 8.20	KWU-S EOC 13 Bundle B59006 Pin Power Comparison for Axial Level 1 and 2 .....	8-28

### List of Figures

Figure 8.21	KWU-S EOC 13 Bundle B59006 Pin Power Comparison for Axial Level 3 and 4 .....	8-29
Figure 8.22	KWU-S EOC 13 Bundle B11330 Pin Power Comparison for Axial Level 1 .....	8-30
Figure 8.23	KWU-S EOC 13 Bundle B58102 Pin Power Comparison for Axial Level 1 and 2 .....	8-31
Figure 8.24	KWU-S EOC 13 Bundle B58102 Pin Power Comparison for Axial Level 3 and 4 .....	8-32
Figure 8.25	KWU-S EOC 13 Bundle B91427 Rod B2 and Rod B4 Axial Ba-140 Distribution Comparison .....	8-33
Figure 8.26	KWU-S EOC 13 Bundle B91427 Rod C7 and Rod G8 Axial Ba-140 Distribution Comparison .....	8-34
Figure 8.27	KWU-S EOC 13 Bundle B59006 Rod G8 and Rod G9 Axial Ba-140 Distribution Comparison .....	8-35
Figure 8.28	KWU-S EOC 13 Bundle B59006 Rod H5 and Bundle B11330 Rod G6 Axial Ba-140 Distribution Comparison .....	8-36
Figure 8.29	KWU-S EOC 13 Bundle B11330 Rod H7 and Rod K5 Axial Ba-140 Distribution Comparison .....	8-37
Figure 8.30	KWU-S EOC 13 Bundle B11330 Rod K8 and Rod K9 Axial Ba-140 Distribution Comparison .....	8-38
Figure 8.31	KWU-S EOC 13 Bundle B58102 Rod B8 and Rod H2 Axial Ba-140 Distribution Comparison .....	8-39
Figure 9.1	Quad Cities Unit 1 EOC2 Assembly Ba-140 Distribution Comparison .....	9-23
Figure 9.2	Quad Cities Unit 1 EOC4 Assembly Ba-140 Distribution Comparison .....	9-24
Figure A.1	BWR-A Cycle 7 MAPLHGR Margin Comparison .....	A-2
Figure A.2	BWR-A Cycle 7 LHGR Margin Comparison .....	A-3

**List of Figures**

Figure A.3 BWR-A Cycle 7 MCPR Margin Comparison ..... A-4

## 1. Introduction

A boiling water reactor (BWR) neutronics design code system consists of a lattice spectrum/depletion code and a steady state reactor core simulator code. A lattice spectrum/depletion code estimates the multi-group neutron spatial spectrum in a heterogeneous fuel lattice composed of fuel and burnable poison rods and structural components. It also determines the lattice nuclide inventories as it is burned through thermonuclear reactions. A reactor simulator code determines the neutronic characteristics of a reactor core containing fuel assemblies, coolant, and structural components. Together these two codes are used to design initial and reload cores, calculate parameters for safety analyses, and perform off-line and on-line core monitoring functions.

As improvements are made in reactor analysis methods through new developments based on experiences gained from operating reactors, it is desirable to utilize these improvements for upgrading the previously approved neutronics design code system. The upgrade of a neutronics design code in a timely manner is important for future operation of BWRs. For instance, an upgraded BWR neutronics code system is needed to more accurately model advanced fuel bundle designs and new operating strategies. Advanced bundle designs incorporate mechanical features that can be better analyzed with a more sophisticated neutronic model. Also more BWRs are operating in a spectral shift mode for a longer fuel cycle length. The design margin for these longer fuel cycles can be more realistically predicted with an improved neutronic model. Specified Accepted Fuel Design Limits (SAFDLs) may be analyzed more accurately resulting in lower probability of fuel failure.

This report presents an upgraded BWR neutronics design code system of Siemens Power Corporation (SPC). The new code system consists of the CASMO-4 lattice spectrum/depletion code<sup>(1)</sup> and the MICROBURN-B2 core simulator code.<sup>(2)</sup> CASMO-4 is an improved version of CASMO-3<sup>(3)</sup> which has been approved for use since 1990. MICROBURN-B2 is an improved version of MICROBURN-B<sup>(4)</sup> which has been approved for use for the same period. The new code system replaces the existing neutronics codes used for the approved SPC BWR neutronic design and safety methodology (Reference 5). All other methodology and procedures presented in Reference 5 remain unchanged.

The new code system incorporates many advanced model features. Among these, the most significant improvement from the previously approved code system is the pin power reconstruction method. The pin powers used for BWR core design and monitoring have been usually determined assuming an infinite medium condition. This assumption is acceptable because a BWR fuel lattice is separated from its neighbors by relatively large water gaps.

However, the core designs employing longer control blade exchange intervals and/or a mixture of UO<sub>2</sub> and MOX bundles need further consideration. These new designs incur relatively large neutron flux gradients across fuel bundles. A long exposure of a bundle to large neutron flux gradients develops a burnup history effect on local pin powers. The burnup history effect in a BWR is a very complex phenomenon involving differential effects on local fuel pins as well as integral effects on the entire lattice. Thus it is appropriate to determine local pin powers using an accurate pin power reconstruction method for these new core designs.

This report establishes a set of methodology evaluation and validation criteria by which a new neutronics design code or code system would be assessed for application to BWR neutronic design. These criteria are established to address the need for more accurate modeling for current and future reactor core/fuel lattice designs and operations. These criteria are then applied to the CASMO - 4/MICROBURN - B2 code system and the results of the assessment are presented in this report. Based on this assessment, it is confirmed that the new code system is acceptable for neutronic designs and licensing evaluations of BWR fuel cycles.

The evaluation and validation of the revised BWR neutronics design methodology described in this report are based on a wide variety of reactor core/fuel lattice designs and address an application to the SPC core monitoring system. Future upgrades of the neutronics methodology will require additional evaluation and validation to assure that the evaluation and validation criteria set forth in this report are met.

## 2. Summary

The upgraded Siemens Power Corporation (SPC) BWR neutronics design code system consists of the CASMO-4 lattice spectrum/depletion code and the MICROBURN-B2 steady state reactor core simulator code. An overview of the SPC standard BWR neutronics design calculation process is shown in Figure 2.1. The CASMO-4 code, developed by Studsvik, is used by nuclear reactor operators throughout the world. Due to such a widespread use, the code is well benchmarked and proven for commercial BWR application. The MICROBURN-B2 code was developed by Siemens and has been applied to European BWR core designs. The code has been extensively benchmarked and is already accepted for European BWR application.

The CASMO-4 code determines a multi-group heterogeneous medium neutron spectrum in a fuel lattice consisting of fuel rods, burnable poison rods, water rods/channels, and structural components. Using this spectrum, CASMO-4 homogenizes the heterogeneous lattice into a neutronicly equivalent homogeneous medium, determines pin power distributions, and depletes nuclides in fuel and burnable poison pins. A multi-group nuclear data library necessary for these calculations is obtained by processing the ENDF/B-IV measured nuclear data library with the support of other internationally recognized libraries such as ENDF/B-III, ENDF/B-V, JEF-1, JEF-2.1 and BNL-84. The main data output from the lattice spectrum/depletion code is a set of two neutron energy group data including microscopic and macroscopic cross sections for a spatially homogenized lattice. Other important output data include pinwise power distribution, exposure distribution, and energy deposition in various components of a fuel lattice. The CASMO-4 code satisfies the lattice code methodology requirement set forth by SPC.

The validation criteria for the lattice code to be used for SPC BWR neutronic design are summarized in Table 2.1. Validation of the CASMO-4 lattice code was carried out by comparing the code predictions with measured data from critical cores, measured isotopic inventory, and results of Monte Carlo simulations. A total of [ ] critical cores were benchmarked to assess the reactivity predicted by CASMO-4. Two PWR and six BWR pin-by-pin fission rate distribution measurements and the Yankee Rowe isotopic measurement were benchmarked. Bundle reactivity and fission rate distributions were compared between CASMO-4 and the MCNP Monte Carlo code for a total of [ ] bundles. Table 2.1 shows the results of the benchmarks. The CASMO-4 code is confirmed to satisfy the validation criteria set forth by SPC.

The lattice neutronic data determined by CASMO-4 is processed by an auxiliary code into a lattice neutronic data library for the MICROBURN-B2 core simulator code. Additional input

data for MICROBURN-B2 are fuel assembly and core inlet thermal-hydraulic data. The MICROBURN-B2 code determines core-wide nodal neutron flux, fission power, and coolant density distributions, reactivity parameters, nodal exposure and nuclide density distributions, channel inlet flow distribution, and fuel thermal performance parameters such as linear heat generation rate (LHGR), axial planar linear heat generation rate (APLHGR), and critical power ratio (CPR). These predicted results are used to design fuel cycles, to assess safety margins, and to monitor operating reactor cores. The MICROBURN-B2 code satisfies the core simulator code methodology requirement set forth by SPC.

A set of validation criteria are established to demonstrate that the new BWR neutronics design code system is acceptable for use in fuel cycle design, licensing, and core monitoring. These criteria, summarized in Table 2.2 and Table 2.3, consist of uncertainty criteria for key parameters calculated by the new code system. The uncertainty of the calculated results is quantified by comparison with measured results. The new code system is validated by simulating a total of [ ] fuel cycles for six selected BWRs which include more than [ ] hot operating state points and a total of [ ] cold critical cores. A total of [ ] full core TIP measurements were benchmarked to validate the predicted TIP distribution. The results of this benchmark are summarized in Table 2.2. The new code system meets the validation requirements.

The local pin power distributions calculated by the new core simulator code are validated by comparison with results from higher order methods and pin gamma scan measurements. A total of [ ] colorset geometries were simulated and the resulting pin power distributions were compared between MICROBURN-B2 and CASMO-3/CASMO-4. The Quad Cities Unit 1 and the KWU-S pin gamma scan measurements were simulated to determine the uncertainty of predicted local pin power distributions. As provided in Table 2.2, the new code system satisfies the validation requirement for local pin power uncertainty.

The measured power distribution uncertainty was verified for the SPC core monitoring system which will use the MICROBURN-B2 code as its core simulator model. The verification is based on a statistical analysis of the predicted-versus-measured TIP distributions and local pin power distributions using the previously approved statistical method.<sup>(5)</sup> The validation requirement and the results of validation are summarized in Table 2.3. The new code meets the validation requirement.

The CASMO-4/MICROBURN-B2 code system is found to satisfy the established methodology and validation requirements. The new code system has been determined to satisfy the previously approved measured power distribution uncertainty. Thus it is valid to apply the new code system to licensing evaluations of BWR neutronic designs.

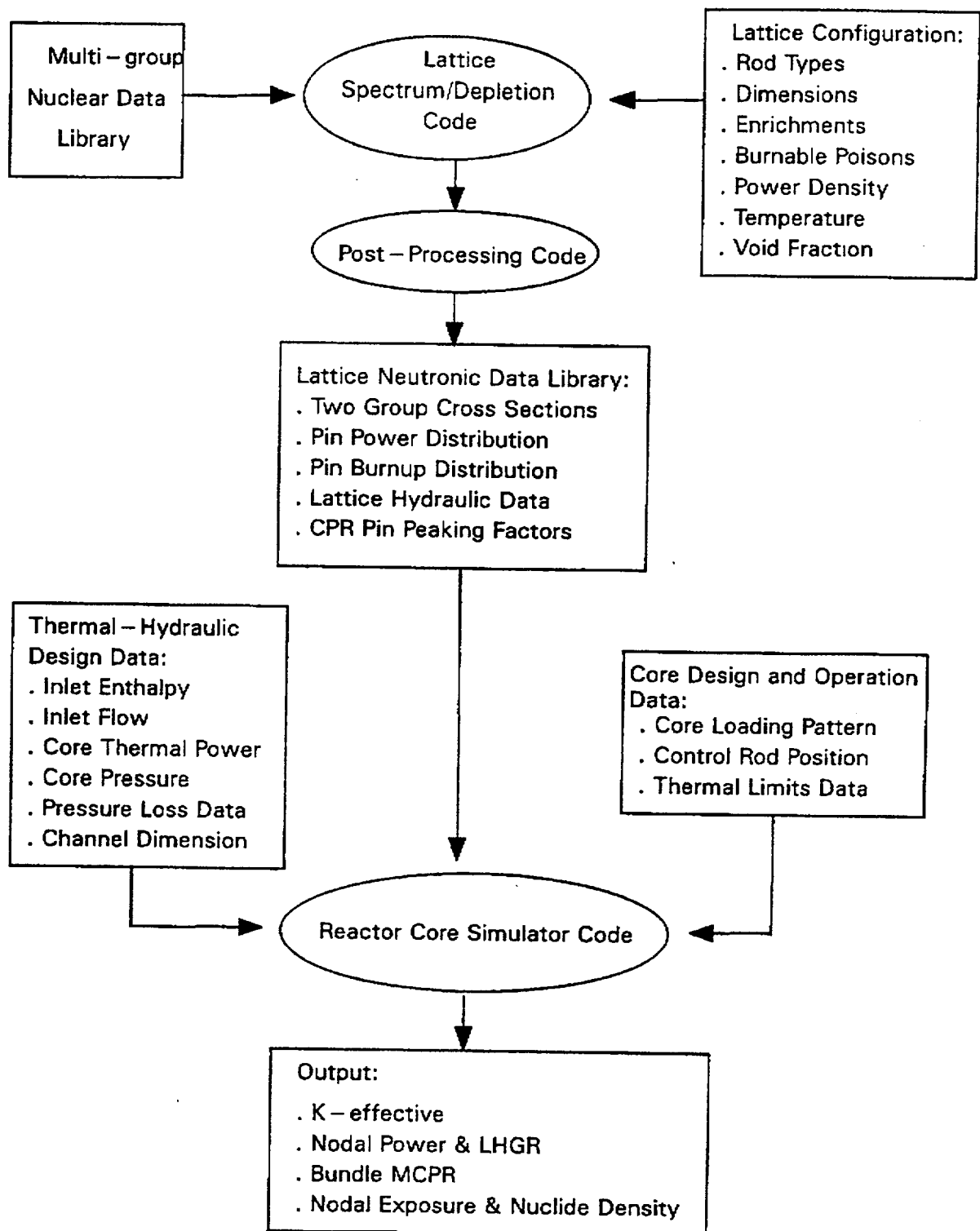


Figure 2.1 SPC Standard BWR Neutronics Calculation Process

Table 2.1 SPC BWR Fuel Lattice Spectrum/Depletion Code Validation Result


Table 2.2 SPC BWR Core Simulator Code Validation Result


**Table 2.3 SPC BWR Core Simulator Code Measured Power Distribution Uncertainty  
Verification**


### 3. Overview

This report first establishes a set of evaluation and validation requirements for assessing a new BWR neutronics design code/code system. The requirements consist of methodology requirements and validation requirements. The methodology requirements are specified in Section 4.0, and briefly describe the required input, modeling, and output capabilities. Requirements associated with the lattice spectrum/depletion code and the core simulator are each addressed. Validation requirements are specified in Section 5.0, and involve comparisons of calculated parameters with measured data. Measured data are available from critical experiments and commercial reactor measurements. Verification of measured power distribution uncertainty is also addressed here.

The evaluation of the CASMO-4/MICROBURN-B2 BWR design code system is presented in Section 6.0. Here the detailed methodology and the input and output features of the new code system are evaluated against the methodology requirements established in Section 4.0. The validation of the new code system is presented in Section 7.0. Benchmark calculations are performed and the results are presented in detail. The validation requirements established in Section 5.0 are applied to assess the acceptability of the benchmark results. The core simulator pin power methodology is validated in Section 8.0. Comparison with CASMO-3/CASMO-4 multi-group heterogeneous transport calculations and with the operating reactor pin gamma scan measurements is presented. The measured power distribution uncertainty of the new code system is determined following the previously approved statistical analysis methodology in Section 9.0.

The impact of the new code system on a typical BWR fuel cycle design is illustrated in Appendix A. Here, the fuel thermal margin parameters predicted by the new code system for a sample fuel cycle are compared to those calculated by the approved design code MICROBURN-B.

## 4. Methodology Requirements

### 4.1 *Lattice Spectrum/Depletion Code Methodology*

#### 4.1.1 Nuclear Data Library

Neutron cross sections for fuel, burnable poison, fission products, and structural components including coolant, fission yield data, and nuclide transmutation constants shall be derived from a nuclear data library and associated processing codes recognized as international standards. Examples of such a library are ENDF/B, JEF, UKNDL, JENDL, and BNL. An example of industry recognized processing codes is the NJOY code (Reference NO TAG).

#### 4.1.2 Lattice Spectrum/Depletion Code

The lattice spectrum/depletion code shall be able to calculate a multi – group neutron spectrum for a heterogeneous medium consisting of various components such as fuel rods, burnable poison rods, water rods/boxes, control rods/blades, metal walls/channels, and a mixture of water and steam and to determine the burnup characteristics of a fuel lattice. The multi – group nuclear data library shall be collapsed into a few group nuclear data suitable for a core simulator code. In detail, the code shall be capable of performing the following tasks:

1. A space – dependent multi – group neutron spectrum can be calculated without any significant pre – homogenization of each component (rigorous treatment of component heterogeneity).
2. Various geometrical configurations of those components can be handled without difficulty in terms of accuracy and input requirement.
3. Nuclides with prominent resonance absorption property can be treated with a well recognized method.
4. The burnup chains of uranium and plutonium can be handled accurately.
5. Explicit modeling of important fission product nuclides can be made.
6. Radial asymmetries can be modeled.
7. Various types of burnable poisons and configurations can be handled.
8. Various types of control rods/blades and configurations can be handled.
9. Modeling of incore instrumentation can be provided.
10. Pin – by – pin power distribution can be calculated.
11. Pin – by – pin exposure and nuclide density distributions can be calculated.

12. Two or four groups of nuclear data can be edited based on the multi-group space-dependent spectrum.
13. A space-dependent multi-group gamma spectrum can be calculated.
14. Heat deposition from fission products, neutron slowdown, and gamma attenuation in various components of a lattice can be generated.

Other features not listed here but generally accepted for lattice calculation should be included.

## 4.2 *Reactor Core Simulator Code*

### 4.2.1 Code Capabilities

The reactor core simulator code shall determine global neutron flux distributions by solving the three-dimensional, two group neutron diffusion equation based on the homogenized lattice nuclear data generated by the lattice spectrum/depletion code described in Section 4.1. An accurate solution of the neutron diffusion equation shall be obtained for a nodalization of the reactor core with assembly size radial and axial meshes. A two-phase thermal-hydraulics model which is capable of calculating nodal coolant flow and density distributions under conditions ranging from cold shutdown to hot operation shall be included. Control blade insertion shall be modeled.

In detail, the following information shall be generated with sufficient accuracy and, if necessary, with conservatism:

- Nodal fast and thermal neutron flux distributions
- Reactor core eigenvalues
- Nodal relative power and LHGR distribution
- Nodal exposure and nuclide distributions
- Nodal coolant density distribution
- Assembly inlet flow distribution
- Assembly pressure drop
- Nodal peak pin LHGR distribution
- Bundle MCPR distribution
- Nodal peak pin exposure distribution
- Neutron or gamma TIP response data
- LPRM response data

In addition to the above, other information necessary for fuel cycle design, startup and operation support, and core monitoring shall be generated.

#### 4.2.2 Compatibility and Consistency with Safety Analysis Methodology

The core simulator code shall be compatible and consistent with the previously approved safety analysis methodology. No degradation of safety margin shall be incurred by a replacement of the core simulator code. Compatibility and consistency shall be maintained with no or a minimum change of the previously approved safety analysis methodology. If significant changes are needed in the safety analysis methodology due to the introduction of a new steady state core simulator code, then the changes shall be evaluated according to the SER requirement of the related safety analysis methodology.

## 5. Validation Requirements

Section 5.1 describes the validation requirements for the lattice spectrum/depletion code. These requirements are mostly based on critical reactor measurements. Validation of a new lattice code shall be performed according to these requirements.

Section 5.2 describes the validation requirements for the core simulator code. The requirements involve comparison of predicted parameter values with measured values from commercially operating BWRs. This validation shall be performed if the lattice spectrum/depletion code or the core simulator code is replaced or modified.

### 5.1 *Critical Experiments and Isotopic Measurements*

The validation of the lattice spectrum/depletion code shall be based on critical experiments, Doppler resonance measurements, and isotopic inventory measurements which are considered to be acceptable measured data within the industry. Examples of critical experiments are KRITZ<sup>(7)</sup> and B&W<sup>(8)</sup>. These experiments provide critical  $k$ -effective and pin-by-pin fission rate measurements. Measured isotopic data from the Yankee Rowe Core I<sup>(9)</sup> provides a well accepted benchmark data base for predicted isotopic inventories.

The critical experiments indicate conditions at which criticality was achieved, i. e., a measured  $k$ -effective of approximately 1.0. The lattice spectrum/depletion code validation shall demonstrate that the predicted  $K$ -effective is within the range of uncertainties previously observed and accepted by the industry and shall not indicate any significant trend with respect to the various conditions considered.

In addition to these measurements, comparisons with results from Monte Carlo simulation codes which are generally accepted by the industry shall be performed for a further validation of the overall methodology of a lattice spectrum/depletion code. An example of an acceptable Monte Carlo code is MCNP.<sup>(10)</sup>

Based on these considerations, the acceptance criteria for validating a new or modified lattice code is defined and provided in Table 5.1. As more measurements become available, these requirements will be augmented.

**Table 5.1 SPC BWR Fuel Lattice Spectrum/Depletion Code Validation Requirement**


**5.2 *Measurements from Commercial Reactors***

**5.2.1 Selection of Reactors**

Diversity of fuel and core loading patterns, operating strategies, and instrumentation system is an important consideration for choosing reactors for benchmark. Fuel loading patterns in the selected reactors shall include available conventional scatter loadings and single rod sequence loadings. Fuel types used in these selected core loadings shall include past and present fuel designs. Symmetric lattice (C-lattice) and/or asymmetric lattice (D-lattice) reactors shall be analyzed depending on availability. Nominal power/flow operation and/or spectral shift operation fuel cycles shall be analyzed depending on availability.

**5.2.2 Hot Operating Condition Measurements**

Steady-state hot operating conditions provide measured power, flow, inlet enthalpy, and control rod pattern. Based on these measured data, core follow calculations shall be performed

for several fuel cycles for the selected reactors. These calculations produce critical  $k$  - effective values which are near 1.0. The variation of critical  $k$  - effectives shall be within the acceptance limit that is established based on previous experience and design uncertainty allowance. Table 5.2 provides the validation requirement for the hot critical  $k$  - effective.

Predictive calculations of nodal TIP distributions shall be performed at cycle exposure points where measured values are available. The measured TIPs shall include available neutron and gamma TIPs. Statistical analysis of TIP comparisons shall be performed. The analysis provides 2 - dimensional (2 - D) radial and 3 - dimensional (3 - D) nodal deviations of the calculated TIPs compared to measured TIPs. These deviations include TIP measurement uncertainty. TIP measurement uncertainty for D - lattice BWRs is typically larger than C - lattice BWRs. For this reason, higher limits are set for TIP deviations in D - lattice BWRs. The 2 - D and 3 - D deviations shall be small and within the acceptance limit which is established based on previous experience and design uncertainty allowance. Table 5.2 provides the validation requirement for calculated TIP distributions.

**Table 5.2 SPC BWR Core Simulator Code Validation Requirement**


### 5.2.3 Cold Shutdown Condition Measurements

The  $k$  – effectives determined by a BWR neutronics design code for critical conditions are an important parameter which determines the predicted shutdown margin. The cold critical  $k$  – effectives determined by a new code system shall be analyzed to confirm that the overall variation of these  $k$  – effectives versus cycle exposure and fuel cycles is within a validation limit. This limit is determined based on previous experience and design uncertainty allowance. The validation requirement for cold critical  $k$  – effectives is provided in Table 5.2.

### 5.2.4 Hot Operating Condition Local Pin Power Measurements

Local pin powers in hot operating fuel bundles are an important safety parameter which has to be monitored to preserve the integrity of fuel cladding. Because pin powers are not directly measurable, monitoring of this parameter should depend on local pin powers calculated by a core simulator. The pin powers used for BWR core design and monitoring have been usually determined assuming an infinite medium condition. This assumption is acceptable because a BWR fuel lattice is separated from its neighbors by relatively large water gaps. However, the core designs employing longer control blade exchange intervals and/or a mixture of UO<sub>2</sub> and MOX bundles need a further consideration. These new designs incur relatively large neutron flux gradients across fuel bundles. A long exposure of a bundle to large neutron flux gradients develop the so – called burnup history effect on local pin powers. The burnup history effect in a BWR is a highly complex phenomenon involving differential effects on local fuel pins as well as integral effects on the entire lattice. Thus the determination of local pin powers in these core designs should be based on an accurate pin power reconstruction method.

Validation of a core simulator pin power method is a costly task. In general, two validation methods could be employed; 1. local pin powers calculated by a core simulator are compared to those calculated by a higher order method (multi – group heterogeneous pin – by – pin transport method) for certain simple geometries representative of real reactor loadings, and 2. core simulator calculated local pin powers are compared to those measured in reactors under hot operating condition. The first method is intended to isolate the neutronic model, to quantify its uncertainty, and to compensate for the lack of real reactor measurements. The second method is intended to consider both neutronic and thermal – hydraulic model and quantify the uncertainty of the entire code system. The second method is very costly and more valuable than the first method but measured data availability is limited.

The real reactor measurement involves measurements of specific fission product isotopic inventories which indirectly reveal fission power distributions in fuel pins immediately before

the measurement. Usually, the La - 140 isotope gamma intensity in each fuel pin is measured. The La - 140 isotope is a short lived daughter of the Ba - 140 fission product isotope. The Ba - 140 isotope is also a relatively short lived so its isotopic concentration is directly proportional to local fission rate before the measurement. Two such measurements are available for the validation of CASMO - 4/MICROBURN - B2 code system. These are the Quad Cities Unit 1 Cycle 2 and Cycle 3 pin gamma scan measurements (Reference NO TAG) and the KWU - S pin gamma scan measurement (Reference NO TAG and NO TAG). The validation requirement on local pin powers is provided in Table 5.3.

### 5.3 *Verification of Measured Power Distribution Uncertainty*

The measured power distribution uncertainty needs to be verified if the new core simulator is used in the POWERPLEX® core monitoring software system (CMSS) or the new lattice code is used to generate input data for POWERPLEX® CMSS. The measured nodal and bundle power distributions are determined by POWERPLEX® CMSS based on measured LPRM signals and calculated nodal power distributions. The determination of nodal and bundle power distributions by POWERPLEX® CMSS is described in detail in Reference 5 (XN - NF - 80 - 19(A), Volume 1, "Advanced Nuclear Fuels Methodology for Boiling Water Reactors"). The measured power distribution determined by POWERPLEX® CMSS contains uncertainties originated from the LPRM measurement and the transformation of measured LPRM signals into measured power distribution. The uncertainty analysis and the limiting uncertainty values presented in Reference NO TAG were approved for application to reload licensing calculations. The purpose for verifying the measured power distribution uncertainty is to confirm that the replacement of the existing core simulator code with the new core simulator code in POWERPLEX® CMSS shall not degrade the core monitoring capability.

The measured power distribution is determined by combining four components which are measured [LPRM signals, synthesized TIP signals, predicted TIP signals, and calculated power distributions]. It is required that the four individual uncertainties and the combined measured power distribution uncertainty generated by the new neutronics design methodology be less than the limit specified in Table 5.3. The limits in this table were determined based on previously approved uncertainties for SPC BWR neutronics methodology.

Measured parameters are utilized to determine uncertainties in the four components of a measured power distribution. These parameters are measured pin power distribution, measured bundle power distribution, and measured TIP distribution. Measured pin power distributions are available from the Quad Cities Unit 1 Cycle 2 through Cycle 3 pin gamma scan measurements and the KWU - S pin gamma scan measurement. Measured TIP distributions

are available from normal operation monitoring data for selected BWRs. Measured bundle power distributions are available from the Quad Cities Unit 1 Cycle 2 and Cycle 4 bundle gamma scan measurements

**Table 5.3 SPC BWR Core Simulator Code Measured Power Distribution Uncertainty Limit**


## 6. Evaluation of CASMO-4/MICROBURN-B2 Methodology

### 6.1 CASMO - 4 Lattice Spectrum/Depletion Code Methodology

The lattice spectrum/depletion code system consists of a 40/70 energy group nuclear data library and the CASMO - 4 code. This code system was originally developed by Studsvik and has been adopted by many nuclear plant operators. Due to its widespread use, the code is well benchmarked and proven for commercial BWR application.

CASMO - 4 selects either a 40 or a 70 group nuclear data library depending on the complexity of a given problem. The data in this library comes primarily from ENDF/B - IV. Whenever necessary to improve accuracy, some data were taken from ENDF/B - III, ENDF/B - V, and other international standard libraries such as JEF - 1, JEF - 2.1, and BNL - 84. In particular, main gadolinia isotopes data were processed from JEF - 2.1. The detailed composition of this library is described in Reference NO TAG.

The CASMO - 4 code is capable of generating heterogeneous medium multi - group neutron spectrum and calculating burnup chain equation solutions for heavy nuclides, fission product nuclides, and burnable poison nuclides in each fuel pin. CASMO - 4 uses deterministic transport methods. At the pin cell level, it exclusively uses collision probability method to collapse the 40/70 group nuclear data into multi - group data. At the lattice level, it uses a characteristics method for the neutron transport equation solution. One improvement of CASMO - 4 compared to its predecessor CASMO - 3 is that CASMO - 4 does not need to perform any pin cell spatial homogenization to perform a 2 - D lattice - wide transport calculation. This capability is important for dealing with burnable poison rods with high gadolinia concentration. CASMO - 4 has been extensively benchmarked and is widely accepted for neutronics design of light water reactors. The primary use of CASMO - 4 within the SPC neutronic method is to determine two group homogenized microscopic and macroscopic cross section data as well as pin power and burnup distributions for fuel lattices. The detailed methodology of CASMO - 4 is found in Reference NO TAG.

The CASMO - 4 lattice spectrum/depletion code satisfies the methodology requirements set forth in Section 4 of this report.

### 6.2 Core Simulator Code Methodology

The core simulator code system consists of an interface code called MICRO - B2 and the MICROBURN - B2 code. The MICRO - B2 code formats lattice nuclear data generated by CASMO - 4 for MICROBURN - B2.

The MICROBURN-B2 code is an improved version of the MICROBURN-B core simulator which has been approved for use since 1990. MICROBURN-B2 solves a two group neutron diffusion equation based on an interface current method, calculates the burnup chain equation solutions for heavy nuclides and burnable poison nuclides, determines nodal power, bundle flow, and void distributions, and determines pin power distributions and thermal margins to technical specification limits. MICROBURN-B2 has several advanced features such as the advanced nodal expansion method solution of diffusion equation, nodal burnup and spectral history gradient model, and a pin power reconstruction model. These features enable MICROBURN-B2 to obtain more accurate nodal and pin power distributions. The detailed methodology is provided in Reference NO TAG.

In addition to the internal SPC review of the methodology, neutronics models contained in MICROBURN-B2 have been published for reviews by industry peers. Examples of such publications are provided in Reference NO TAG and NO TAG. Recently the CASMO-3/MICROBURN-B2 methodology was reviewed and accepted by the German licensing authority (TUV) for [ ]

The MICRO-B2/MICROBURN-B2 core simulator code system satisfies the methodology requirements set forth in Section 4.

### 6.3 *Compatibility and Consistency with Safety Analysis Methodology*

No change in the approved safety analysis methodology of SPC has been identified as necessary for the application of MICROBURN-B2 to BWR core designs. MICROBURN-B2 is compatible with the approved safety analysis codes and consistent with the approved neutronic safety analysis methodologies of SPC provided in Reference 5.

A sample comparison of neutronic input to transient analyses is provided in Table 6.1. Here major neutronic input parameters for a transient analysis are compared for various power/flow conditions between the new code system and the currently approved code system. There are only minor differences in most of the input parameters except for the void reactivity coefficient. The new data (CASMO-4/MICROBURN-B2) are about [10-20 % less negative] than the current data (CASMO-3/MICROBURN-B). The new data is considered to be more accurate because of the improved nature of the new code system. The new neutronics input data is collectively validated through comparison to core follow measurements, reactor transient measurements, and BWR stability decay ratio measurements. The core follow measurements provide various power/flow point criticality and TIP data. Comparison of the predicted critical  $k$ -effectives and TIPs with measured data

at different power/flow conditions provides evidence that the base neutronic data and models supporting reactivity coefficients are accurate. Such a comparison is provided in Section 7.0 of this report. Comparisons to reactor transient measurements and stability decay ratio measurements provide evidence that the neutronic input to the transient safety analysis codes is compatible with the approved transient methodology.

**Table 6.1 Sample Comparison of Neutronics Input Data for BWR Transient Analysis**

┌

└

## 7. Validation of CASMO-4/MICROBURN-B2 Methodology

### 7.1 *Critical Experiments and Isotopic Measurements*

CASMO-4 was validated against available critical experiments including KRITZ measurements and B&W experiments. Most of the critical cores analyzed were operated at room temperature (290 – 300 °K) but several of the KRITZ cores were also measured at higher temperatures close to operating conditions (500 – 520 °K). The boron concentration varied from 0 to 1670 ppm and the fuel enrichment varied from 1.3 to 3.0 %. The KRITZ experiments covered several core types: KRITZ-1 and KRITZ-2 are regular pin cell cores, KRITZ-3 contains PWR lattices and KRITZ-4 contains BWR assemblies. The B&W experimental cores were made up of 3x3 PWR assemblies with 2.46 % enrichment. Five cores were selected and all measurements were made at room temperature.

Additional description of critical measurements and detailed results of validation are presented in Reference NO TAG. For all calculated critical cores (37 cases) CASMO-4 predicted  $k_{eff} = 1.00032 + 0.000123$ . Two PWR and six BWR fission rate distribution measurements were analyzed. The experimental uncertainty in each pin is about 1 % and the RMS difference between calculations and measurements is also 1 %. No trends were found for fission rates in pins around small or large water holes, along water gaps, in corner locations, around absorbers, or in the gadolinia rods.

CASMO-4 calculated fission rate distributions were compared with those calculated by the MCNP Monte Carlo code. Included in this comparison are several BWR bundles of modern designs:

1. SIEMENS Design: 8x8, 9x9, ATRIUM-9, ATRIUM-10, and ATRIUM-10 MOX
2. ABB-Atom Design: 8x8, SVEA-63, SVEA-64, SVEA-96, SVEA-100, and SVEA-96 MOX
3. GE Design: GE6, GE7, GE8, GE9, GE10, GE11, GE12, and GE 7x7 Pu Island

Comparisons were made for four different moderator density conditions: cold, zero void, 40 % void, and 80 % void. The overall RMS deviation of CASMO-4 predictions compared to MCNP reference results was 1 %. There was no noticeable trend versus the moderator density, and the bundle design. MOX bundles showed the same magnitude of deviation as the UO2 bundles. Control rod worths and gadolinia rod worths showed a maximum deviation of less than 3.0 %. A detailed description of this benchmark is presented in Reference NO TAG.

The Yankee Rowe Core I isotopic data measurement was analyzed with CASMO - 4. Isotopic data from 173 asymptotic spectrum measurements were compared with calculated U - 235, U - 236, Pu - 239, Pu - 240, Pu - 241, and Pu - 242 atom percents as well as the ratios of Pu - 239/U - 238, Pu - 239/Pu - 240, Pu - 240/Pu - 241, and Pu - 241/Pu - 242. The CASMO - 4 isotopic data was found to agree extremely well with the measured data, which verifies the isotopic inventories from the CASMO - 4 depletion calculation. A detailed description of this benchmark is presented in Reference NO TAG.

**7.2 Validation against Commercial Reactors**

Six commercial BWRs were selected for validating the CASMO - 4/MICROBURN - B2 code system. These are BWR - A, BWR - B, BWR - C, BWR - D, BWR - E, and KWU - S. Except for KWU - S, all reactors were monitored with neutron TIPs (Traversing Incore Probes). KWU - S was monitored with gamma TIPs. BWR - C and BWR - D are D - lattice (asymmetric water gap) reactors and the remaining reactors are C - lattice (symmetric water gap) reactors. Table 7.1 provides pertinent information about these reactors.

**Table 7.1 Selection of Commercial BWRs for Benchmark Analysis**


Core follow calculations are performed for these reactors over a total of [ ] fuel cycles. These calculations are based on measured critical core conditions (control rod pattern, power, flow,

core inlet enthalpy, and cycle exposure) at or nearly at equilibrium xenon condition. The  $k$ -effectives calculated for these conditions are called hot operating condition critical  $k$ -effectives, which are an important parameter for measuring the accuracy of a BWR core neutronics method. TIP distributions are generated at state points where measured TIP data are available. Occasionally, reactor startup measurements yield cold critical conditions. The  $k$ -effectives calculated for these conditions are called cold critical  $k$ -effectives, which are an important parameter for determining reactor shutdown margin. The zero power cold critical cores are analyzed using measured conditions which include core temperatures, control rod patterns, and xenon transient data. The short-lived fission product (Xe-135 and Sm-149) decay/buildup and the transmutation of Np-239 to Pu-239 are modeled based on the measured shutdown cooling time. Transmutation of other pertinent actinide nuclides were also modeled in the same manner.

### 7.2.1 Hot Operating Condition Critical K-effectives

BWRs operate at varying power/flow conditions, which affect in feedback the neutronic response of the fuel bundle. Due to the inherent uncertainty of measured critical conditions and that of the reactor physics code system, the critical  $k$ -effectives determined by a core simulator are usually scattered around the mathematical criticality ( $k$ -effective = 1). For this reason, a typical BWR core design and monitoring relies on target  $k$ -effectives rather than the mathematical criticality. A great deal of information about the performance of a core simulator is obtained by combining all of the important parameters affecting the calculated critical  $k$ -effectives. Thus the presentation in this section will show the measured core power/flow, and inlet subcooling trends, and the calculated core void fraction, pressure drop, and axial power/exposure tilts for all of the fuel cycles modeled. This is followed by a plot of calculated critical  $k$ -effectives versus cycle exposure and a table showing cycle average critical  $k$ -effective and its scattering (standard deviation).

The seven cycles (Cycle 1 to 7) of BWR - A are presented in Figure 7.1 through Figure 7.3 and in Table 7.2. The core power level is almost constant at or near 100 % of the rated power. The core flow varies depending on each cycle exposure, usually staying at 80 - 90 % level from BOC through MOC and increasing to 100 % level toward EOC. In general,  $k$ -effectives vary within [ ] to [ ] increasing from BOC to EOC. There is a consistency in trend for all the cycles. The overall cycle average  $k$ -effectives range from [ ] to [ ], which means the cycle-to-cycle variation of hot critical  $k$ -effectives is small. The maximum in-cycle scattering for a given cycle is [ ].

The nine cycles (Cycle 1 to 9) of BWR - B are presented in Figure 7.8 through Figure 7.10 and in Table 7.4. The core power level is almost constant at or near 100 % of the rated power.

The core flow variation within each cycle is relatively small except for Cycle 9. The reactor went through a power uprate at BOC 8 but kept on using the original rated power and flow as reference values. Thus Cycle 8 and Cycle 9 power/flow plot shows that the reactor operated at or above the original rated condition. In general,  $k$ -effectives vary within [ ] to [ ] increasing from BOC to EOC. There is a consistency in trend for all the cycles. The overall cycle average  $k$ -effectives range from [ ] to [ ], which means the cycle-to-cycle variation of hot critical  $k$ -effectives is small. The maximum in-cycle scattering for a given cycle is [ ].

The eight cycles (Cycle 8 to 15) of BWR-C are presented in Figure 7.15 through Figure 7.17 and in Table 7.6. The core power level shows a large swing in a relatively short time period as this reactor is operated in a load follow maneuver. The core flow variation shows a similarly large swing. Despite this large variation in core conditions, the critical  $k$ -effective range is within [ ] to [ ]. There is a consistency in trend for all the cycles. The overall cycle average  $k$ -effectives are found between [ ] to [ ]. The maximum cycle-to-cycle variation of the cycle average  $k$ -effective is [ ]. The maximum in-cycle scattering for a given cycle is [ ].

The four cycles (Cycle 1 to 4) of BWR-D are presented in Figure 7.22 through Figure 7.24, and in Table 7.8. The core power level shows a large swing as this reactor goes through several mid-cycle shutdowns and low power operations. The core flow variation shows a similarly large swing. The core follow calculation state points contain transient xenon points which were assumed to be equilibrium xenon points due to the lack of fine time step measured transient state points. Despite this deficiency in measured core conditions, the critical  $k$ -effective range is within [ ] to [ ]. The overall cycle average  $k$ -effectives are found between [ ] to [ ]. The validation criteria set forth in Section 5.2.2 exclude transient state points from the statistical analysis. Thus the maximum cycle-to-cycle variation of the cycle average  $k$ -effective ([ ]) and the maximum in-cycle scattering for a given cycle ([ ]) will not be considered for the overall statistical result although they are within the acceptance limits.

The thirteen cycles (Cycle 1 to 13) of KWU-S are presented in Figure 7.28 through Figure 7.30 and in Table 7.9. The core power level is almost constant at or near 100 % of the rated power until near EOC. The reactor was operated in a long coastdown mode near EOC. Thus the core power decreases gradually to near 80 % of rated and the core flow increases to above 100 % of rated. In general,  $k$ -effectives vary within [ ] to [ ] except for a few xenon transient state points, the lowest occurring at BOC 1 and staying nearly constant over each cycle. There is a consistency in trend for all the cycles. The overall cycle average  $k$ -effectives are between [ ] to [ ], which means the

cycle-to-cycle variation is small. The maximum in-cycle scattering for a given cycle is [ ].

The twelve cycles (Cycle 1 to 12) of BWR-E are presented in Figure 7.35 through Figure 7.37 and in Table 7.11. The core power level is almost constant at or near 100 % of the rated power. The reactor was operated in a spectral shift mode, so the core flow is lower than rated flow (nearly 80 %) until near EOC at which point the core flow creeps up to near 100 % of rated. In general, k-effectives vary within [ ] to [ ]. There is a consistency in trend for all the cycles. The overall cycle average k-effectives are between [ ] and [ ], which means the cycle-to-cycle variation is small. The maximum in-cycle scattering for a given cycle is [ ].

In summary, six BWRs with a combined [ ] fuel cycles were benchmarked to verify the hot critical k-effectives calculated by the CASMO-4/MICROBURN-B2 code system. The maximum cycle-to-cycle change of the cycle average k-effectives is [ ] and the maximum in-cycle scattering of k-effectives for a given cycle is [ ]. Thus the quality of the new code system satisfies the validation requirement set forth in Section 5.2.2.

### 7.2.2 Cold Critical K-effectives

A total of [ ] criticals were analyzed for BWR-A. The result of analysis is presented in Figure 7.4 and Table 7.3. The k-effectives vary between [ ] and [ ] showing a slight decreasing trend as a function of cycle exposure. The BOC average k-effectives are found within the band of [ ] and [ ] with a maximum cycle-to-cycle change of [ ]. The maximum within-cycle scattering of BOC k-effectives is [ ].

A total of [ ] criticals were analyzed for BWR-B. The result of analysis is presented in Figure 7.11 and Table 7.5. The k-effectives vary between [ ] and [ ] showing a slight decreasing trend as a function of cycle exposure. The BOC average k-effectives are found within the band of [ ] and [ ] with a maximum cycle-to-cycle change of [ ]. The maximum within-cycle scattering of BOC k-effectives is [ ].

A total of [ ] criticals were analyzed for BWR-C. The result of analysis is presented in Figure 7.18 and Table 7.7. The k-effectives vary between [ ] and [ ]. The BOC average k-effectives are found within the band of [ ]

and [ ] with a maximum cycle-to-cycle change of [ ]. The maximum within-cycle scattering of BOC k-effectives is [ ].

A total of [ ] critical cores at BOC of Cycle 9 to 13 were analyzed for KWU-S. These critical cores were local criticals where a part of the core drives the whole core to the criticality. The result of analysis is presented in Figure 7.31 and Table 7.10. The k-effectives vary between [ ] and [ ]. The BOC average k-effectives are found within the band of [ ] and [ ] with a maximum cycle-to-cycle change of [ ]. The maximum within-cycle scattering of BOC k-effectives is [ ].

A total of [ ] criticals were analyzed for BWR-E. The result of analysis is presented in Figure 7.38 and Table 7.12. The k-effectives vary between [ ] and [ ]. The BOC average k-effectives are found within the band of [ ] and [ ] with a maximum cycle-to-cycle change of [ ]. The maximum within-cycle scattering of BOC k-effectives is [ ].

In summary, a total of [ ] critical cores were benchmarked. The critical k-effectives range from [ ] to [ ] with a maximum within-cycle BOC k-effective scattering of [ ]. The maximum cycle-to-cycle change in BOC average k-effectives is less than [ ]. This result satisfies the validation requirement set forth in Section 5.2.3.

### 7.2.3 Detector Reaction Rate Comparison

Calculated TIPs were compared to measured TIPs for selected BWRs. For each measurement, TIP data plots were generated and inspected to verify the agreement between predicted and measured TIPs. A statistical analysis was performed and 2-D and 3-D relative standard deviations (STDs) between calculated and measured TIPs were determined.

A total of [ ] TIP measurements were analyzed for BWR-A Cycle 2 through Cycle 7. The 2-D radial, 3-D nodal, and 3-D planar relative STDs between the predicted TIP distributions and the measured TIP distributions and their frequency distributions are presented in Figure 7.5 through Figure 7.7. These figures also show the measured TIP asymmetry STDs. [

] The frequency distribution of relative differences between predicted TIPs and measured TIPs shows a near normal distribution.

A total of [ ] TIP measurements were analyzed for BWR – B Cycle 2 through Cycle 9. The 2 – D radial, 3 – D nodal, and 3 – D planar relative STDs between the predicted TIP distributions and the measured TIP distributions and their frequency distributions are presented in Figure 7.12 through Figure 7.14. These figures also show the measured TIP asymmetry STDs. [

] The frequency distribution of relative differences between predicted TIPs and measured TIPs shows a near normal distribution.

A total of [ ] TIP measurements were analyzed for BWR – C Cycle 8 through Cycle 15. The 2 – D radial, 3 – D nodal, and 3 – D planar relative STDs between the predicted TIP distributions and the measured TIP distributions and their frequency distributions are presented in Figure 7.19 through Figure 7.21. These figures also show the measured TIP asymmetry STDs. [

] The frequency distribution of relative differences between predicted TIPs and measured TIPs shows a near normal distribution.

A total of [ ] TIP measurements were analyzed for BWR – D Cycle 1 through Cycle 3. The 2 – D radial, 3 – D nodal, and 3 – D planar relative STDs between the predicted TIP distributions and the measured TIP distributions and their frequency distributions are presented in Figure 7.25 through Figure 7.27. These figures also show the measured TIP asymmetry STDs. [

] Due to this reason, the 2 – D frequency distribution of relative differences shows a slight abnormality.

A total of [ ] TIP measurements were analyzed for KWU – S Cycle 9 through Cycle 13. The 2 – D radial, 3 – D nodal, and 3 – D planar relative STDs between the predicted TIP distributions and the measured TIP distributions and their frequency distributions are presented in Figure 7.32 through Figure 7.33. These figures also show the measured TIP asymmetry STDs. [

] The relatively small calculated TIP uncertainty for this reactor is typical of a gamma TIP system. The frequency distribution of relative

differences between predicted TIPs and measured TIPs shows a center peaked distribution. This is due to the excellent agreement between predicted and measured TIP distributions.

A total of [ ] TIP measurements were analyzed for BWR – E Cycle 9 through Cycle 13. The 2 – D radial, 3 – D nodal, and 3 – D planar relative STDs between the predicted TIP distributions and the measured TIP distributions and their frequency distributions are presented in Figure 7.39 through Figure 7.41. These figures also show the measured TIP asymmetry STDs. [

] The frequency distribution of relative differences between predicted TIPs and measured TIPs shows a near normal distribution.

In summary, the verification of MICROBURN – B2 predicted TIPs considered a total of [ ] full core TIP measurements; [ ] measurements for C – lattice and [ ] measurements for D – lattice. The overall 2 – D TIP STD including measurement uncertainty is [

] The overall 3 – D TIP STD including measurement uncertainty is [

] Thus the validation requirement set forth in Table 5.2 of Section 5.2.2 is satisfied.

### 7.3 *Independent Validation of MICROBURN – B2 Methodology*

Validation of the MICROBURN – B2 methodology was made by KWU for European BWRs. For example, Reference NO TAG describes the validation of the CASMO – 3/MICROBURN – B2 code system using measured data from KWU – K, KWU – S and KWU – C BWRs located in Germany. The core design and operation characteristics of these BWRs are similar to those of domestic BWRs. All three of these BWRs use gamma TIPs for periodic in – core measurements. KWU – S and KWU – C BWRs had several MOX bundles loaded in their late and current cycles. These reactors provide an additional variation in the validation basis for the MICROBURN – B2 core simulator. The German licensing authority (TUV) for the KWU – S BWR determined the CASMO – 3/MICROBURN – B2 code system acceptable for designing UO2 and MOX cores.

For the above three BWRs, the in – cycle 1 $\sigma$  scattering of hot critical k – effectives was of 1 to 3 mk. Many of the cold critical measurements in these BWRs were done for local critical conditions. The cycle exposure dependency and the cycle – to – cycle variation of cold critical

k – effectives were similar to the global criticals measured in domestic BWRs. There was no discrepancy between local criticals and global criticals. The TIP 2 – D relative standard deviation was of 2 – 4 % and the TIP 3 – D relative standard deviation was of 3 – 5 %. One noticeable observation was that TIPs calculated using MICROBURN – B2 for the MOX bundle locations showed an agreement with measured TIP data as good as for UO2 bundle locations.

#### **7.4 Summary of CASMO – 3/MICROBURN – B2 Validation**

Critical experiments and isotopic measurements were analyzed to validate CASMO – 4. The analysis indicates that the CASMO – 4 lattice spectrum/depletion code provides a level of accuracy acceptable for SPC BWR fuel bundle and core design. Six operating BWRs were chosen to validate the CASMO – 4/MICROBURN – B2 code system. Hot operating condition critical k – effectives, TIP measurements, and cold critical measurements were analyzed for a combined total of [ ] fuel cycles. These fuel cycles were loaded with various types of fuel mechanical designs from different vendors. The results of analysis indicate that the CASMO – 4/MICROBURN – B2 code system provides accurate predictions of important core physics parameters examined. The level of predictive accuracy is independent of core loading patterns, fuel assembly types, and core operating modes. In summary, the CASMO – 4/MICROBURN – B2 code system satisfies the validation requirements set forth in Section 5.0.

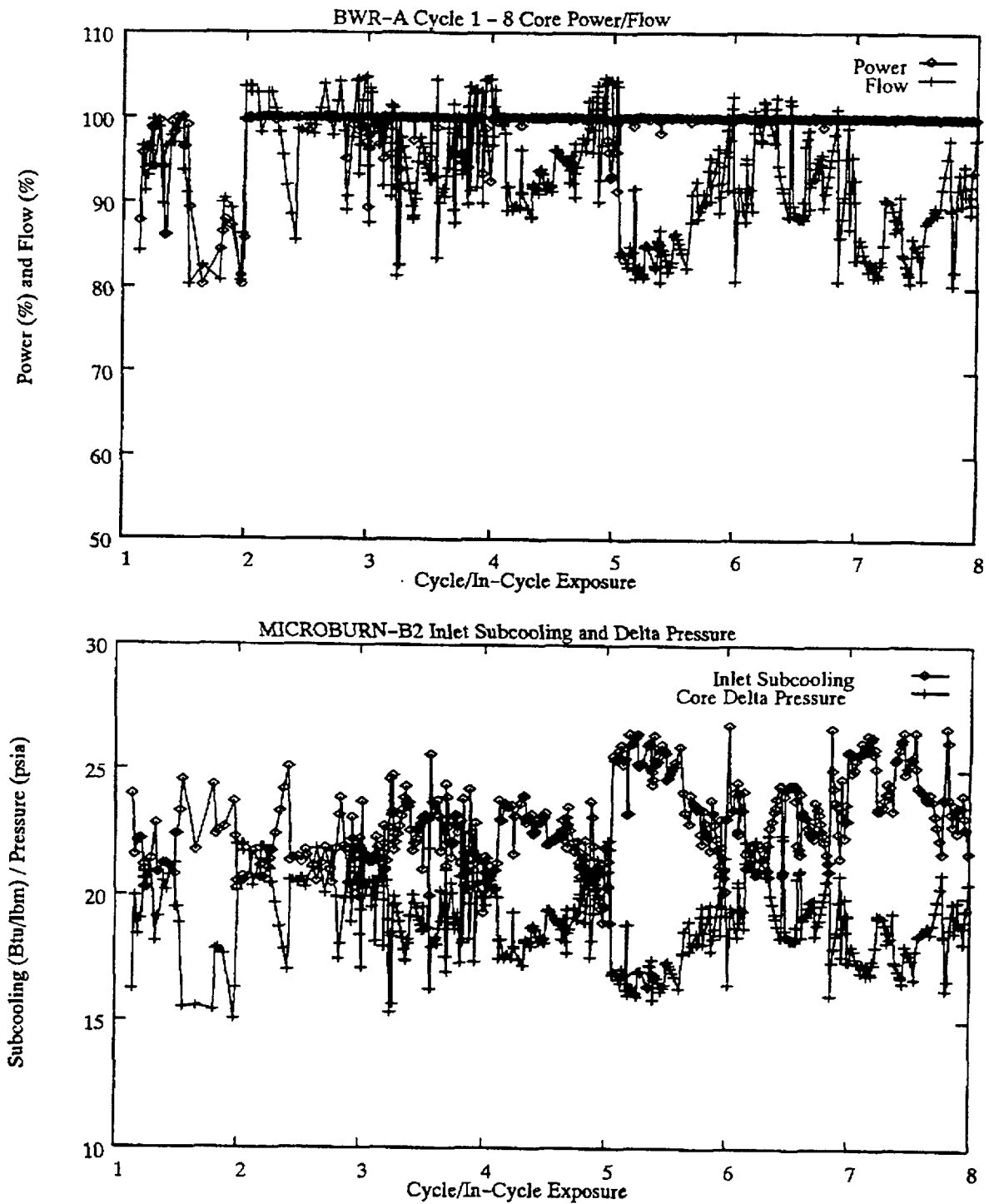


Figure 7.1 BWR - A Core Power/Flow and Inlet Subcooling/Core Pressure Drop Trend

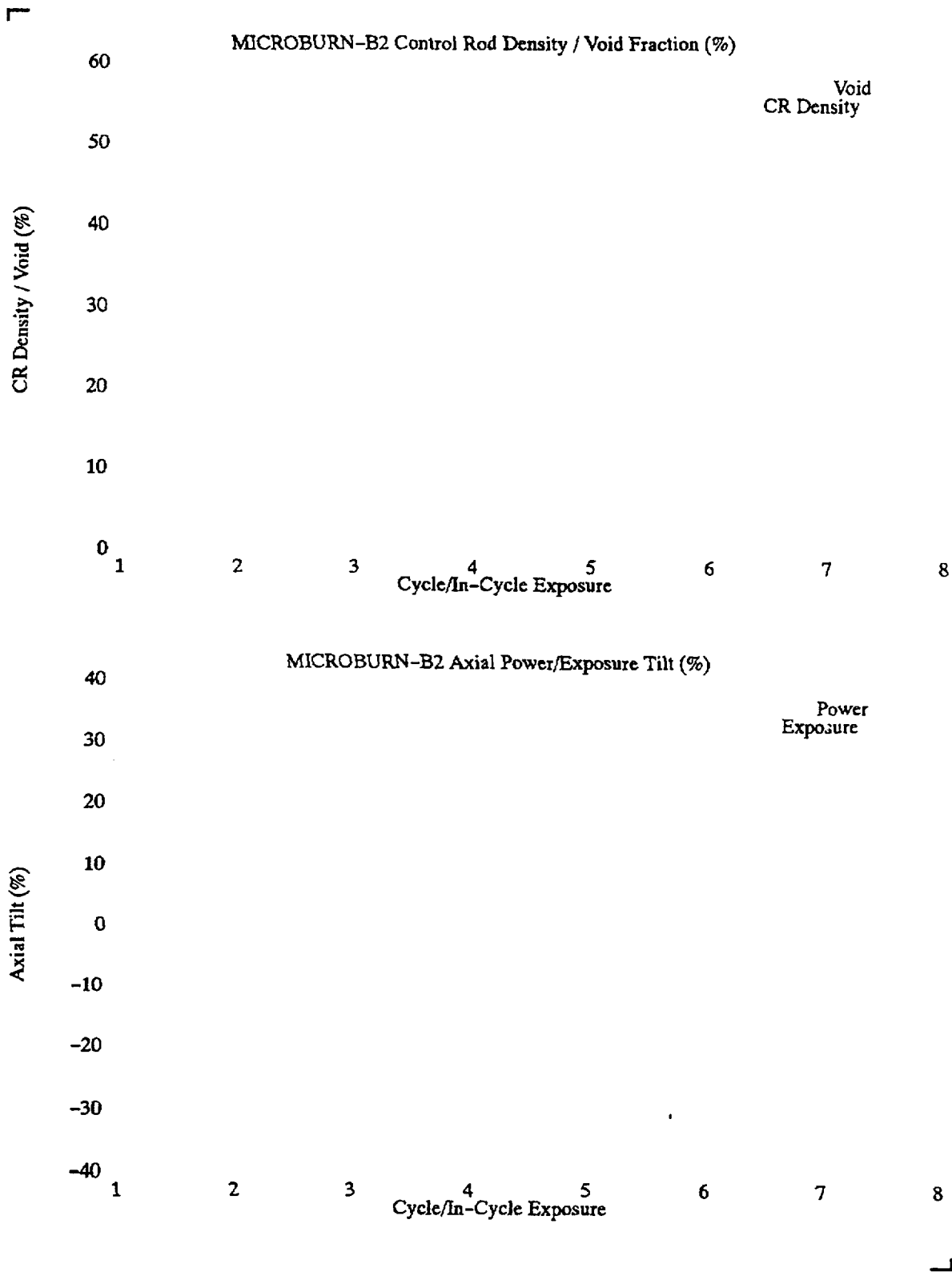


Figure 7.2 BWR – A Core Void/Control Density, and Axial Power/Exposure Tilt Trend

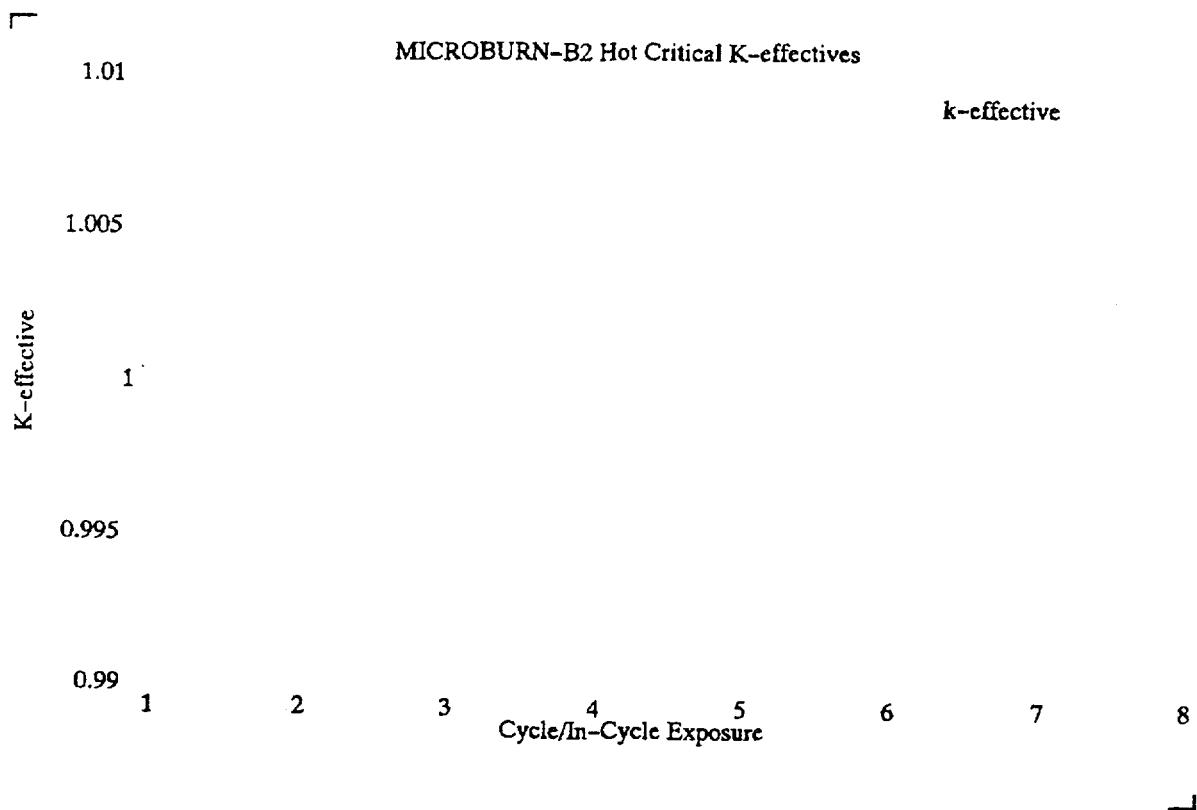


Figure 7.3 BWR – A Hot Critical K – effective Trend

Table 7.2 BWR – A Cycle Average Hot Critical K – effectives

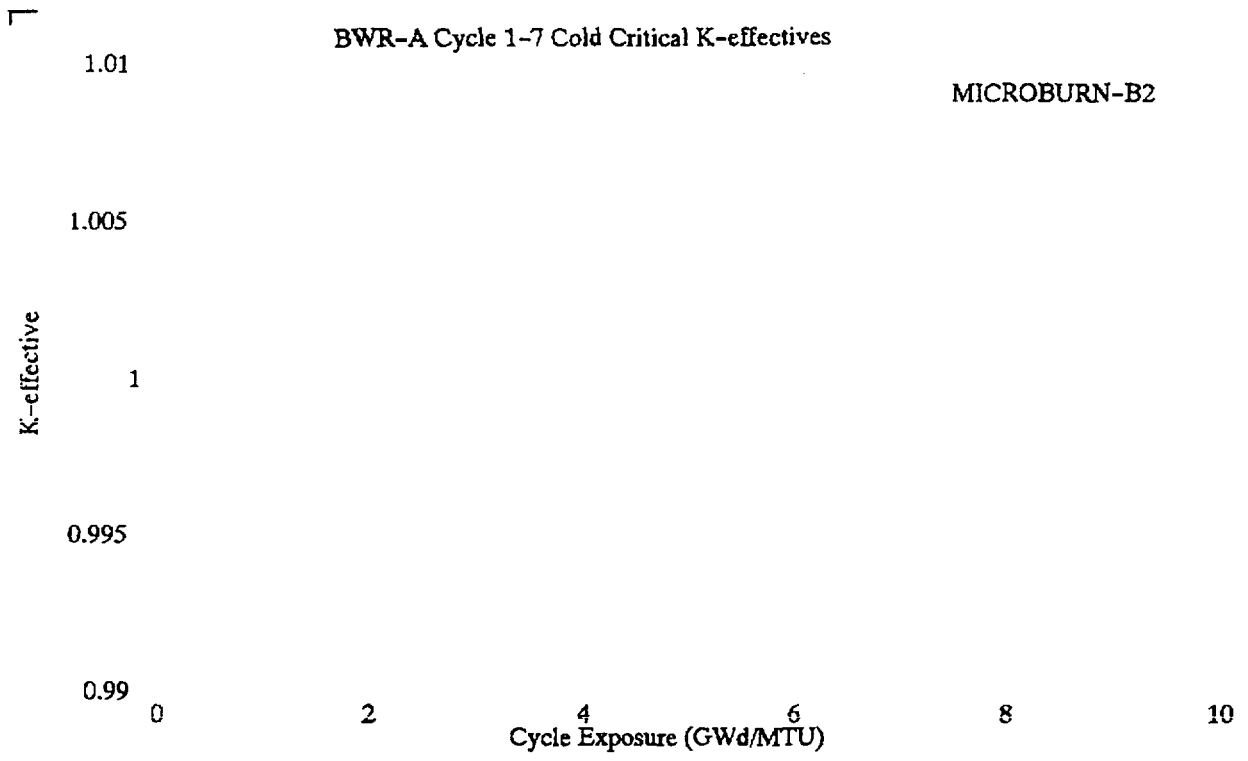



Figure 7.4 BWR – A Cycle 1 to 7 Cold Critical K – effective Trend

Table 7.3 BWR – A Beginning of Cycle Average Cold Critical K – effectives

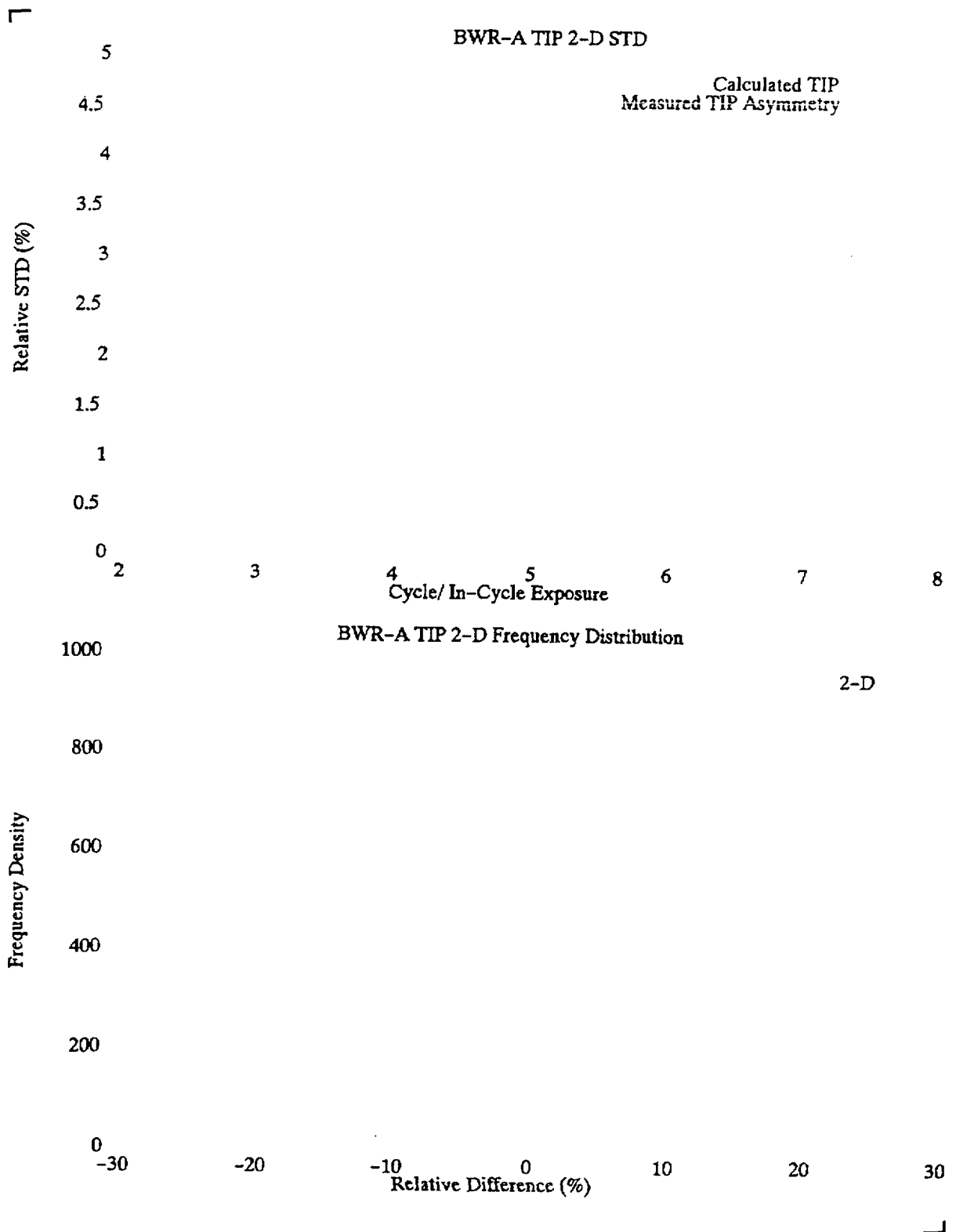
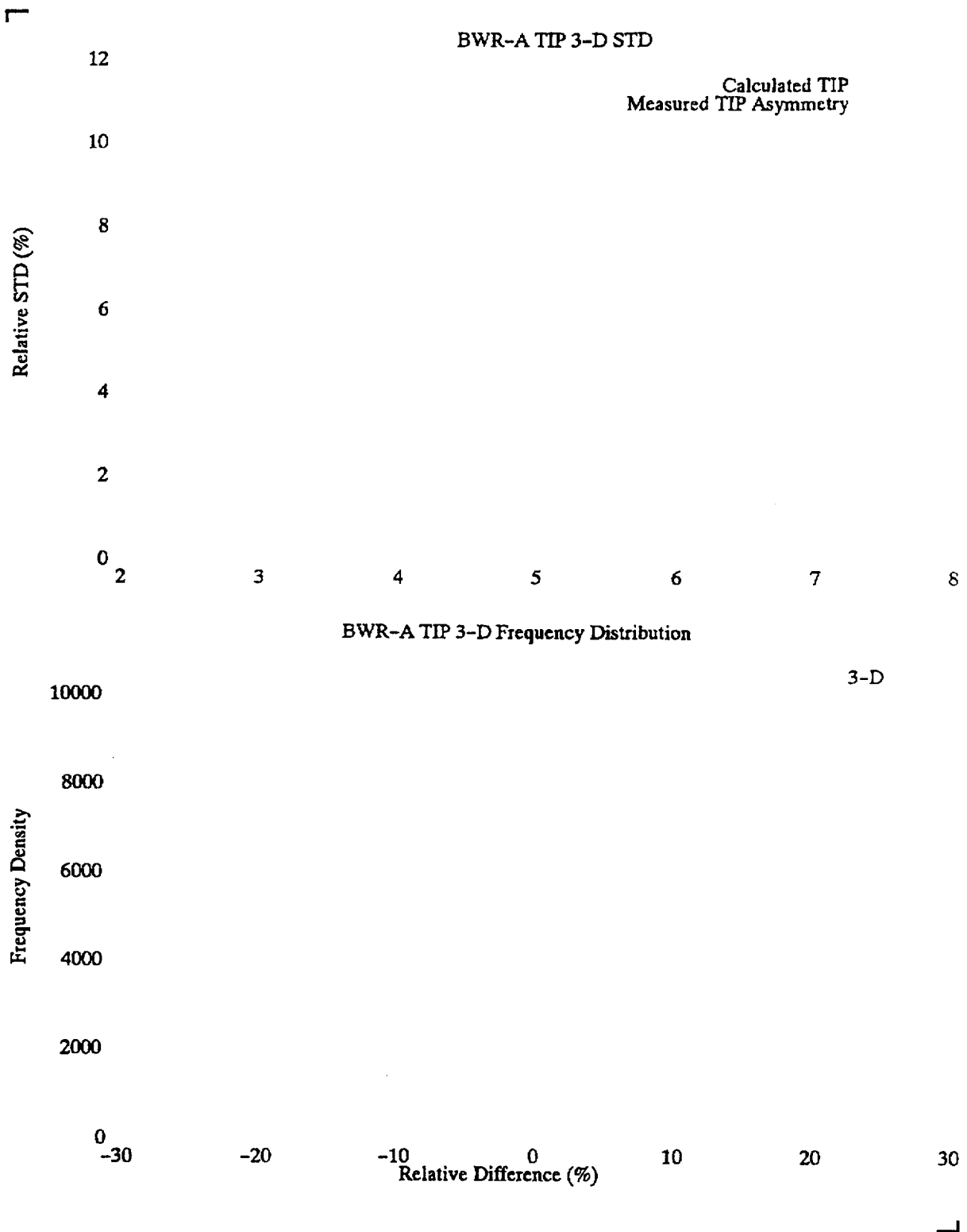
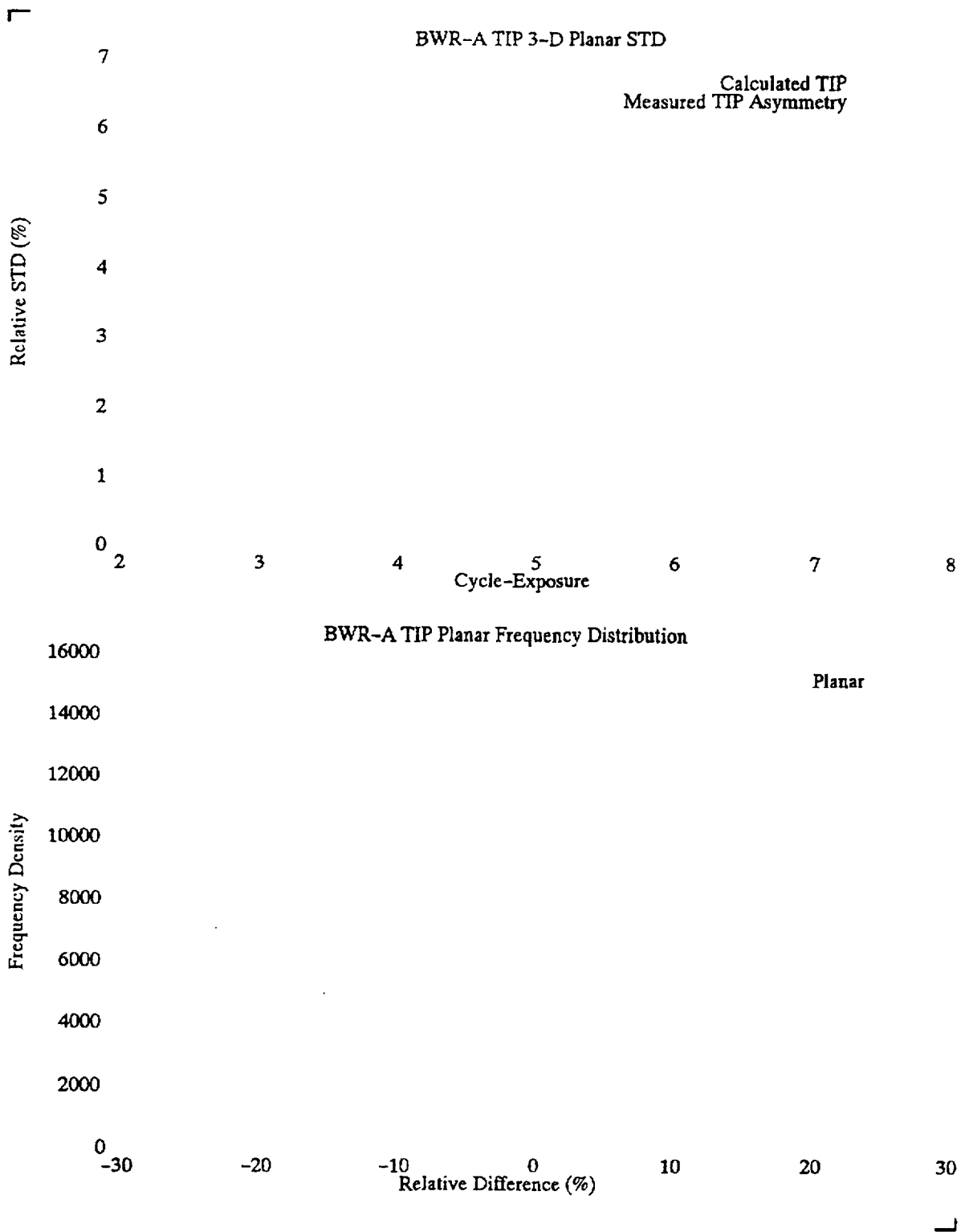



Figure 7.5 BWR – A TIP 2 – D Radial Relative Standard Deviations and Frequency Distribution of Relative Differences



**Figure 7.6 BWR – A TIP 3 – D Nodal Relative Standard Deviations and Frequency Distribution of Relative Differences**



**Figure 7.7 BWR – A TIP 3 – D Planar Relative Standard Deviations and Frequency Distribution of Relative Differences**

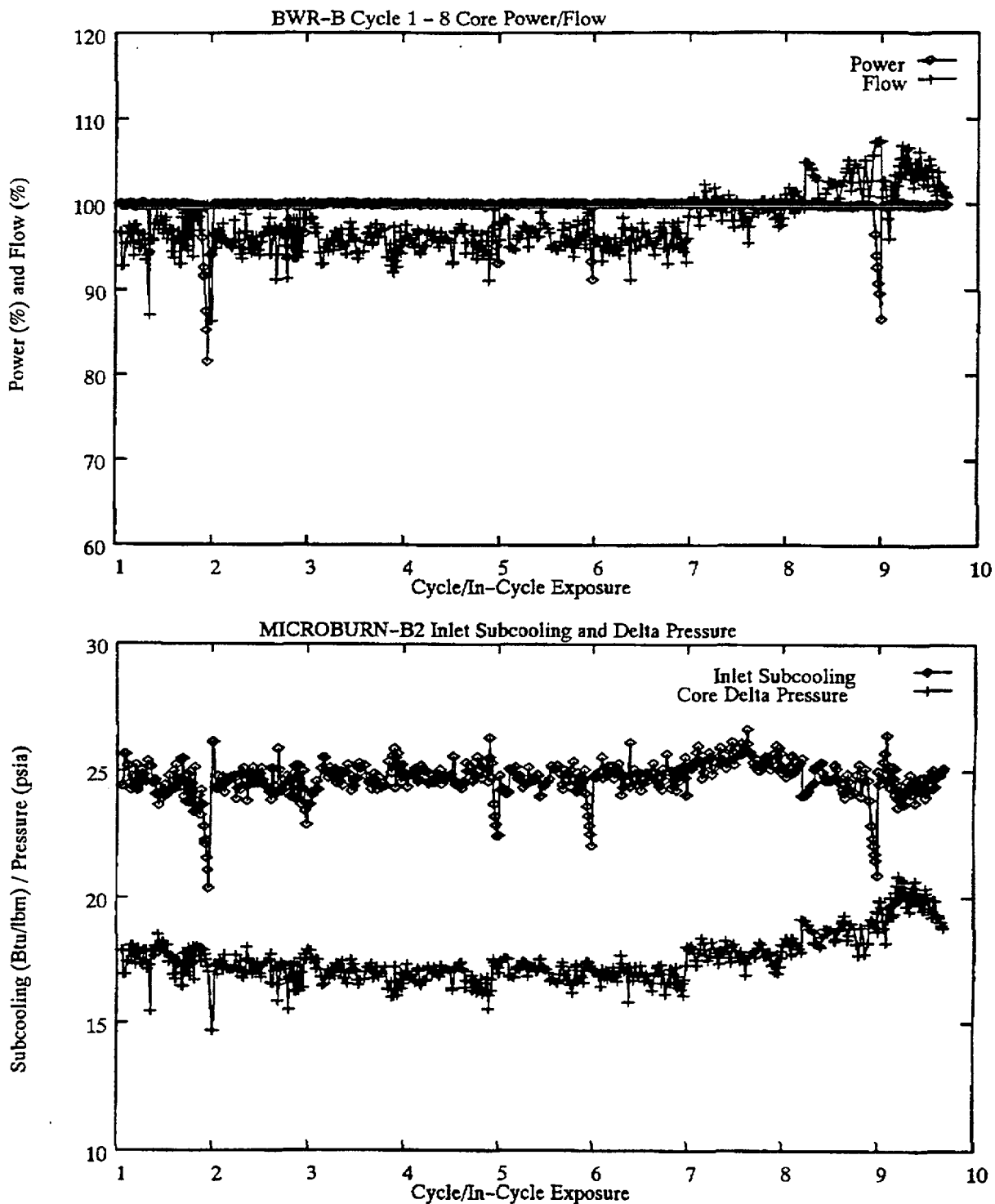


Figure 7.8 BWR - B Core Power/Flow and Inlet Subcooling/Core Pressure Drop Trend

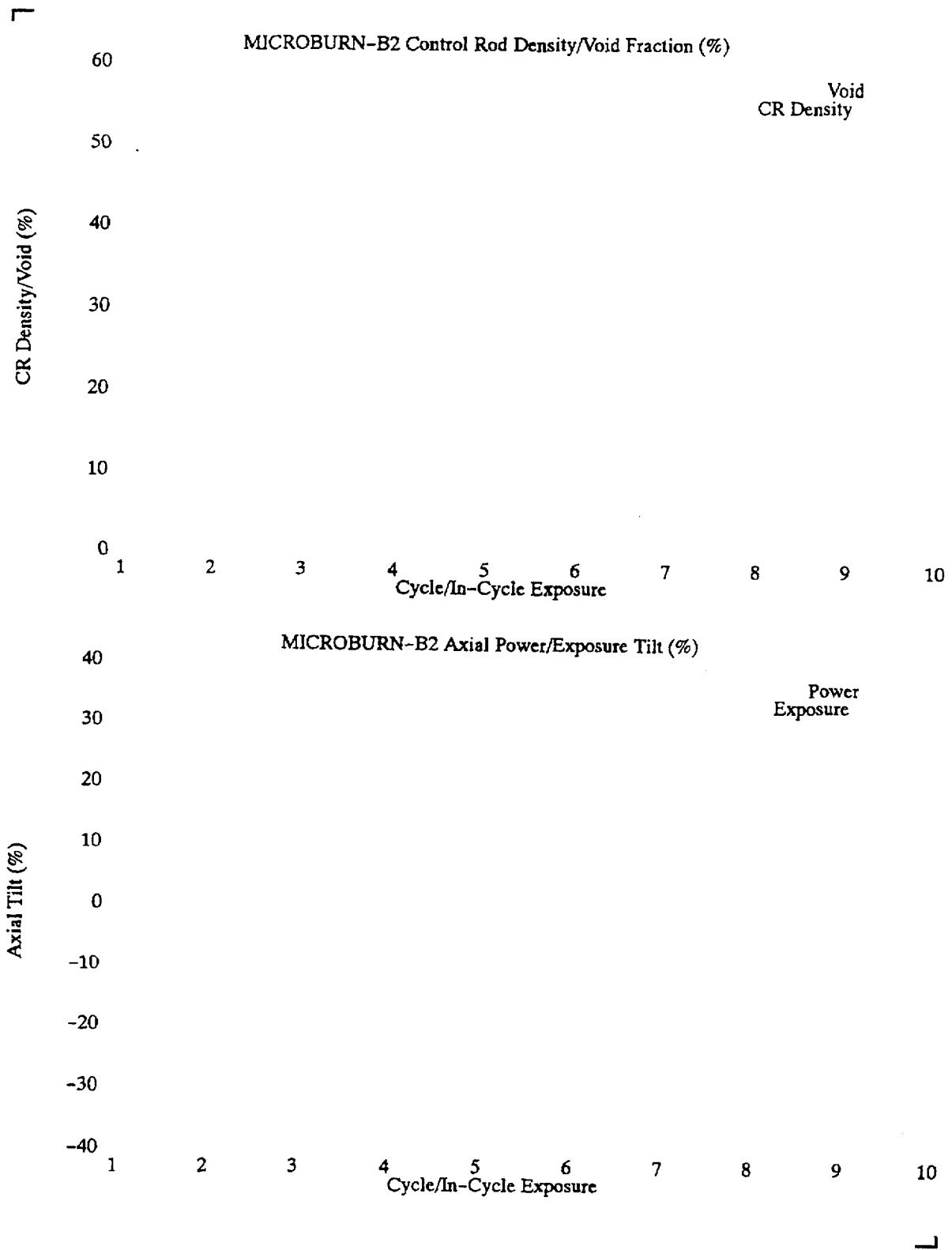


Figure 7.9 BWR – B Core Void/Control Density, and Axial Power/Exposure Tilt Trend

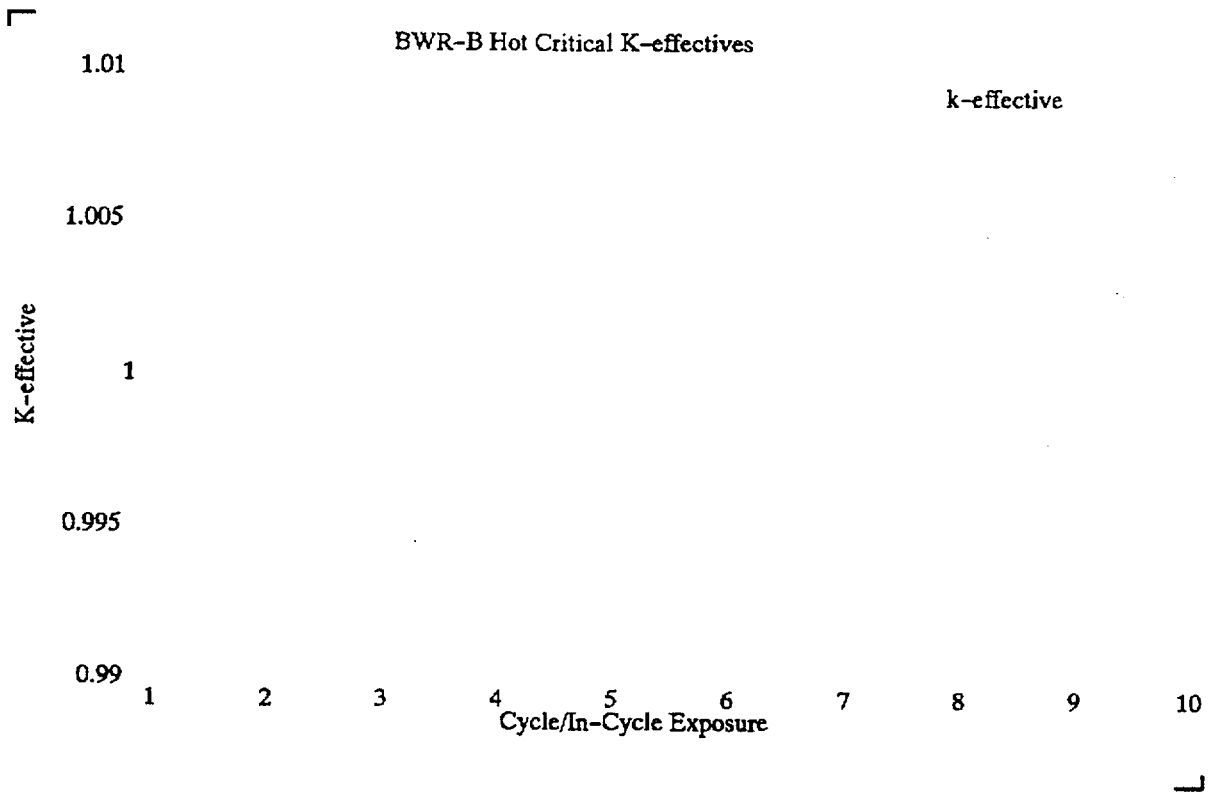


Figure 7.10 BWR – B Hot Critical K – effectives

Table 7.4 BWR – B Cycle Average Hot Critical K – effectives

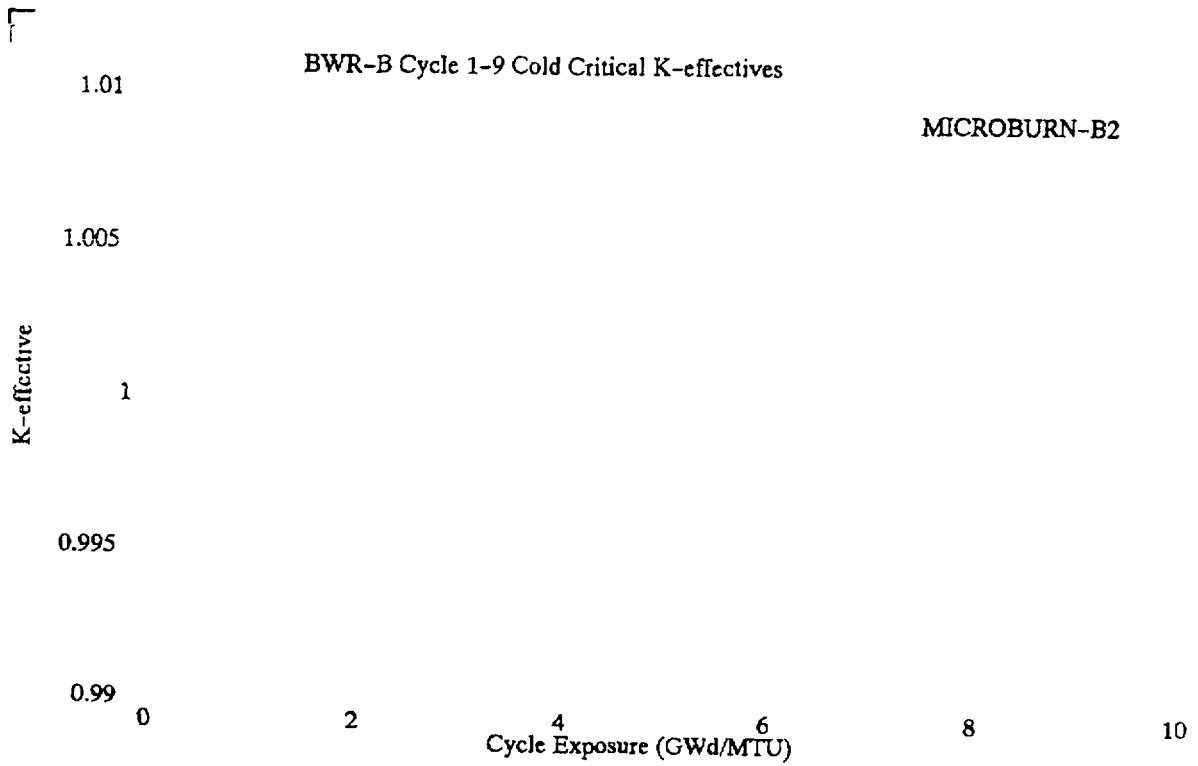
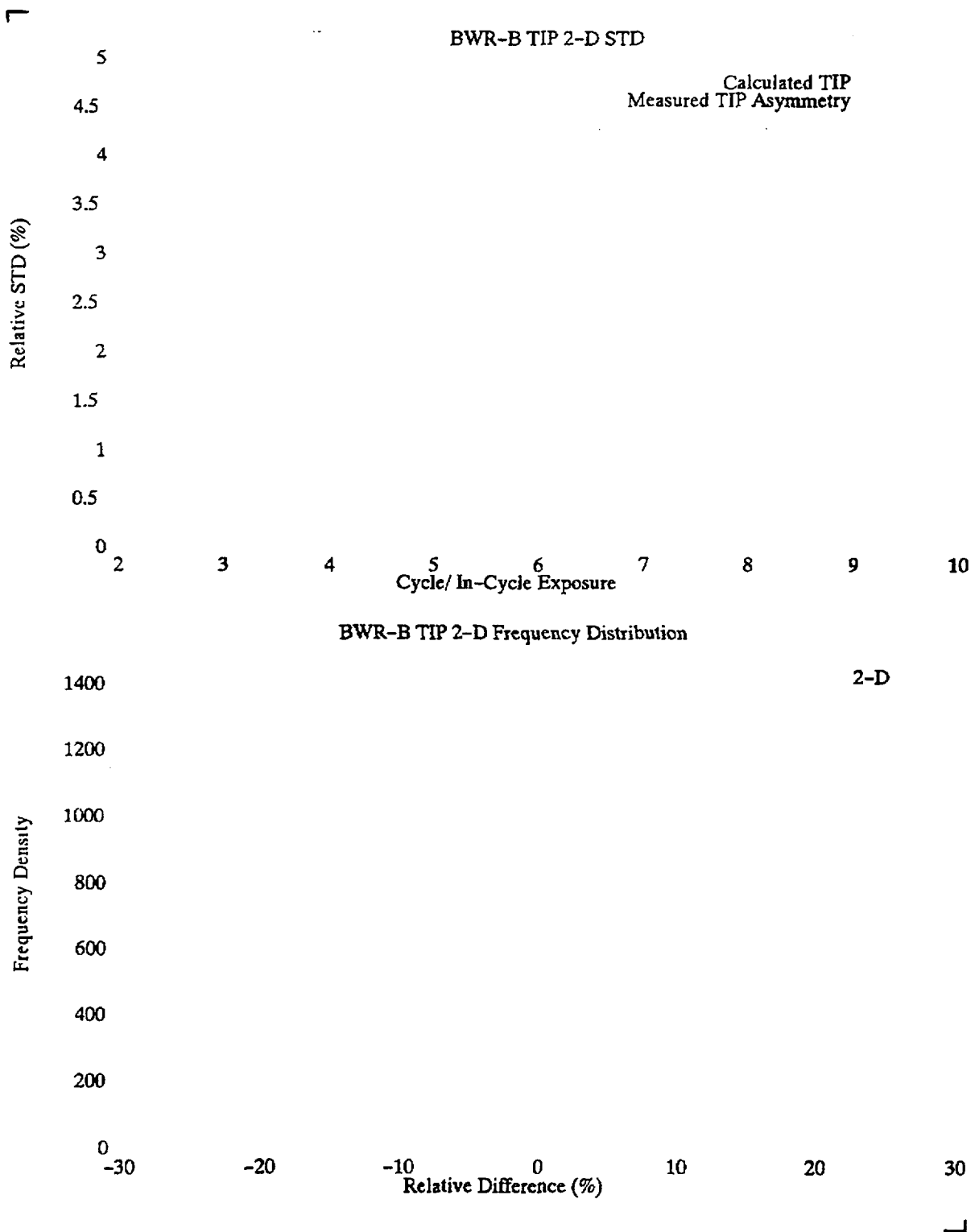
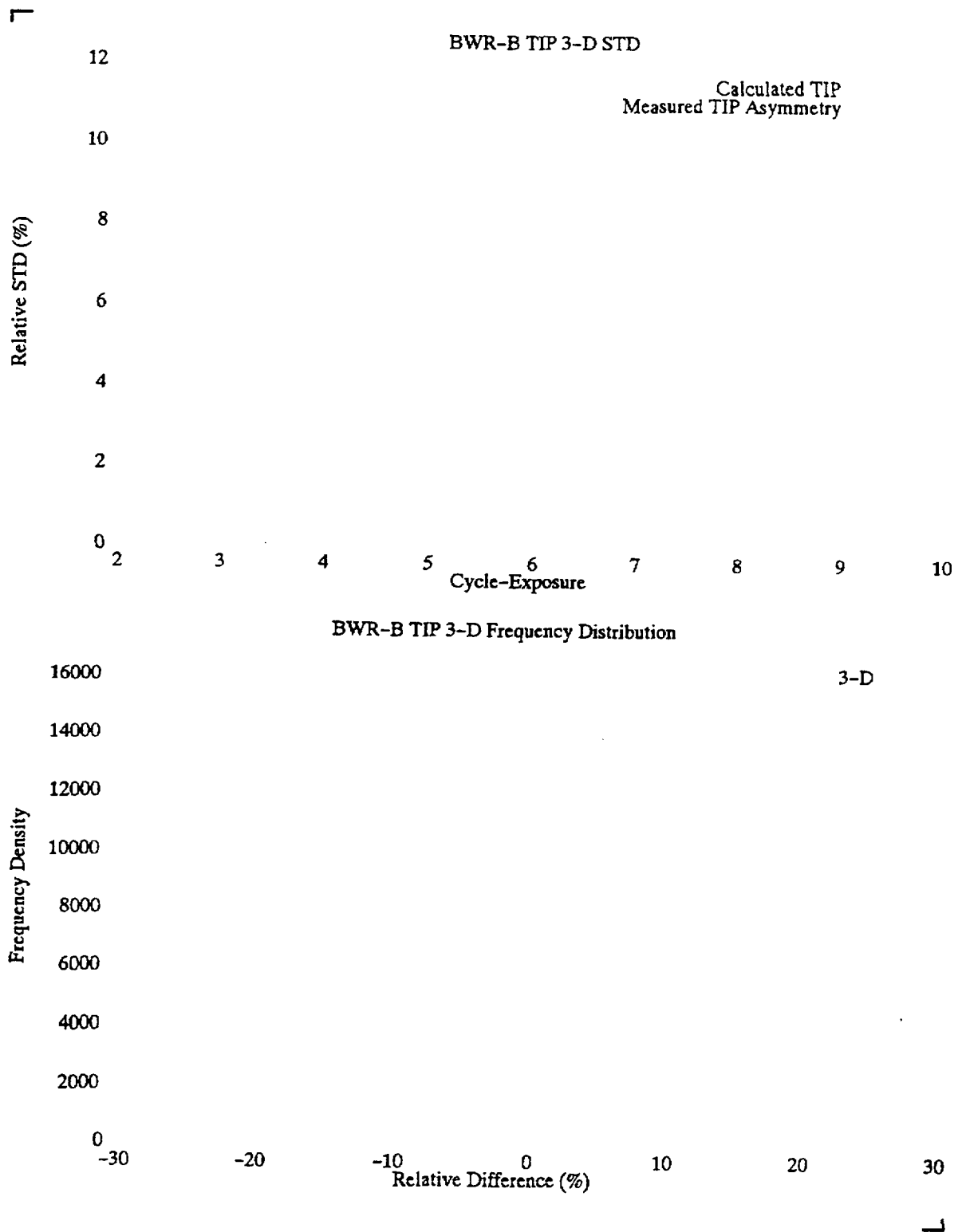



Figure 7.11 BWR - B Cycle 1 to 9 Cold Critical K - effectives

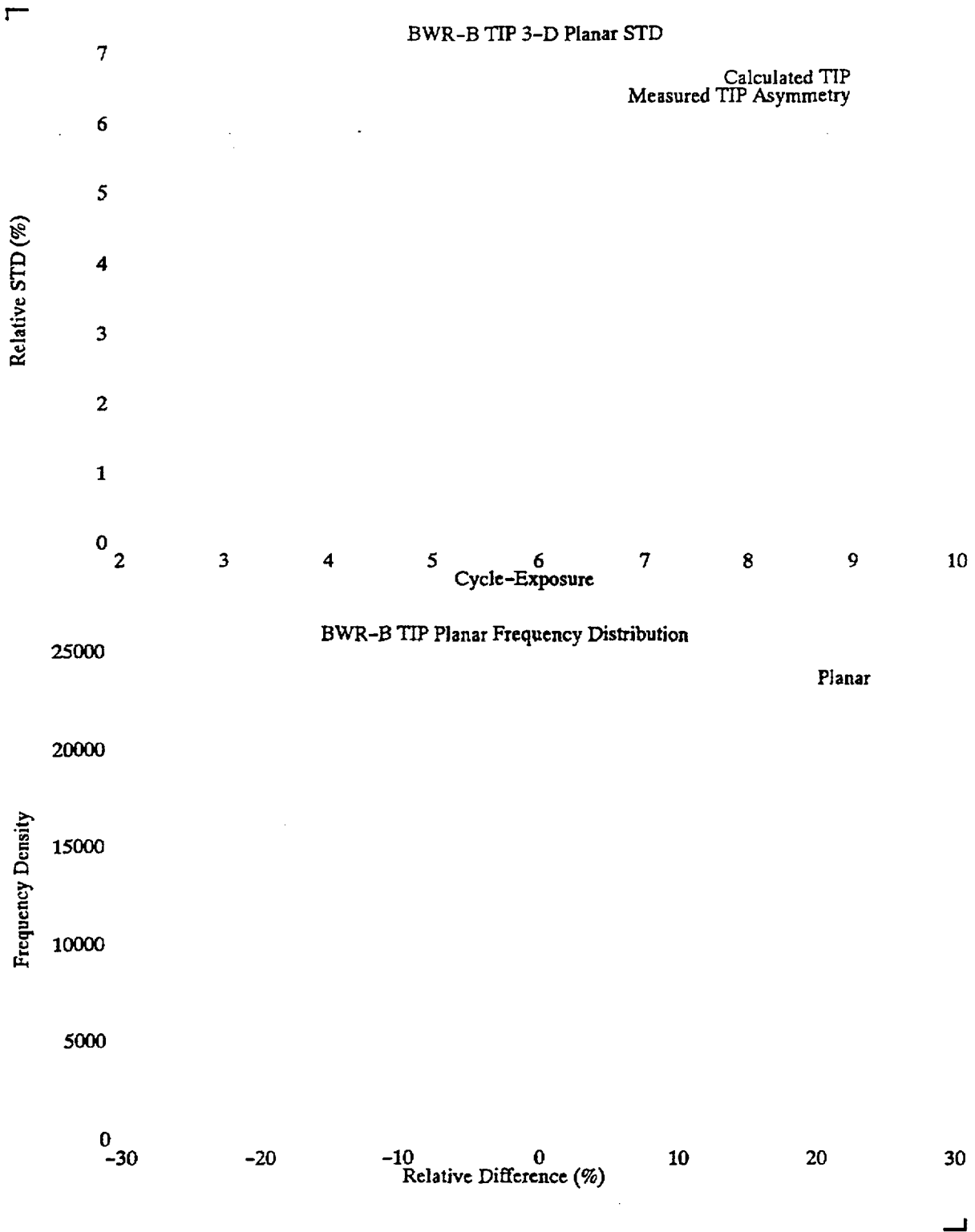
Table 7.5 BWR-B Beginning of Cycle Average Cold Critical K - effectives

**Figure 7.12 BWR – B TIP 2 – D Radial Relative Standard Deviations and Frequency Distribution of Relative Differences**



**Figure 7.13 BWR – B TIP 3 – D Nodal Relative Standard Deviations and Frequency Distribution of Relative Differences**



**Figure 7.14 BWR – B TIP 3 – D Planar Relative Standard Deviations and Frequency Distribution of Relative Differences**

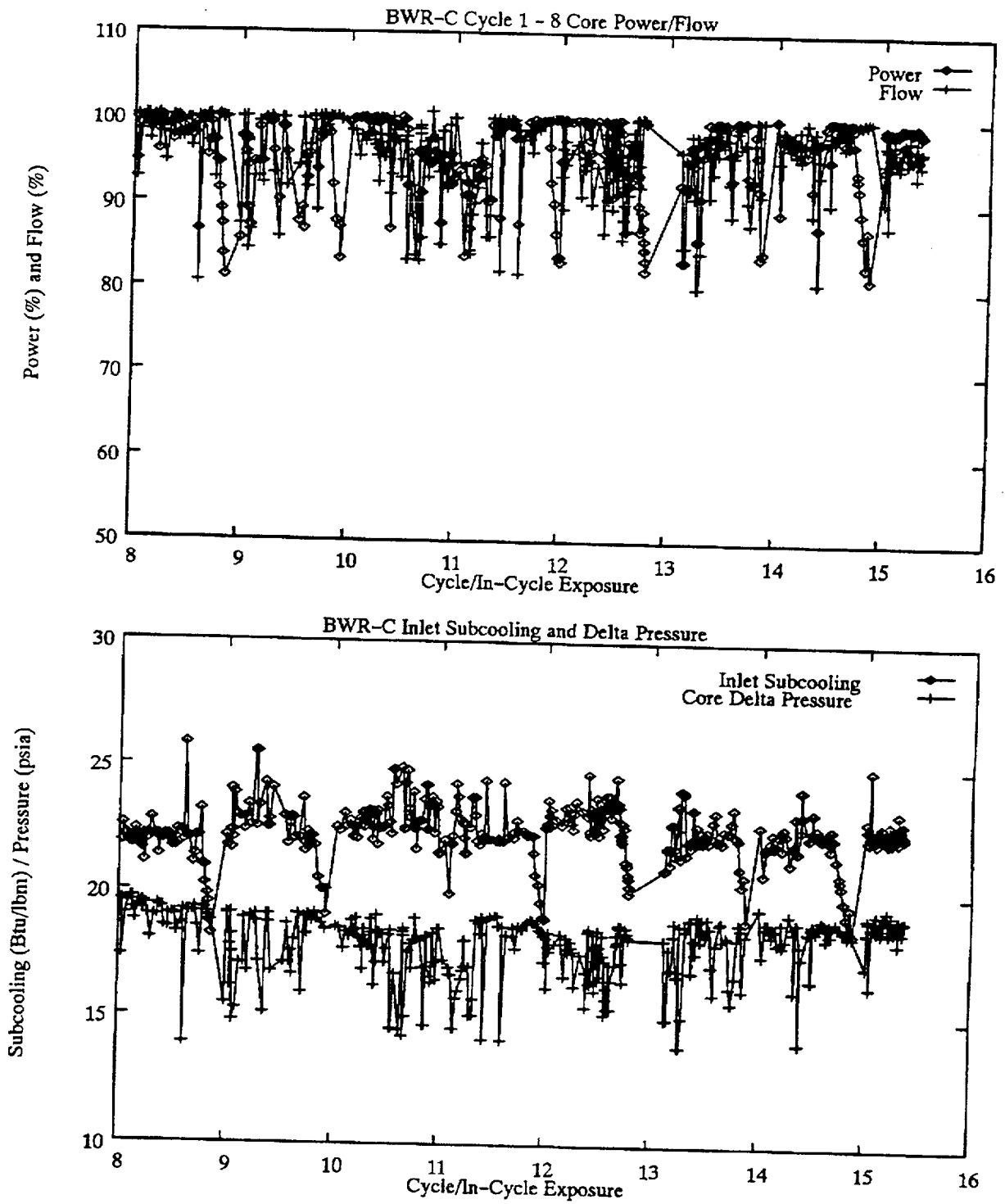


Figure 7.15 BWR - C Core Power/Flow and Inlet Subcooling/Core Pressure Drop Trend

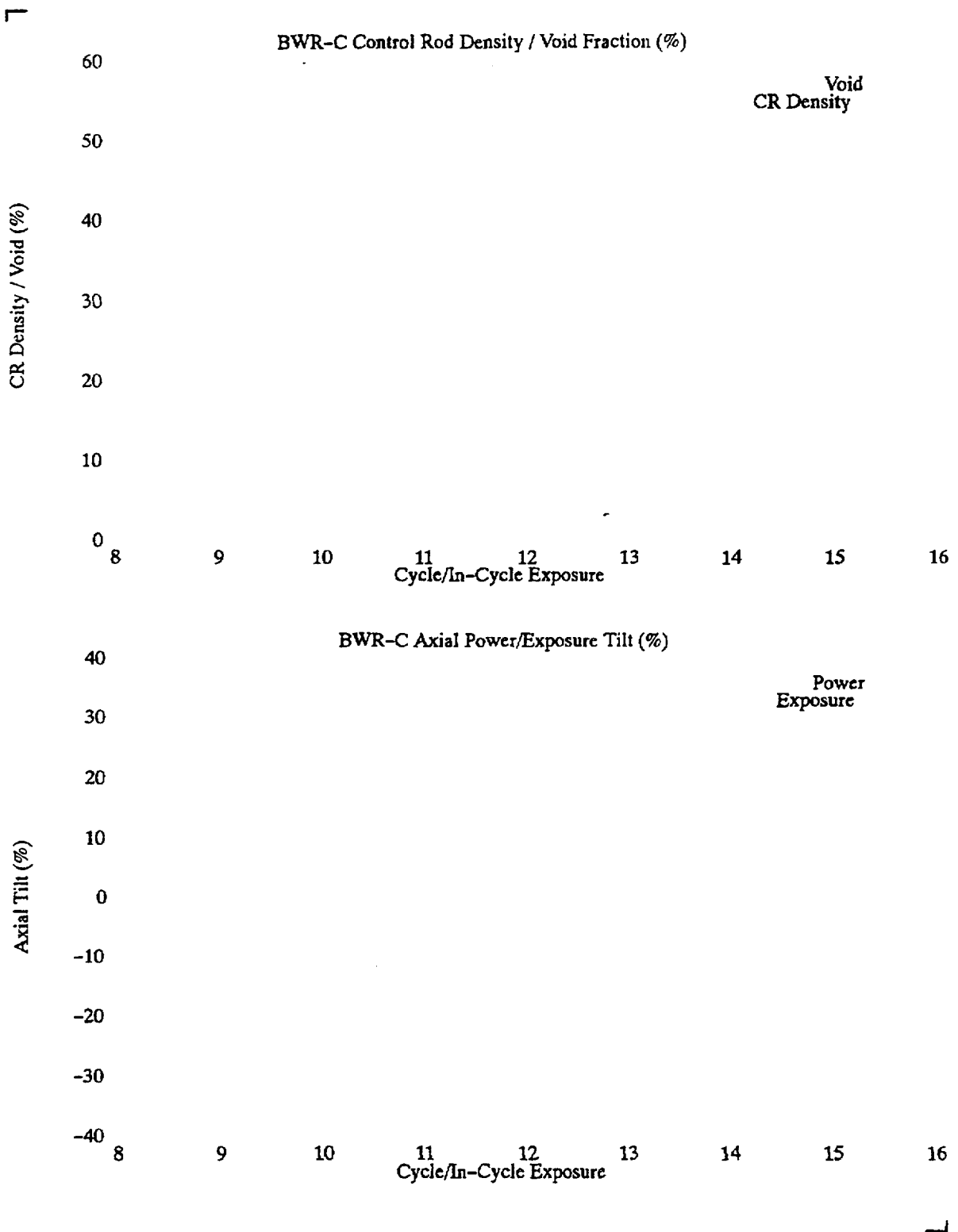


Figure 7.16 BWR – C Core Void/Control Density, and Axial Power/Exposure Tilt Trend

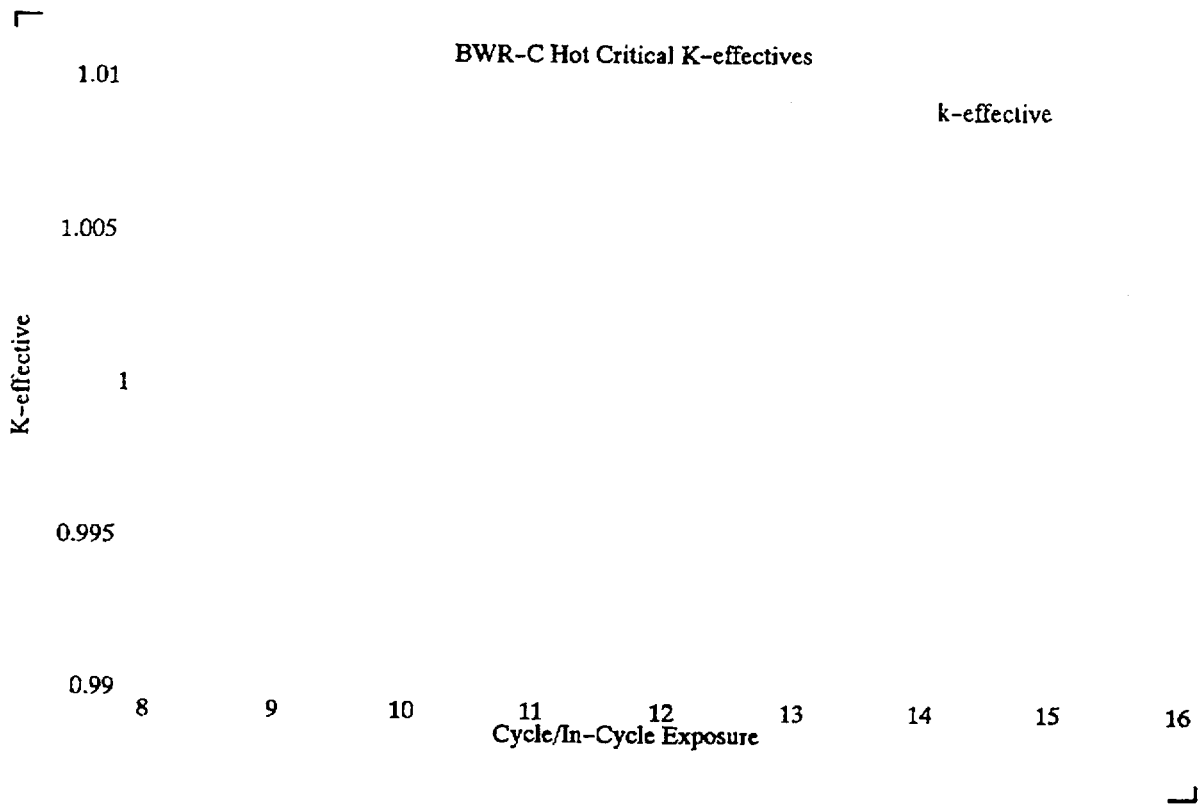


Figure 7.17 BWR - C Hot Critical K - effectives

Table 7.6 BWR - C Cycle Average Hot Critical K - effectives

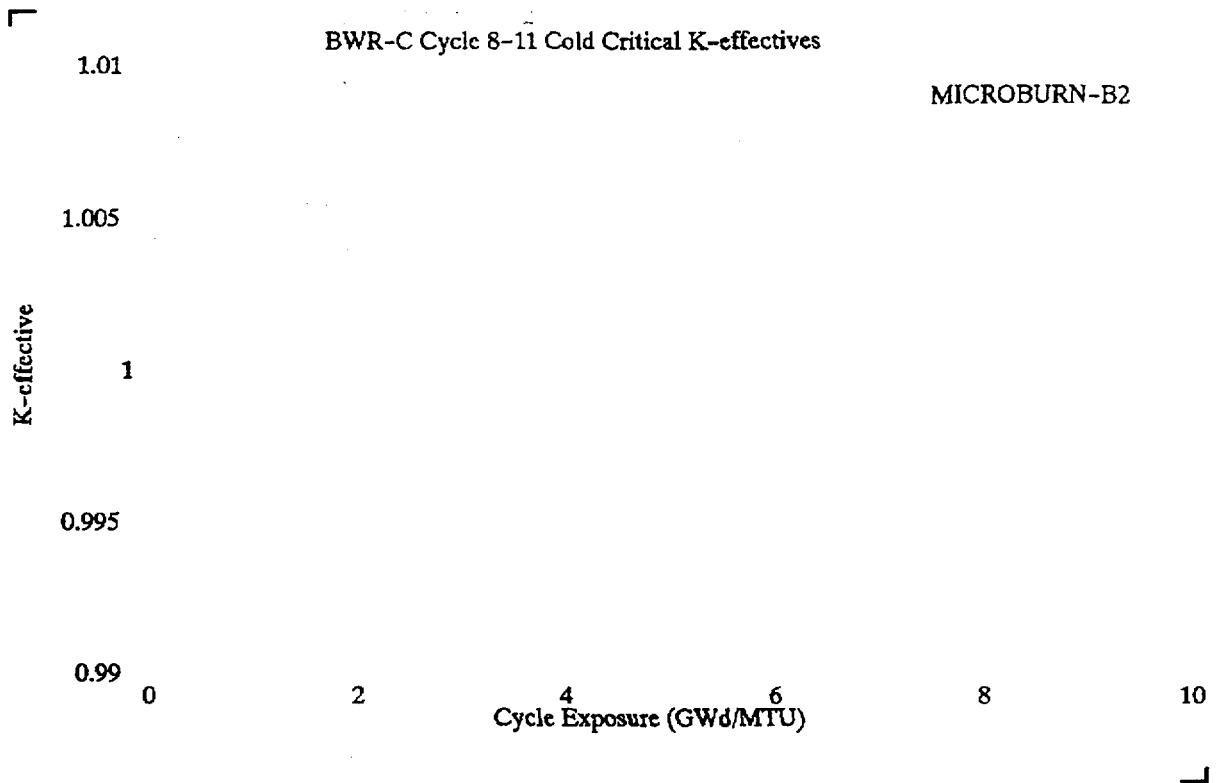
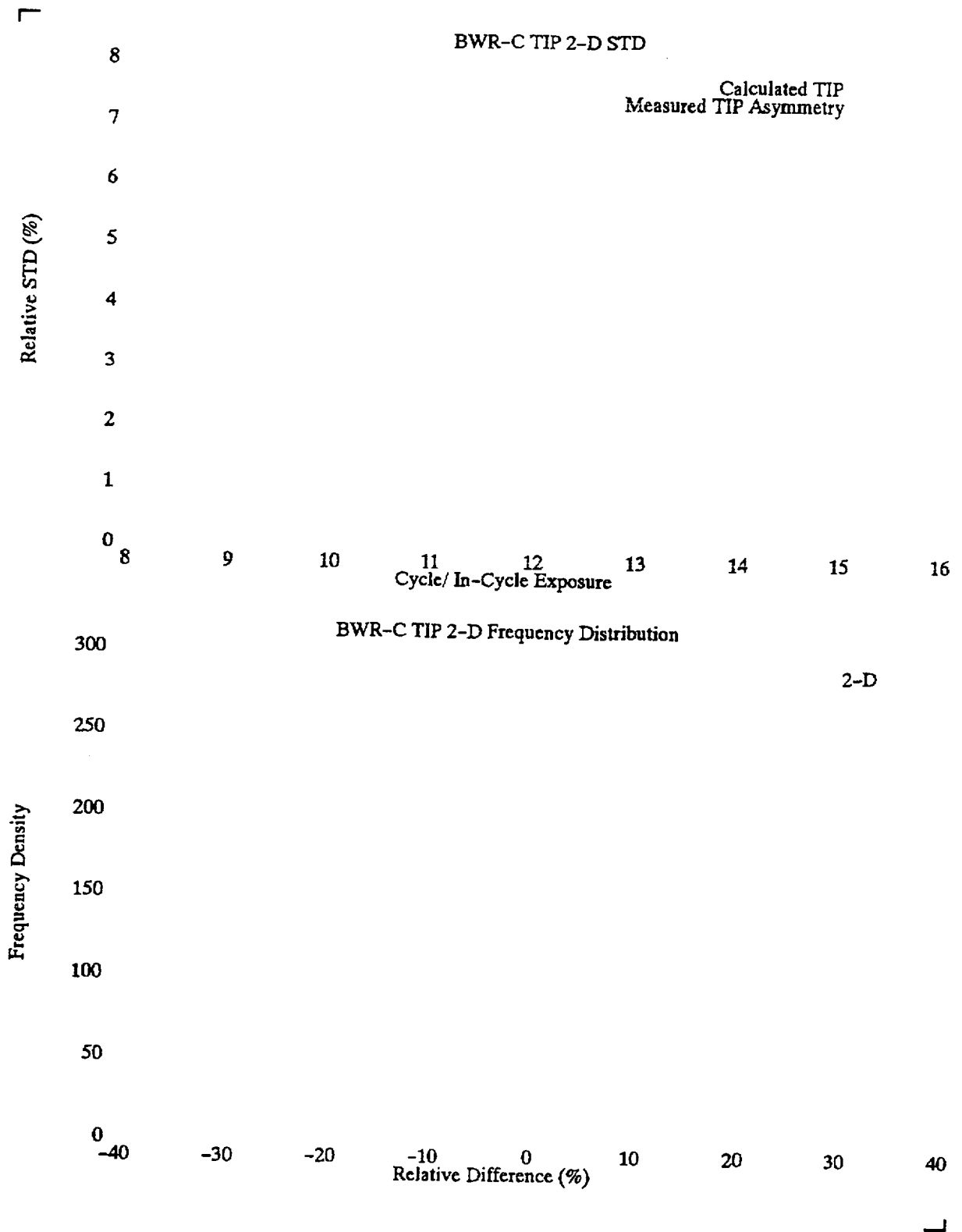
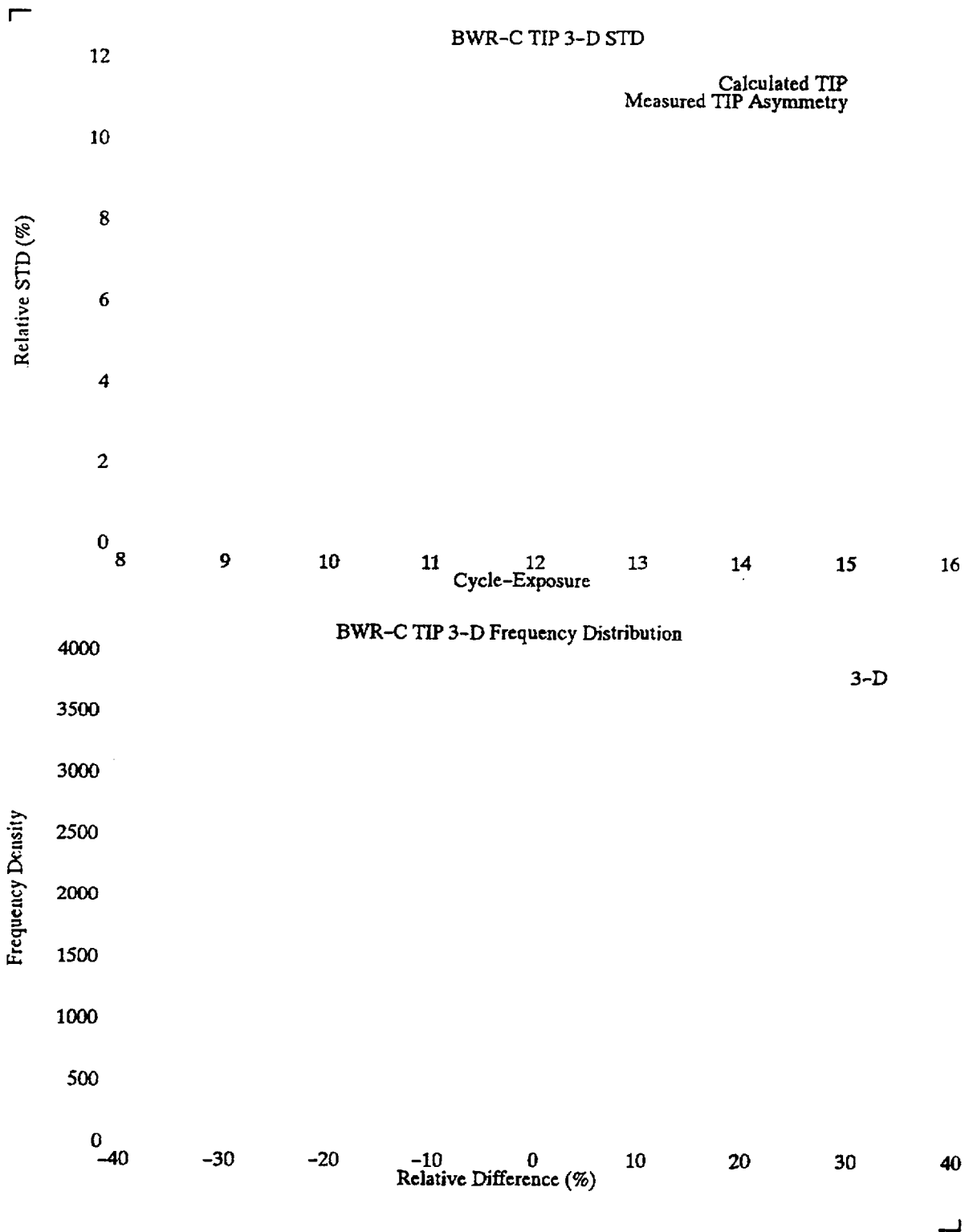



Figure 7.18 BWR – C Cycle 8 to 11 Cold Critical K – effectives

Table 7.7 BWR-C Beginning of Cycle Average Cold Critical K – effectives

**Figure 7.19 BWR – C TIP 2 – D Radial Relative Standard Deviations and Frequency Distribution of Relative Differences**



**Figure 7.20 BWR – C TIP 3 – D Nodal Relative Standard Deviations and Frequency Distribution of Relative Differences**

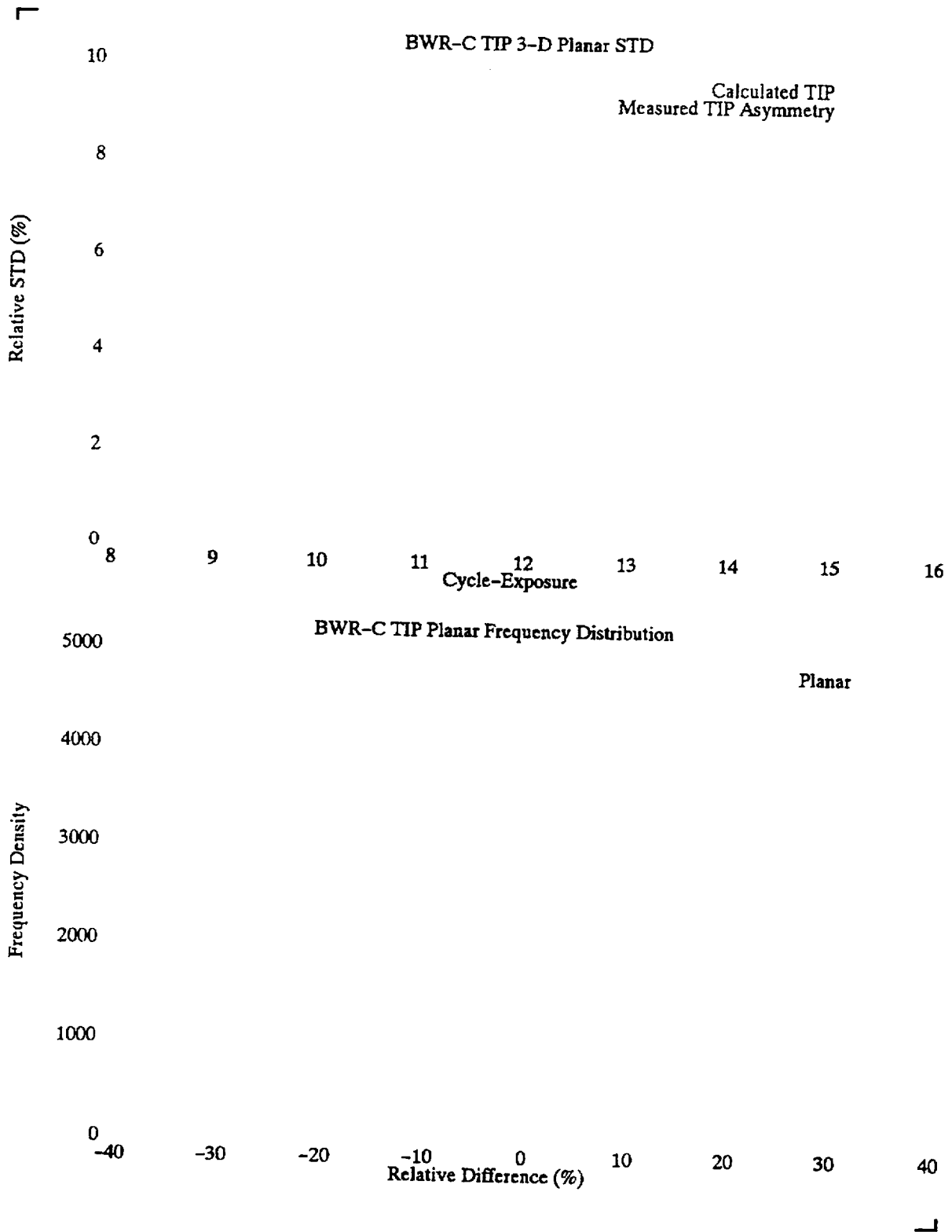


Figure 7.21 BWR - C TIP 3 - D Planar Relative Standard Deviations and Frequency Distribution of Relative Differences

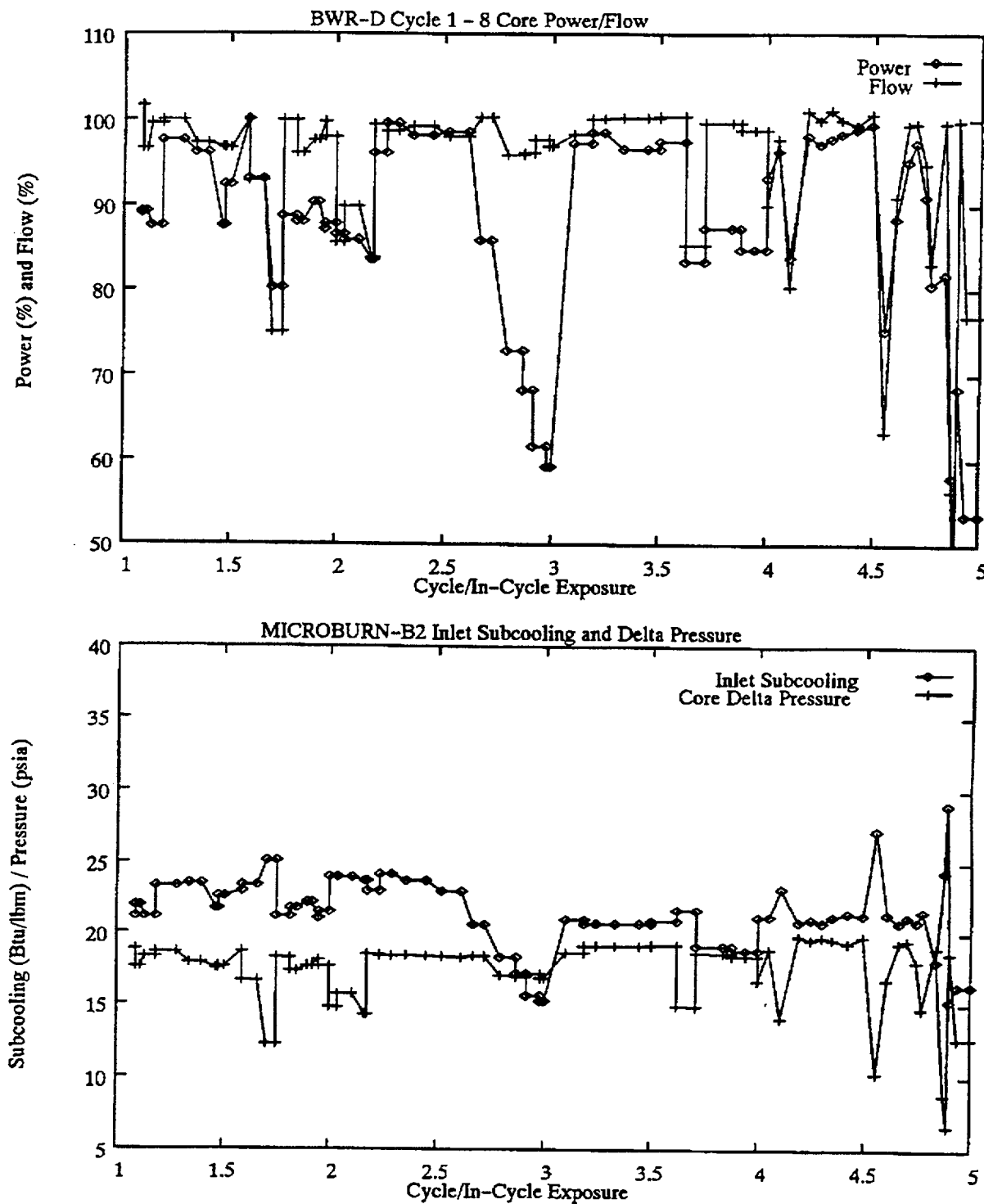


Figure 7.22 BWR - D Core Power/Flow and Inlet Subcooling/Core Pressure Drop Trend

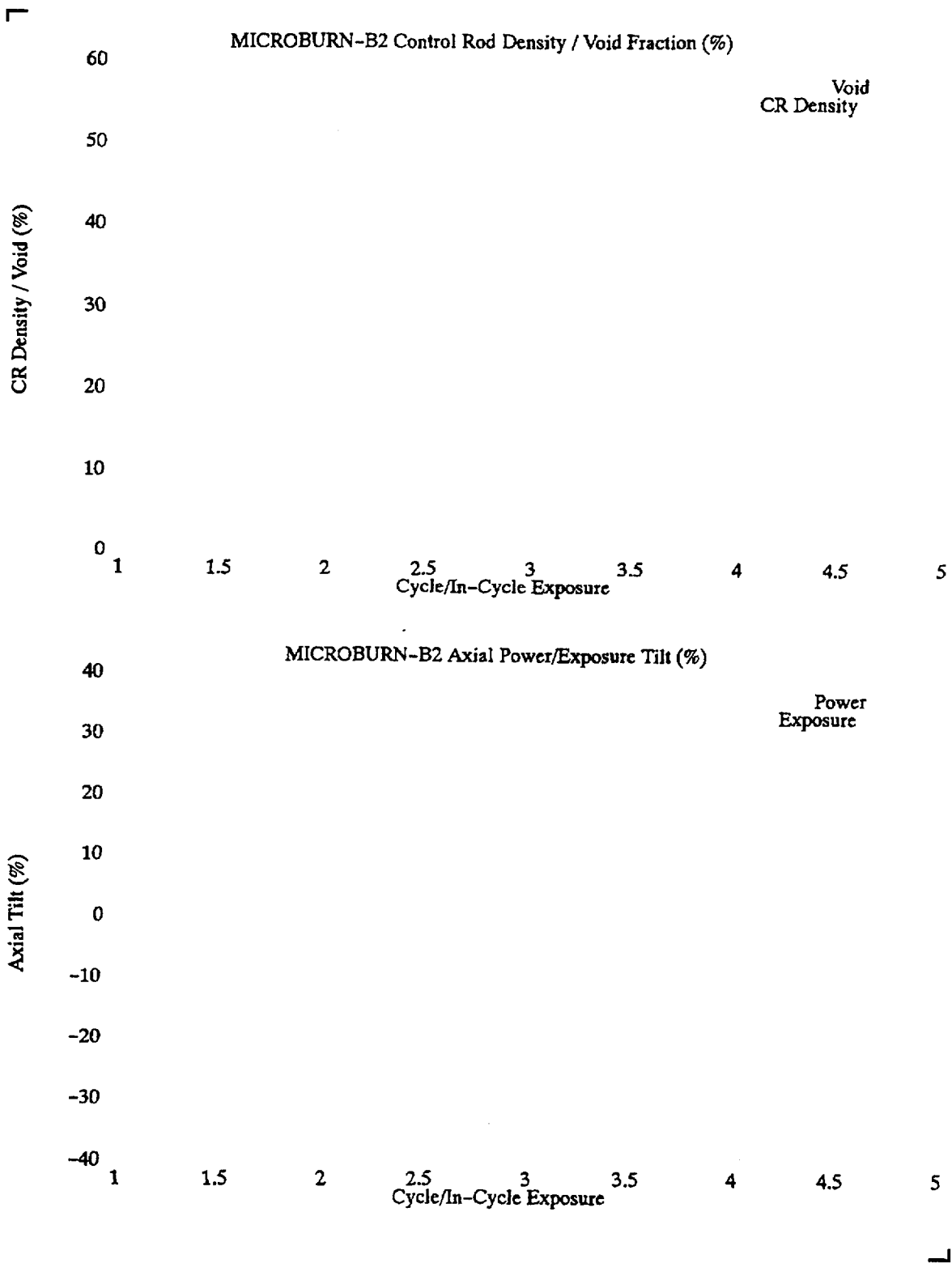


Figure 7.23 BWR – D Core Void/Control Density, and Axial Power/Exposure Tilt Trend

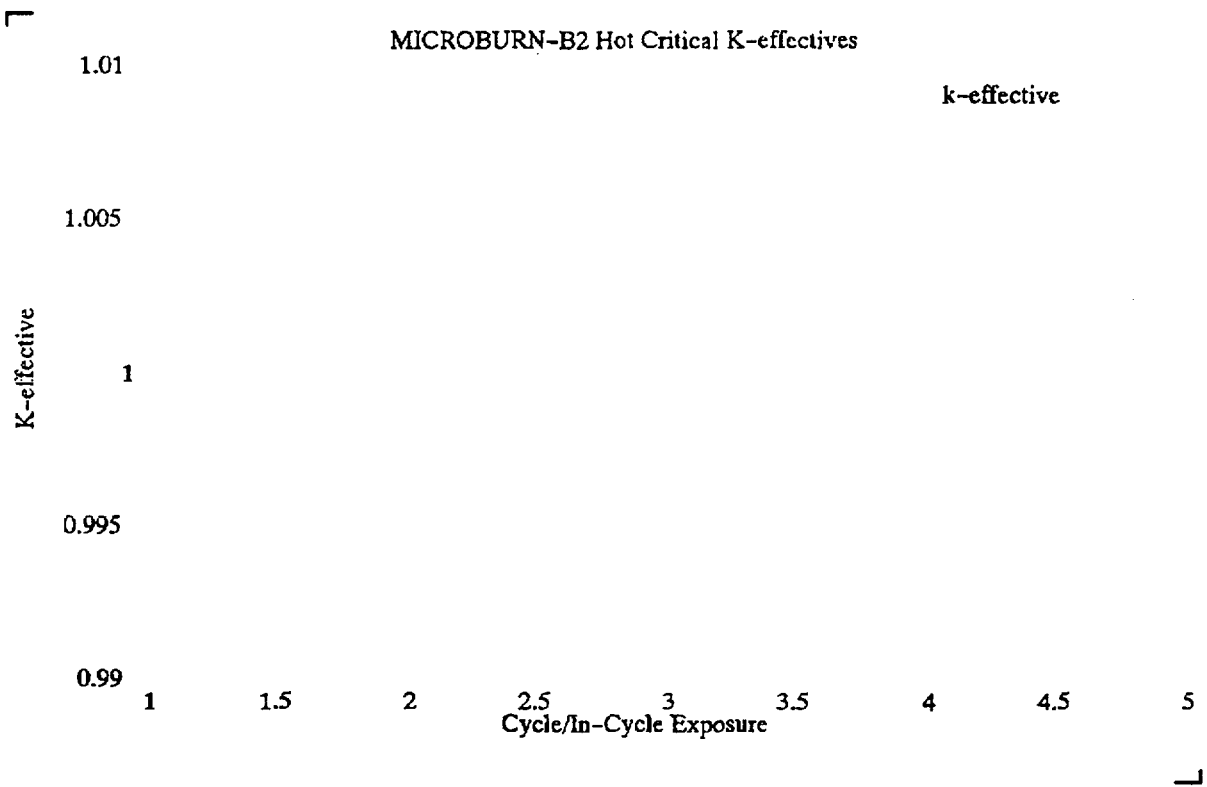


Figure 7.24 BWR – D Hot Critical K – effectives

Table 7.8 BWR-D Cycle Average Hot Critical K – effectives

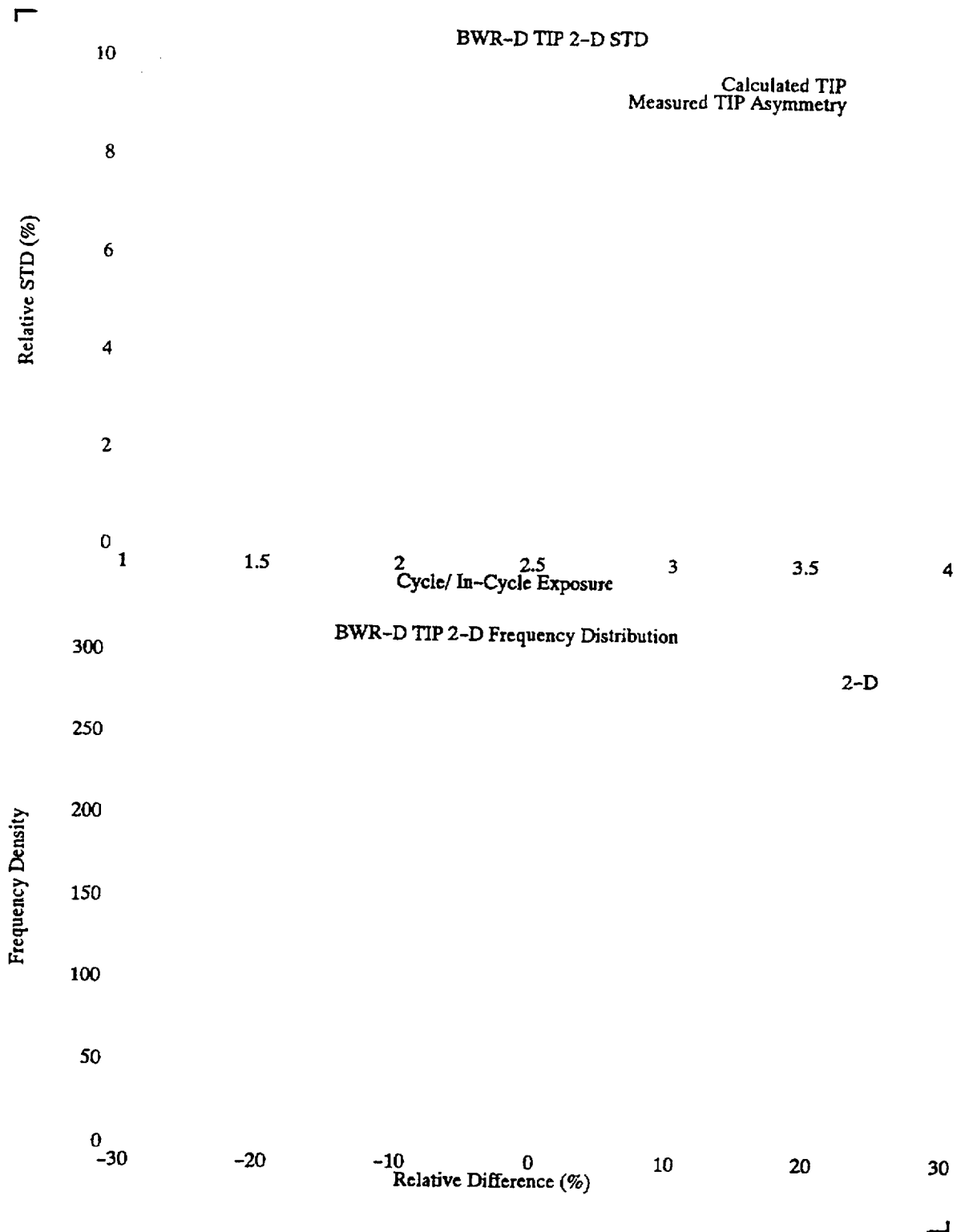
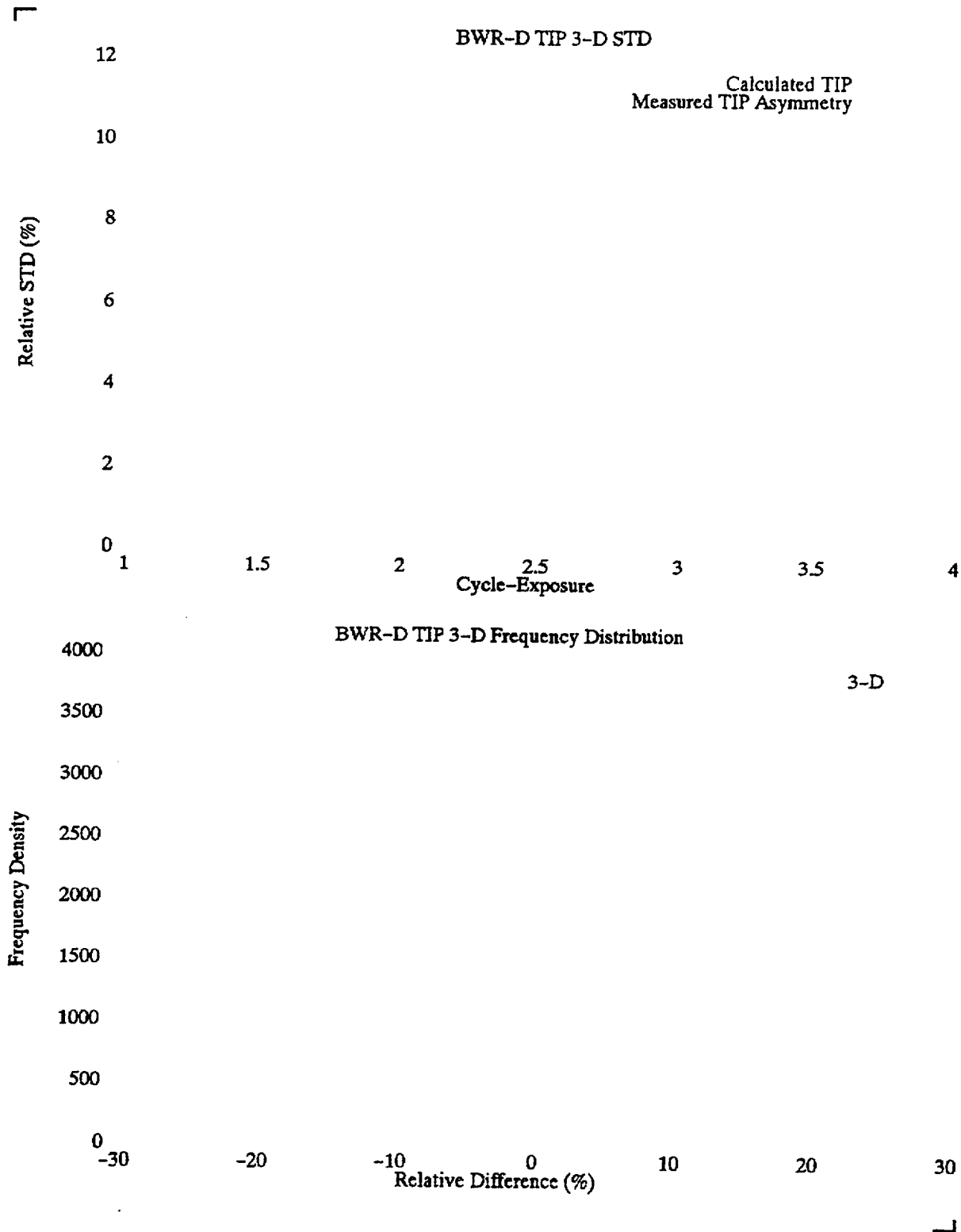
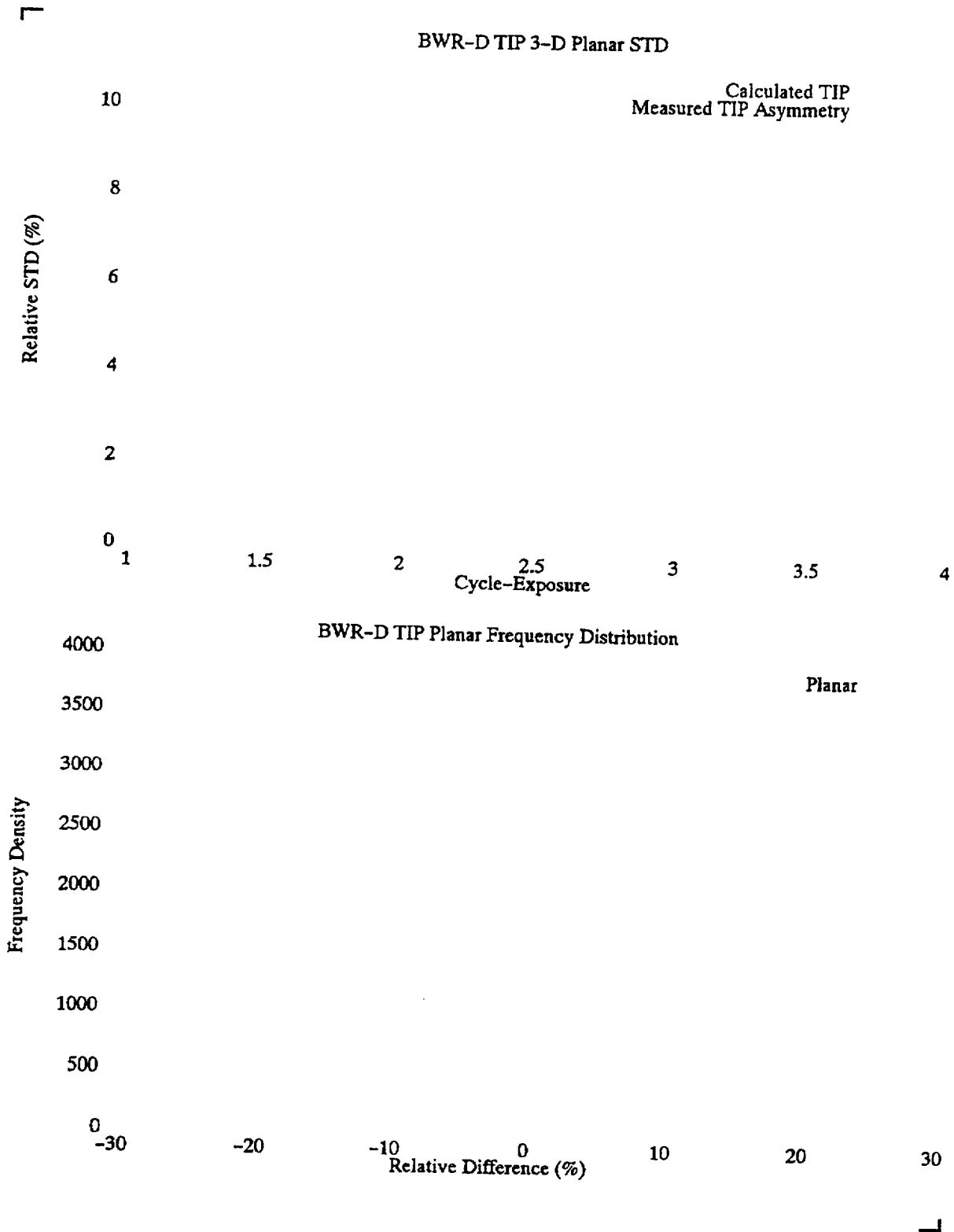



Figure 7.25 BWR – D TIP 2 – D Radial Relative Standard Deviations and Frequency Distribution of Relative Differences



**Figure 7.26 BWR – D TIP 3 – D Nodal Relative Standard Deviations and Frequency Distribution of Relative Differences**



**Figure 7.27 BWR – D TIP 3 – D Planar Relative Standard Deviations and Frequency Distribution of Relative Differences**

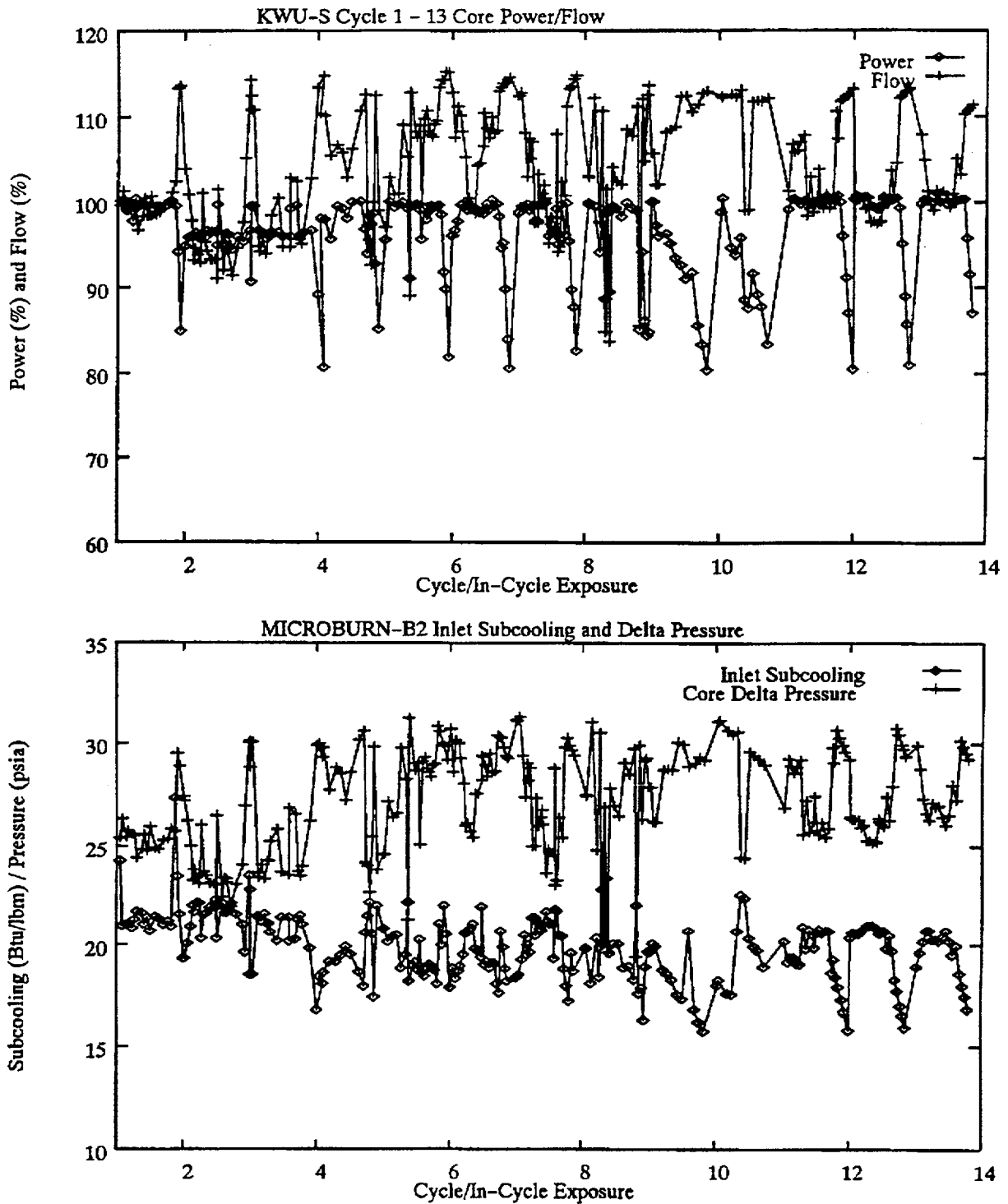


Figure 7.28 KWU-S Core Power/Flow and Inlet Subcooling/Core Pressure Drop Trend

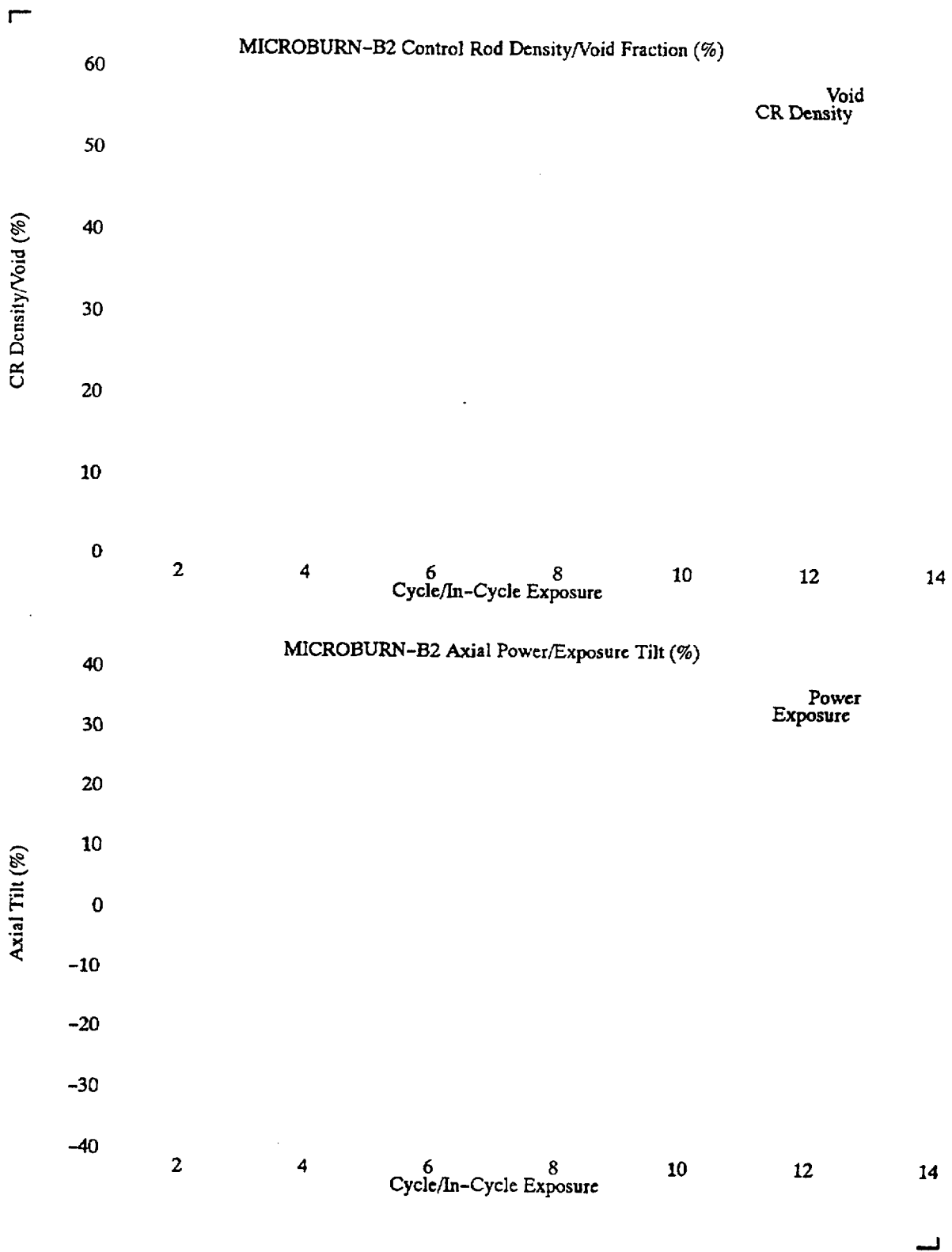


Figure 7.29 KWU – S Core Void/Control Density, and Axial Power/Exposure Tilt Trend



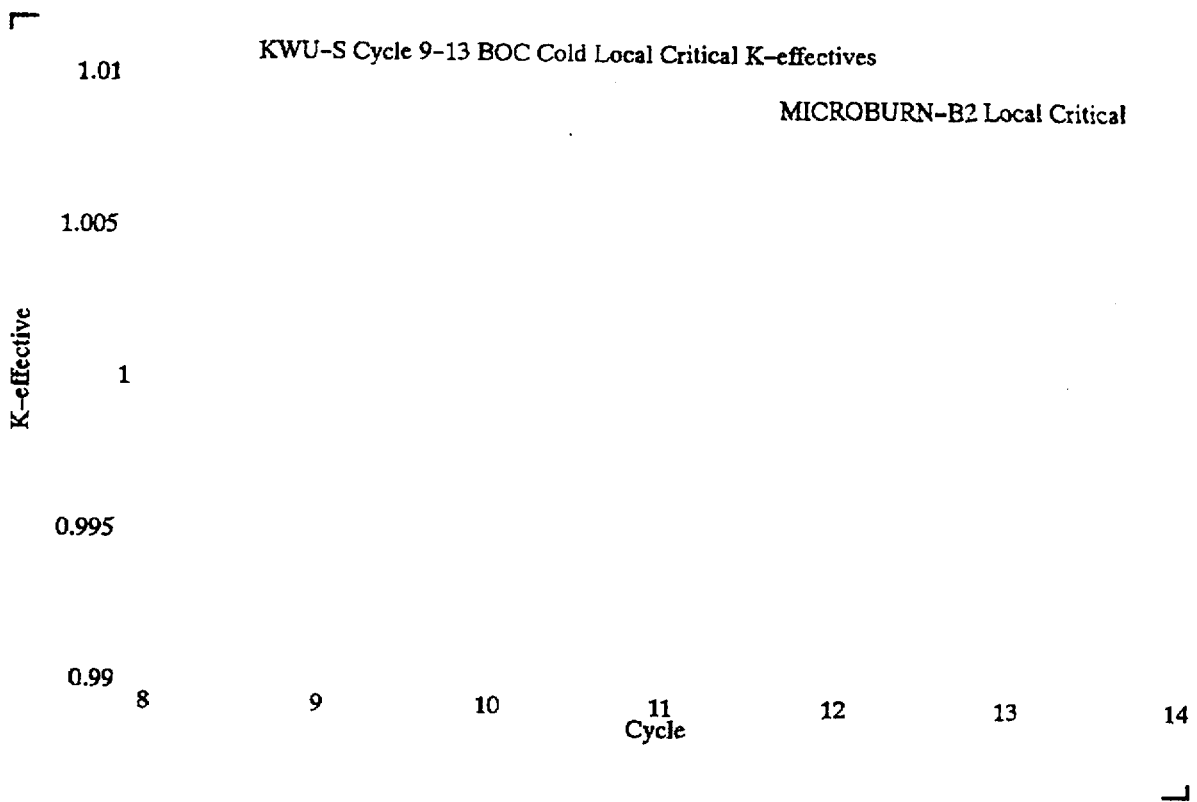
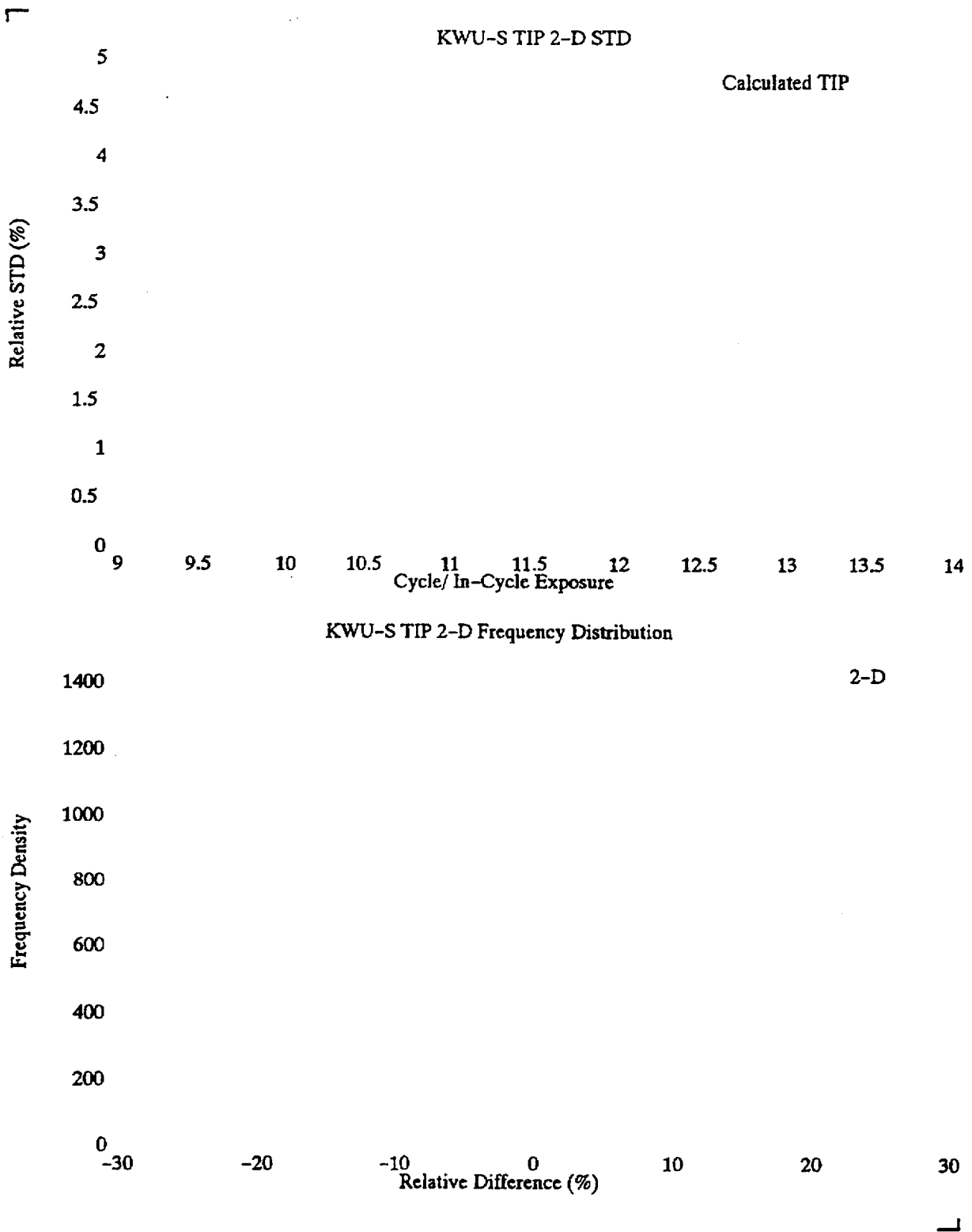


Figure 7.31 KWU – S Beginning of Cycle Cold Local Critical K – effectives

Table 7.10 KWU-S Beginning of Cycle Average Cold Critical K – effectives

**Figure 7.32 KWU – S TIP 2 – D Radial Relative Standard Deviations and Frequency Distribution of Relative Differences**

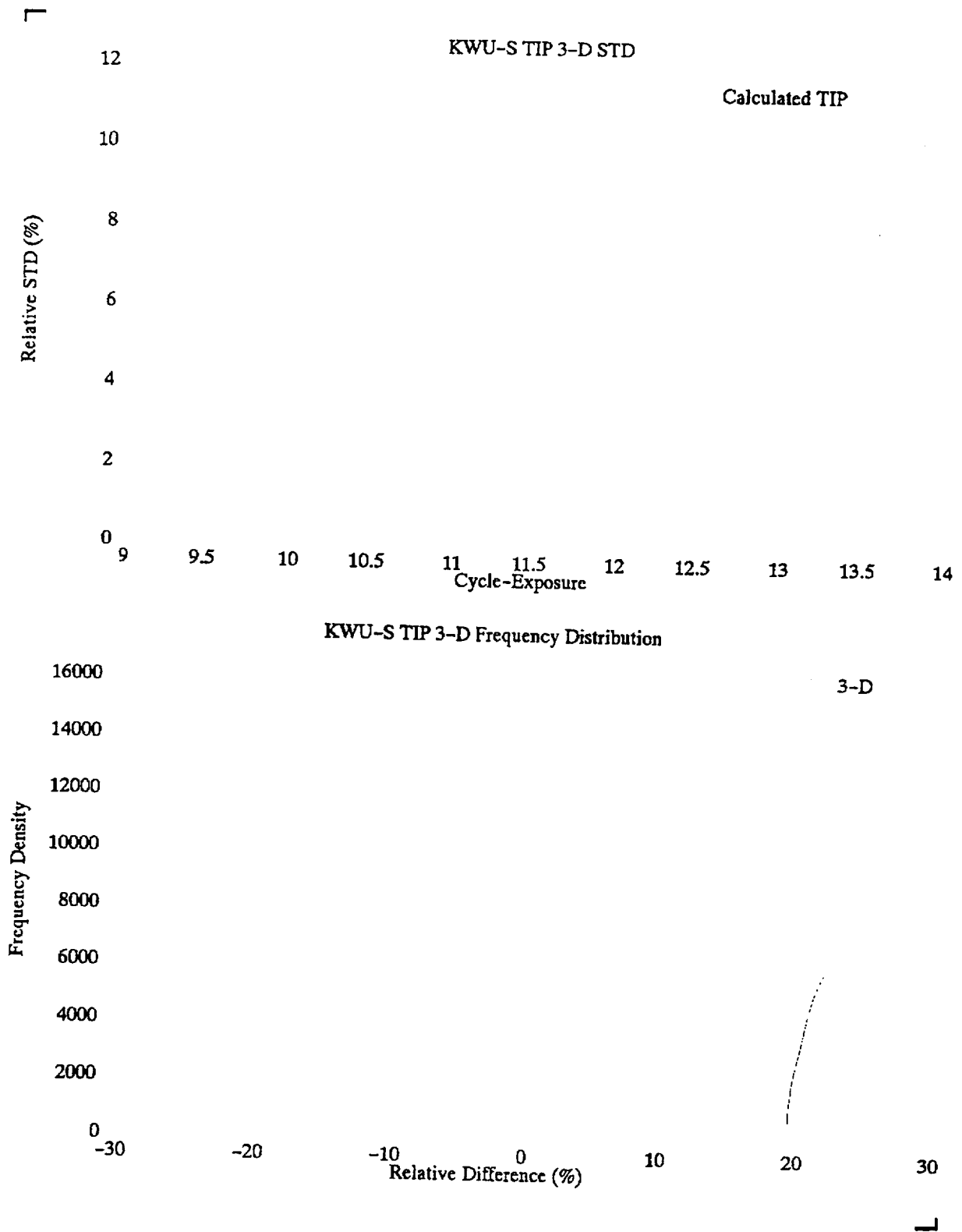
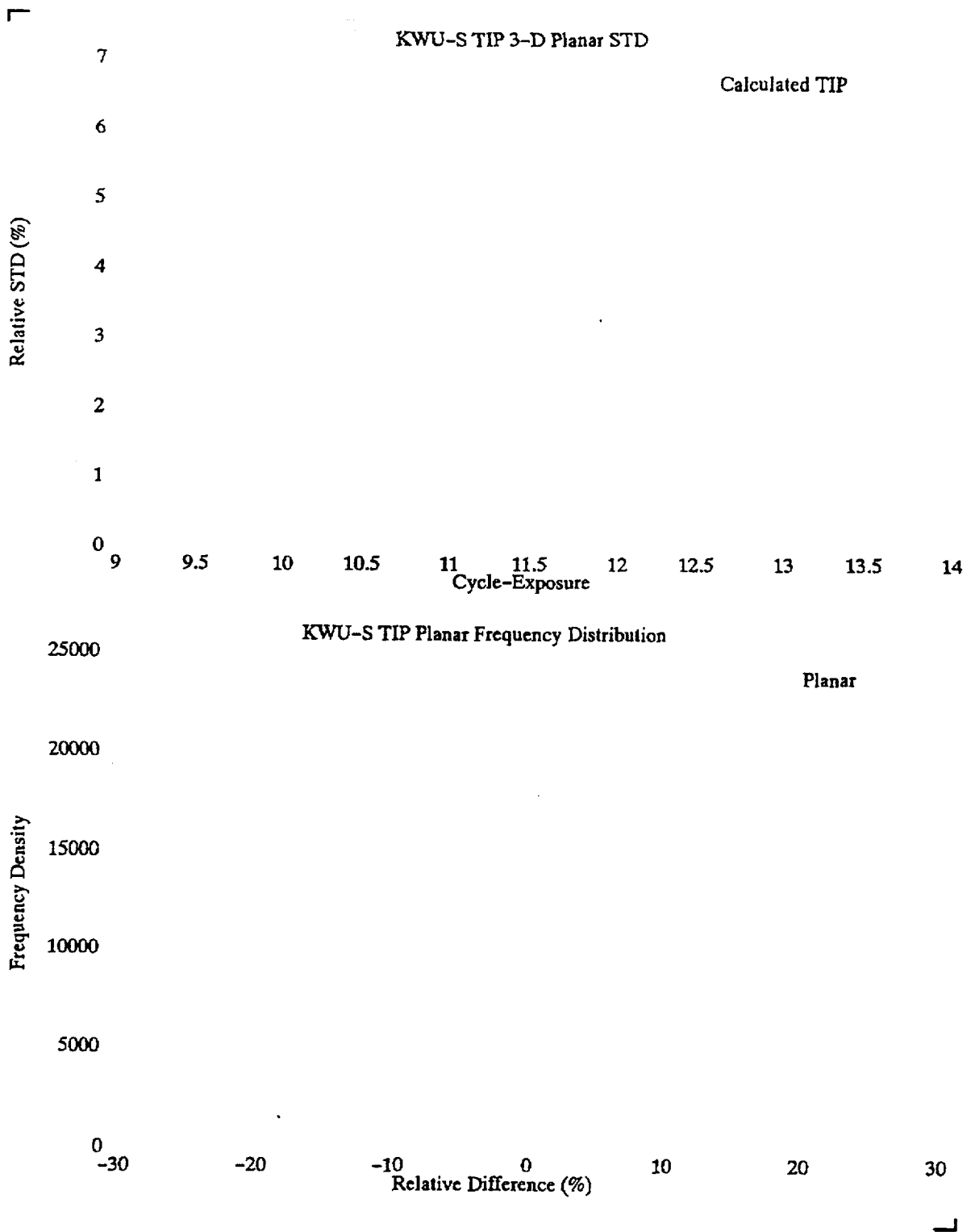


Figure 7.33 KWU – S TIP 3 – D Nodal Relative Standard Deviations and Frequency Distribution of Relative Differences



**Figure 7.34 KWU-S TIP 3-D Planar Relative Standard Deviations and Frequency Distribution of Relative Differences**

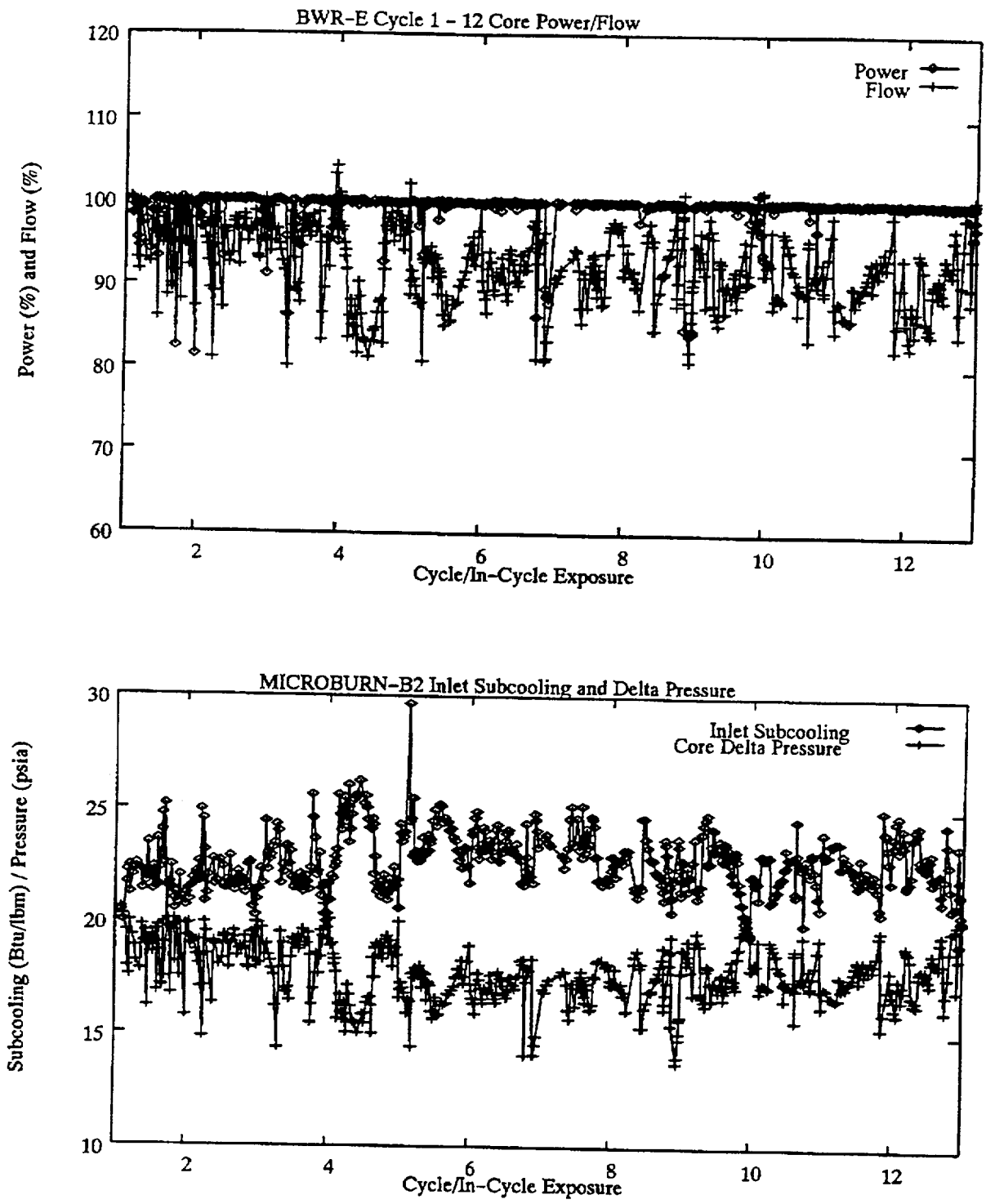


Figure 7.35 BWR-E Core Power/Flow and Inlet Subcooling/Core Pressure Drop Trend

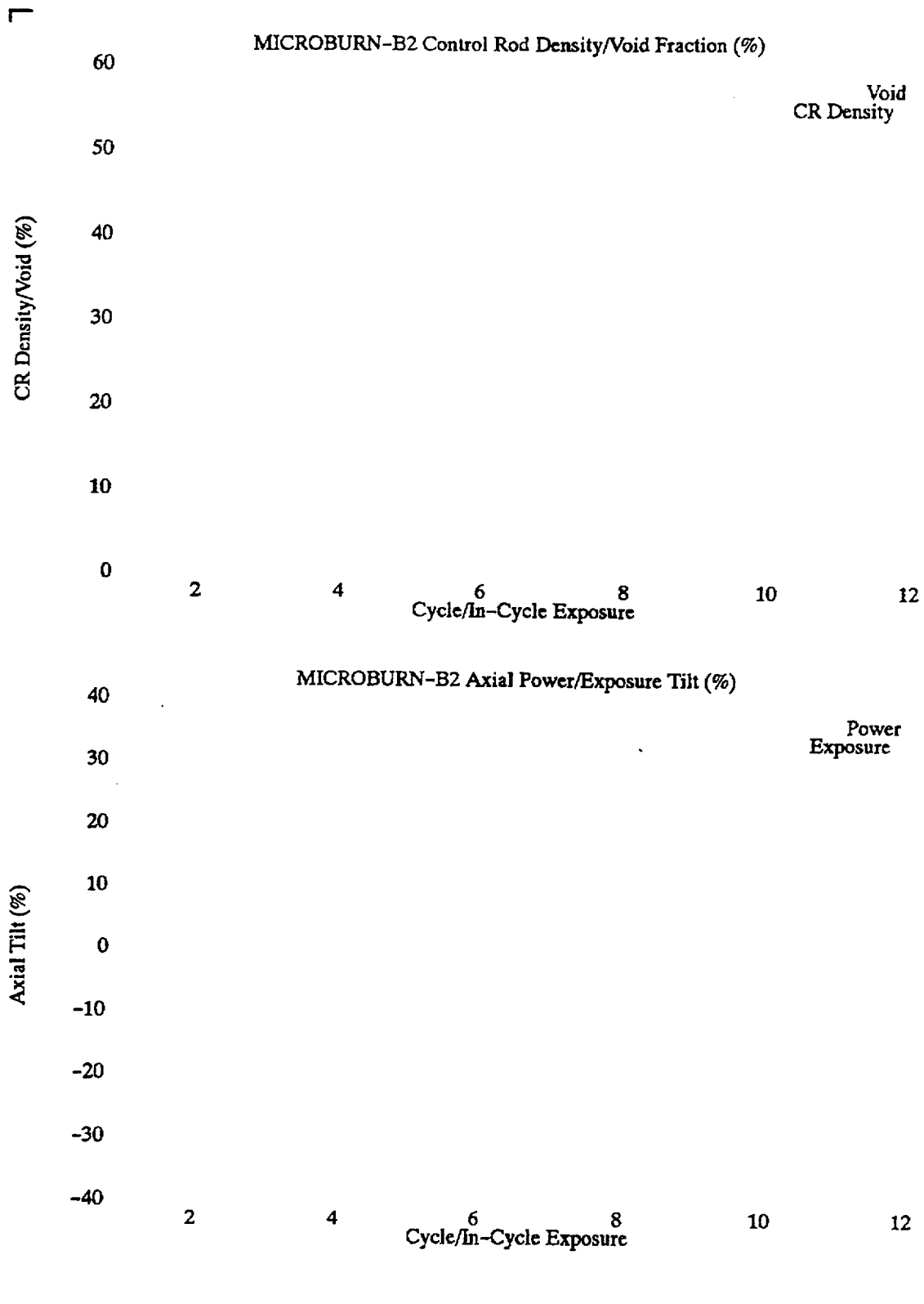


Figure 7.36 BWR – E Core Void/Control Density, and Axial Power/Exposure Tilt Trend





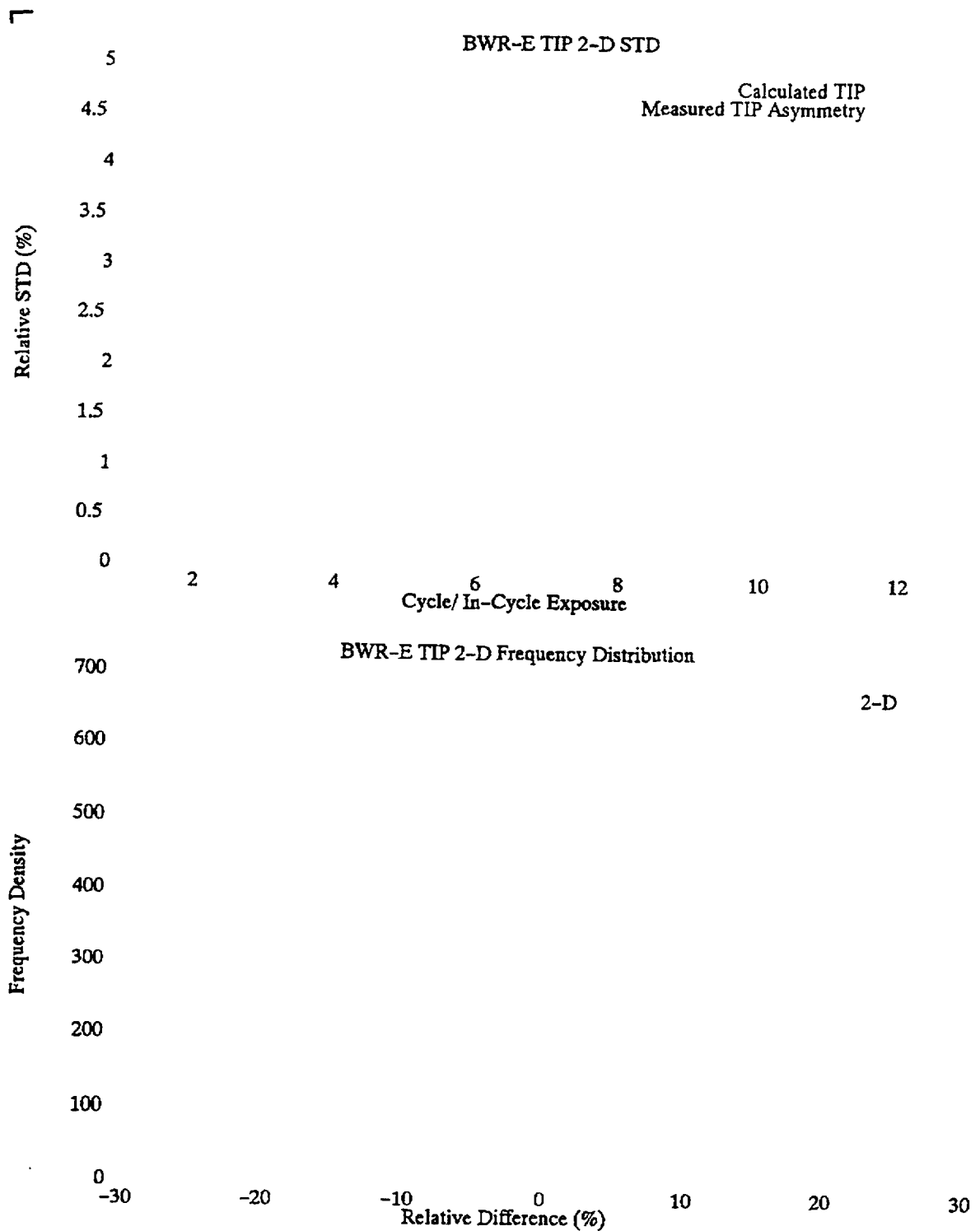
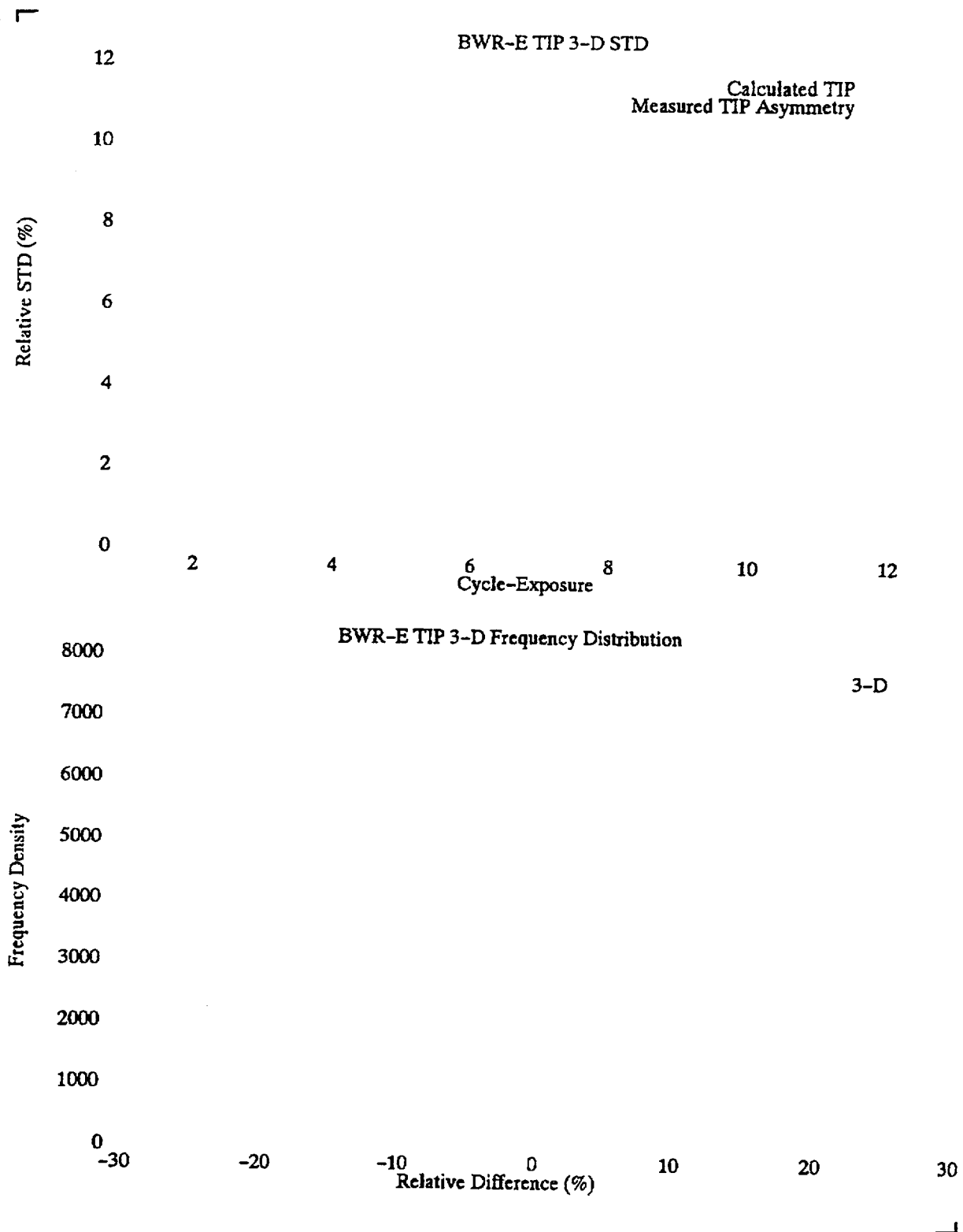
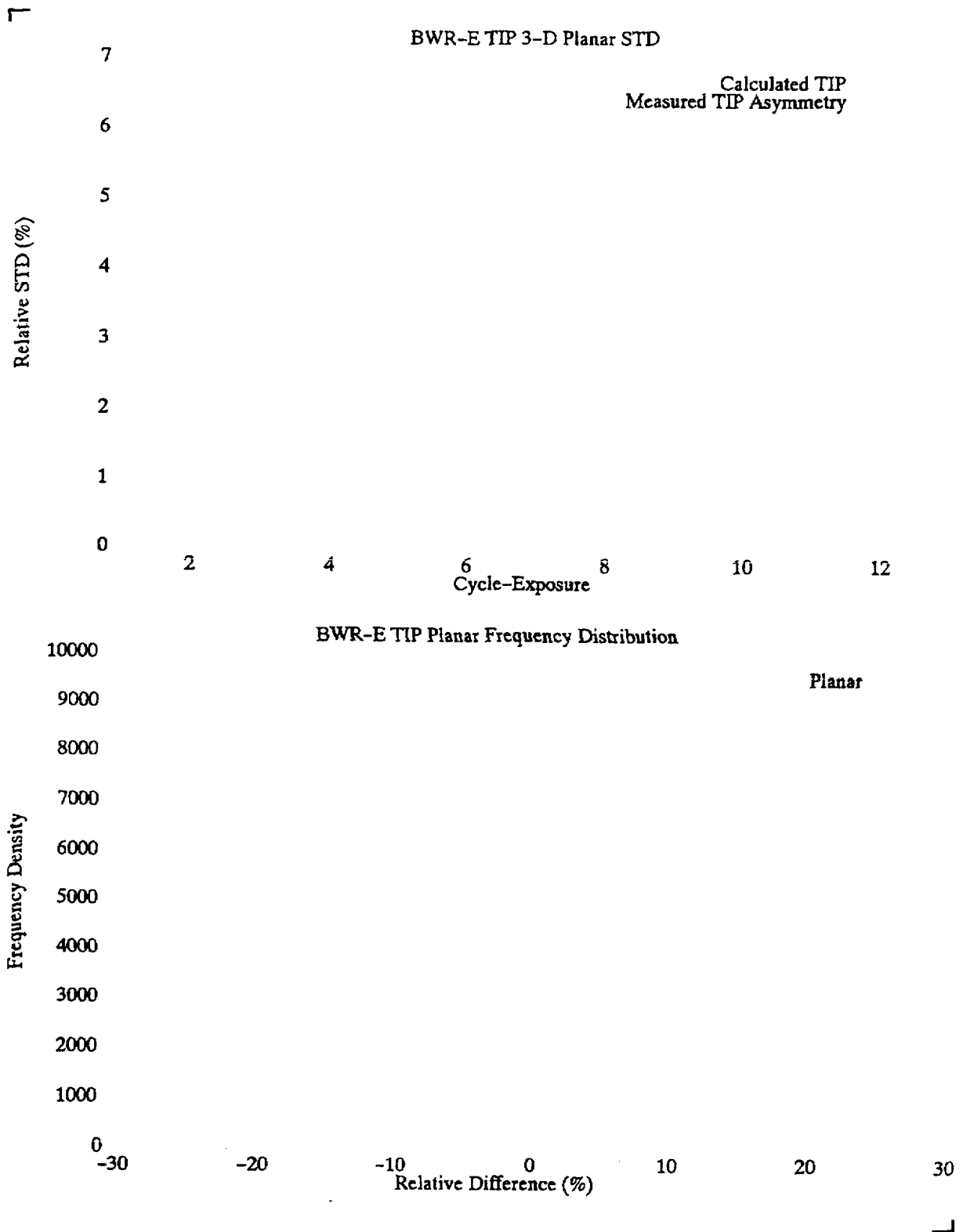


Figure 7.39 BWR – E TIP 2 – D Radial Relative Standard Deviations and Frequency Distribution of Relative Differences



**Figure 7.40 BWR – E TIP 3 – D Nodal Relative Standard Deviations and Frequency Distribution of Relative Differences**



**Figure 7.41 BWR – E TIP 3 – D Planar Relative Standard Deviations and Frequency Distribution of Relative Differences**

## 8. Validation of CASMO-4/MICROBURN-B2 BWR Pin Power Methodology

### 8.1 *Validation Against Higher Order Method*

Both CASMO - 3 and CASMO - 4 are multi - group transport codes and determine pin power distributions in a heterogeneous bundle. Both codes have been benchmarked against Monte Carlo codes for modern BWR fuel assemblies. The benchmarks indicate that the deviation of CASMO - 3 and CASMO - 4 from reference Monte Carlo results is of 1.0 % range, which is about the statistical uncertainty of Monte Carlo methods. Thus both CASMO - 3 and CASMO - 4 are acceptable higher order methods which can provide adequate references for benchmarking the pin power method in a core simulator.

A colorset geometry consists of four bundles facing each other in a configuration representative of real reactor fuel loadings. Each geometry forms a small core with an imposed boundary condition (usually reflective or periodic condition). These model cores are then burned for a typical BWR cycle length. To cover diverse loading configurations, many such geometries are analyzed. In particular, control blade history effect is thoroughly tested by varying controlled bundle initial exposure and duration of controlled depletion. For each geometry, a CASMO - 3 or CASMO - 4 calculation is run and generates reference solution (core k - effectives, bundle powers, and pin power distributions). The same geometry is run with MICROBURN - B2 which uses standard two group cross section libraries from single bundle calculations. MICROBURN - B2 calculations are done with the same coolant density and fuel temperature as used by CASMO. Two examples of colorset geometries are shown in Figure 8.1.

Table 8.1 describes colorset geometries used for validation. A total of 14 colorsets were simulated. Bundle types used in this simulation are 8x8 - 2, 9x9 - 2, 9x9 - 1, 9x9 - 5, and 10x10 - 9. All of these bundles have gadolinia pins loaded in various locations of simulated bundles. Five colorsets contain [

]. Eight colorsets simulate controlled depletion up to [ ].

Control blade is withdrawn at the end of controlled depletion generating large power spikes in bundles experiencing control blade history effect. The colorset simulation of control blade history effect is more rigorous and realistic than a single bundle controlled depletion simulation.

Table 8.2 presents results of validation. The overall absolute standard deviation in local pin power is [ ] for approximately 40,000 data points.

] This satisfies the validation requirement set forth in Section 5.2.4.





uncertainty generated in this conversion process is included in the results of comparison between measured and calculated Ba - 140 density distributions.

Quad Cities Unit 1 gamma scan measurements of pin power distribution were performed at EOC 2 and EOC 3 (Reference NO TAG). The two gamma scan campaigns yielded 8 full bundle measurements which are adopted for the current validation. The bundles were 7x7 and 8x8 lattice types. Two of the bundles contained 10 PuO<sub>2</sub> fuel rods (out of a total of 49 fuel rods). The measurement was made at 8 axial elevations with reported measurement uncertainty of 1.7 %. The measurement also reports a measurement uncertainty of 1.2 % for 4 axial elevation data which is derived by collapsing the 8 axial elevation data.

The result of comparison between measured and calculated Ba - 140 density distribution at 8 axial elevations is shown in Table 8.3 for EOC 2 and Table 8.4 for EOC 3. The overall relative standard deviation from the EOC 2 comparison without including MO2 bundle (GEB159) is [ ] for [ ] data points. The EOC 3 comparison without including MO2 bundle (GEB159) produces an overall relative standard deviation of [ ] for [ ] data points. The randomly combined EOC 2 and EOC 3 relative standard deviation without including MO2 bundles is [ ] for [ ] data points. The randomly combined EOC 2 and EOC 3 relative standard deviation with MO2 bundles included is [ ] for [ ] data points. The pure calculation uncertainty is [ ] for UO<sub>2</sub> bundles only and [ ] for UO<sub>2</sub> and MO2 bundles combined. A pin-by-pin comparison of Ba - 140 density is provided in Figure 8.2 through Figure 8.17 for 4 axial elevations.

### 8.2.2 KWU - S Measurement

The KWU - S gamma scan measurement of pin power distribution was performed at EOC 13 (Reference and NO TAG and NO TAG). One full MOX bundle and 3 half UO<sub>2</sub> bundles were measured at 4 axial elevations. In addition, a continuous axial measurement was performed for 16 fuel rods. The MOX bundle is [ ]

[ ] Two UO<sub>2</sub> bundles are a 9x9 lattice type with 4 gadolinia rods and 1 water rod. The remaining UO<sub>2</sub> bundle is 10x10 lattice type with 11 gadolinia rods and 9 water rods. The measurement uncertainty is conservatively assumed to be [ ].

The result of comparison between measured and calculated Ba - 140 density distribution is shown in Table 8.5. The overall relative standard deviation is [ ] for [ ] data points of UO<sub>2</sub> bundles and [ ] for [ ] data points of UO<sub>2</sub> and MOX bundles combined. The pure calculation uncertainty is [ ] for UO<sub>2</sub> bundles only and [ ] for UO<sub>2</sub> and MOX bundles combined. A pin-by-pin comparison of Ba - 140 density is provide in Figure 8.18 through Figure 8.24 for four axial elevations.

A comparison on the continuous axial measurement yields a statistical result provided in Table 8.6. Axial plots of calculated and measured Ba – 140 density distribution are provided in Figure 8.25 through Figure 8.31. This axial comparison is provided here as a supporting evidence of the axial TIP comparison. The calculated and the measured TIP comparisons adequately represent the axial power distribution uncertainty. Thus there is no validation requirement on the axial comparison of measured Ba – 140 density distribution. The uncertainty of the axial Ba – 140 distribution is very close to the axial TIP uncertainty given in Section 7. The overall agreement shown in the accompanied plots is satisfactory.

**Table 8.3 Summary of Quad Cities Unit 1 EOC 2 Pin Power Benchmark**

**Table 8.4 Summary of Quad Cities Unit 1 EOC 3 Pin Power Benchmark**

**Table 8.5 Summary of KWU-S EOC 13 Pin Power Benchmark**

**Table 8.6 Summary of KWU-S EOC 13 Axially Continuous Pin Power Benchmark**


┌

└

**Figure 8.2 Quad Cities Unit 1 EOC2 Bundle CX672 Pin Power Comparison for Axial  
Level 1 and 2**

┌

└

**Figure 8.3 Quad Cities Unit 1 EOC2 Bundle CX672 Pin Power Comparison for Axial  
Level 3 and 4**

┌

└

**Figure 8.4 Quad Cities Unit 1 EOC2 Bundle GEH02 Pin Power Comparison for Axial  
Level 1 and 2**

┌

└

**Figure 8.5 Quad Cities Unit 1 EOC2 Bundle GEH02 Pin Power Comparison for Axial  
Level 3 and 4**

┌

└

**Figure 8.6 Quad Cities Unit 1 EOC2 Bundle CX214 Pin Power Comparison for Axial  
Level 1 and 2**

┌

└

**Figure 8.7 Quad Cities Unit 1 EOC2 Bundle CX214 Pin Power Comparison for Axial  
Level 3 and 4**

┌

└

**Figure 8.8 Quad Cities Unit 1 EOC2 Bundle GEB159 Pin Power Comparison for Axial  
Level 1 and 2**

┌

└

**Figure 8.9 Quad Cities Unit 1 EOC2 Bundle GEB159 Pin Power Comparison for Axial  
Level 3 and 4**

┌

└

**Figure 8.10 Quad Cities Unit 1 EOC3 Bundle L2593 Pin Power Comparison for Axial  
Level 1 and 2**

┌

└

**Figure 8.11 Quad Cities Unit 1 EOC3 Bundle L2593 Pin Power Comparison for Axial  
Level 3 and 4**

┌

└

**Figure 8.12 Quad Cities Unit 1 EOC3 Bundle GEB159 Pin Power Comparison for  
Axial Level 1 and 2**

┌

└

**Figure 8.13 Quad Cities Unit 1 EOC3 Bundle GEB159 Pin Power Comparison for  
Axial Level 3 and 4**

└

└

**Figure 8.14 Quad Cities Unit 1 EOC3 Bundle GEH06 Pin Power Comparison for Axial  
Level 1 and 2**

┌

└

**Figure 8.15 Quad Cities Unit 1 EOC3 Bundle GEH06 Pin Power Comparison for Axial  
Level 3 and 4**

┌

└

**Figure 8.16 Quad Cities Unit 1 EOC3 Bundle L2532 Pin Power Comparison for Axial  
Level 1 and 2**

┌

└

**Figure 8.17 Quad Cities Unit 1 EOC3 Bundle L2532 Pin Power Comparison for Axial  
Level 3 and 4**

┌

└

**Figure 8.18 KWU – S EOC 13 Bundle B91427 Pin Power Comparison for Axial Level 1  
and 2**

┌

└

**Figure 8.19 KWU – S EOC 13 Bundle B91427 Pin Power Comparison for Axial Level 3  
and 4**

┌

└

**Figure 8.20 KWU – S EOC 13 Bundle B59006 Pin Power Comparison for Axial Level 1  
and 2**

┌

└

**Figure 8.21 KWU – S EOC 13 Bundle B59006 Pin Power Comparison for Axial Level 3  
and 4**

┌

└

**Figure 8.22 KWU – S EOC 13 Bundle B11330 Pin Power Comparison for Axial Level 1**

┌

└

**Figure 8.23 KWU – S EOC 13 Bundle B58102 Pin Power Comparison for Axial Level 1  
and 2**

┌

└

**Figure 8.24 KWU – S EOC 13 Bundle B58102 Pin Power Comparison for Axial Level 3  
and 4**

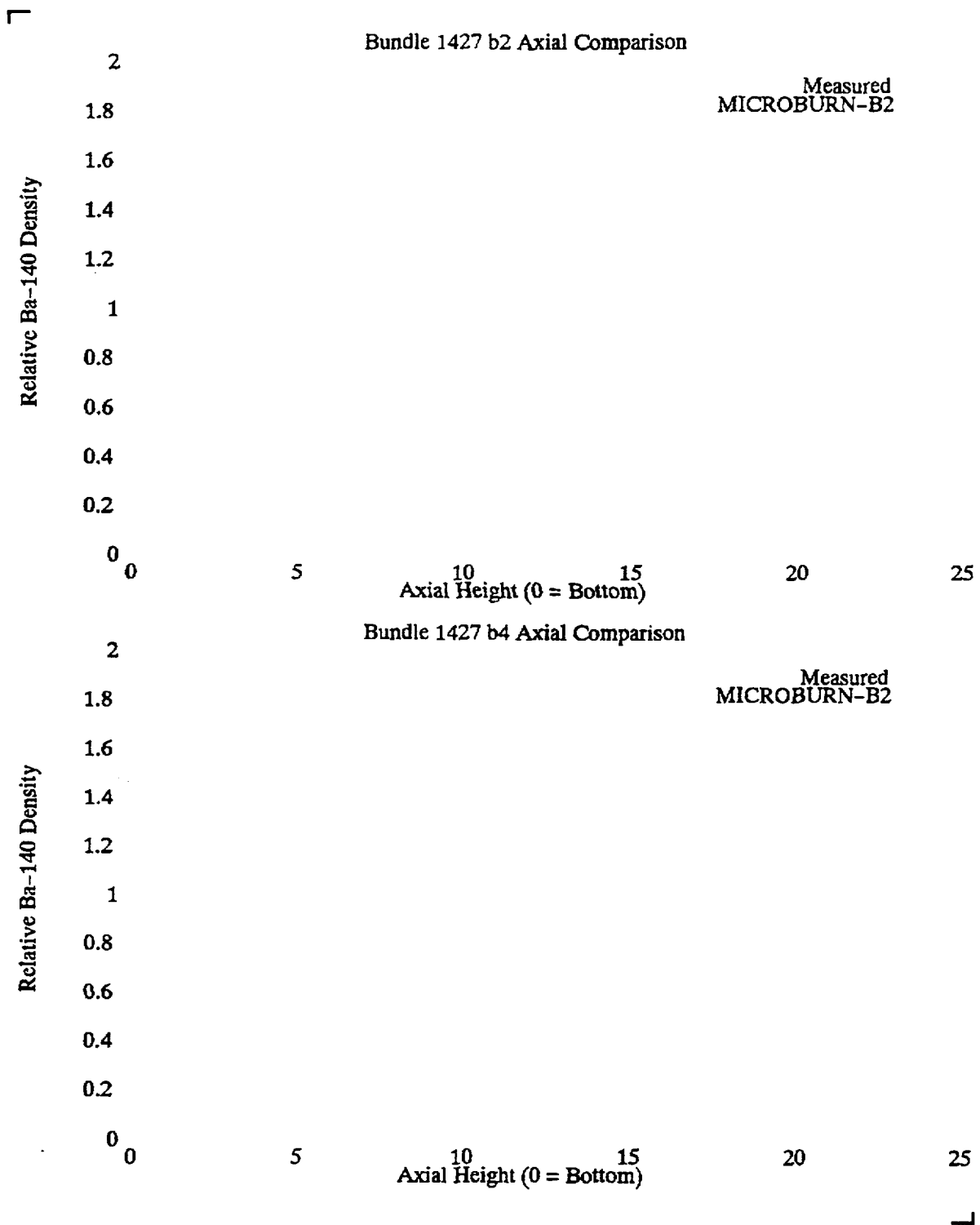


Figure 8.25 KWU - S EOC 13 Bundle B91427 Rod B2 and Rod B4 Axial Ba - 140  
 Distribution Comparison

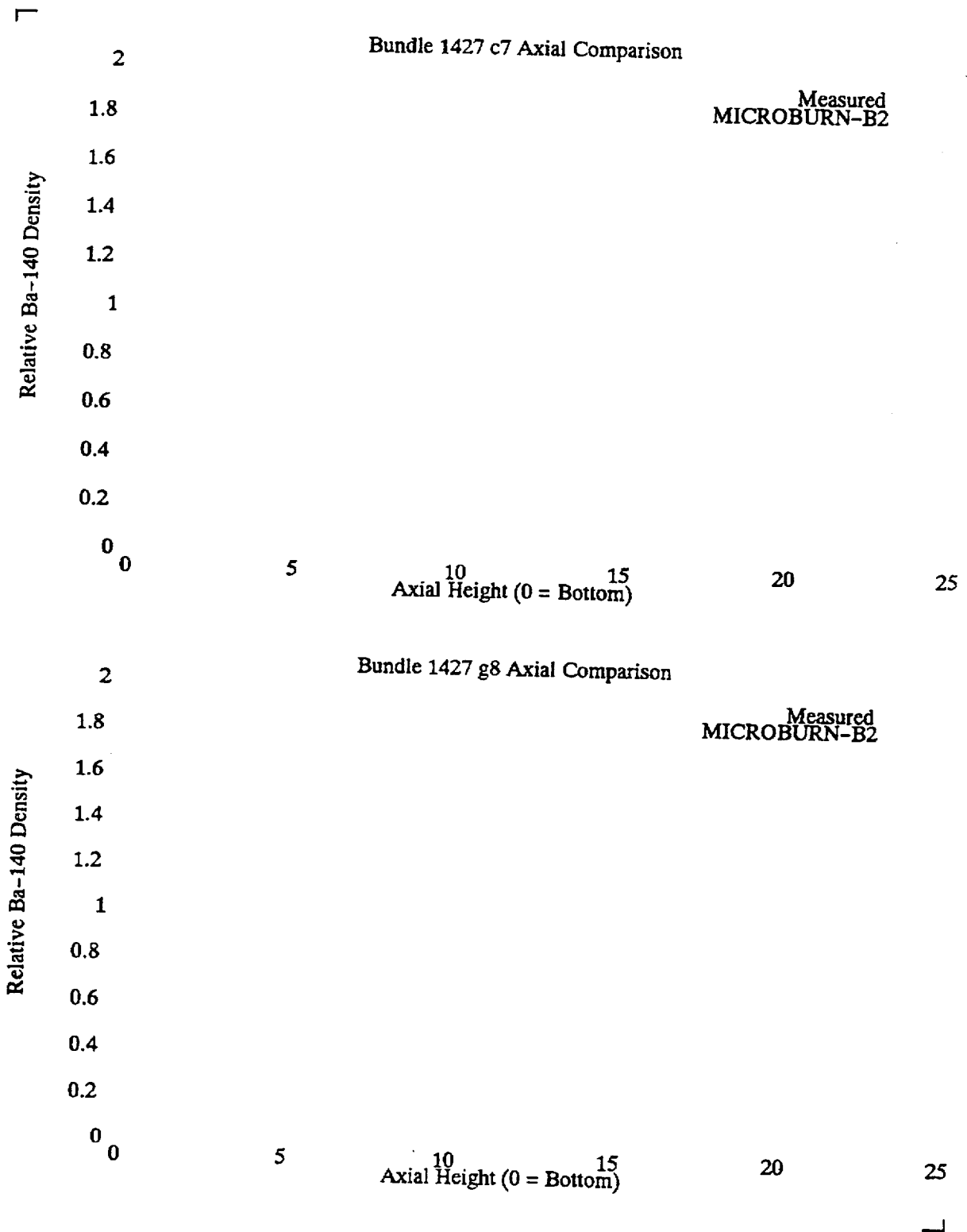
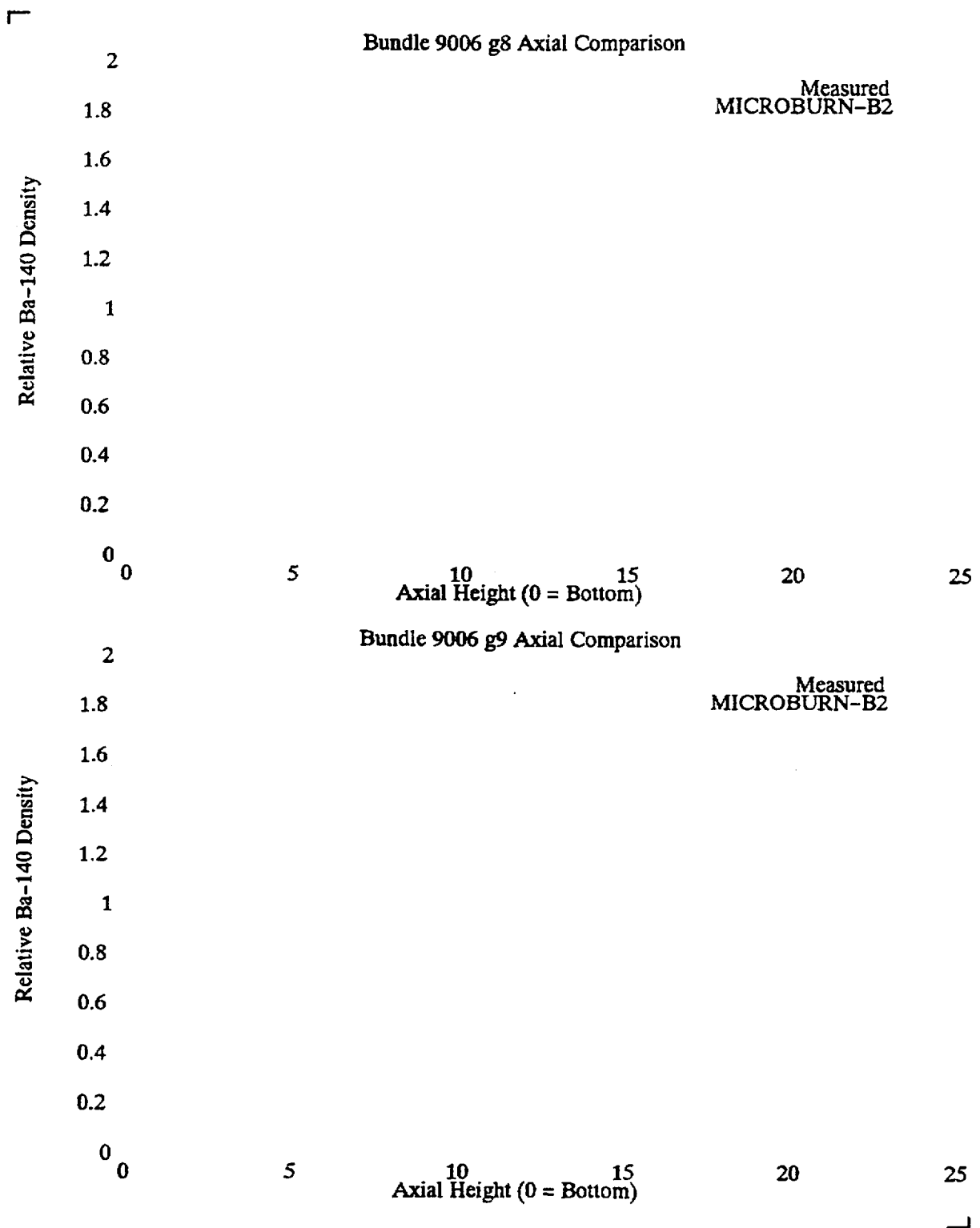
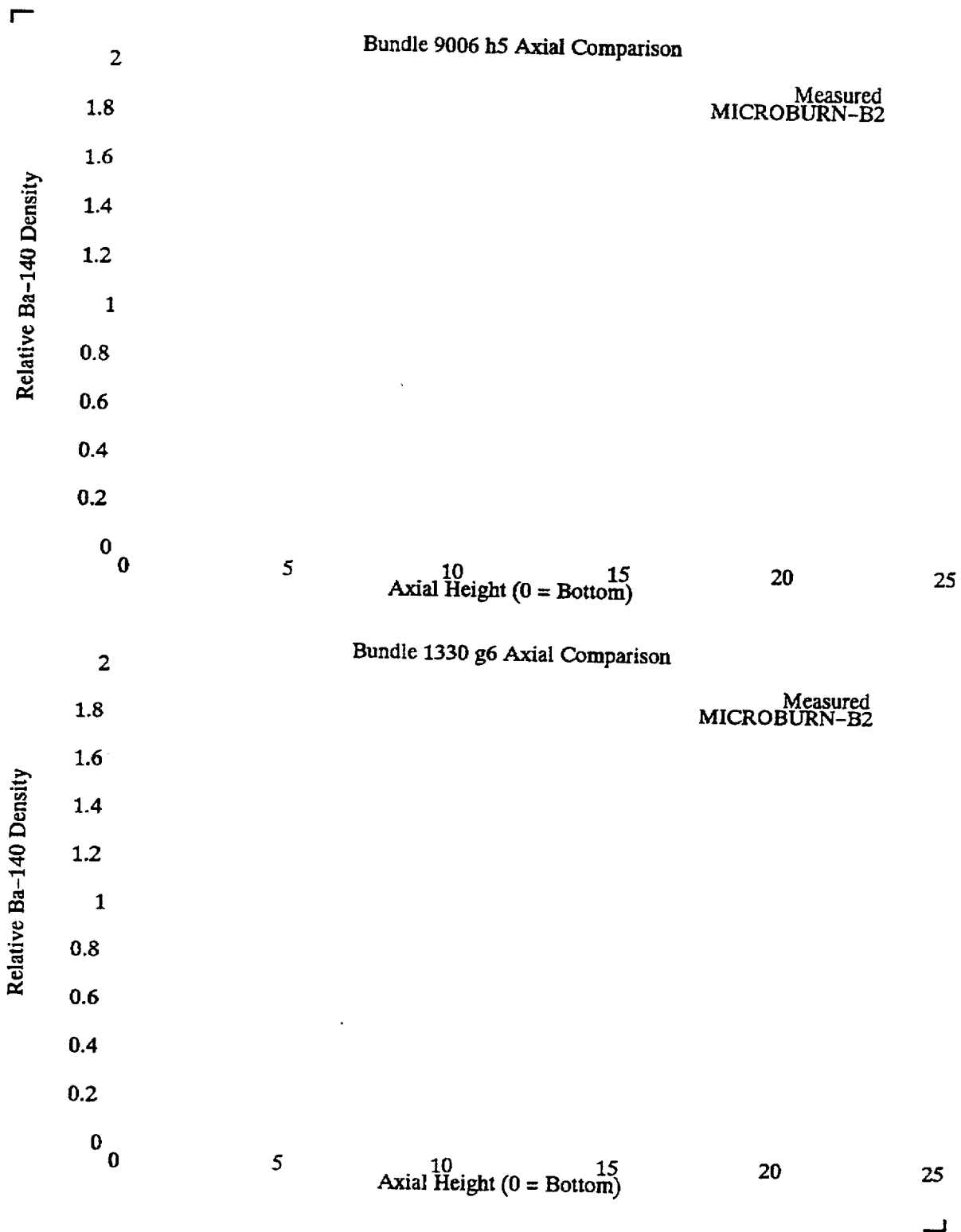


Figure 8.26 KWU-S EOC 13 Bundle B91427 Rod C7 and Rod G8 Axial Ba - 140 Distribution Comparison



**Figure 8.27 KWU - S EOC 13 Bundle B59006 Rod G8 and Rod G9 Axial Ba - 140 Distribution Comparison**



**Figure 8.28 KWU – S EOC 13 Bundle B59006 Rod H5 and Bundle B11330 Rod G6  
 Axial Ba – 140 Distribution Comparison**

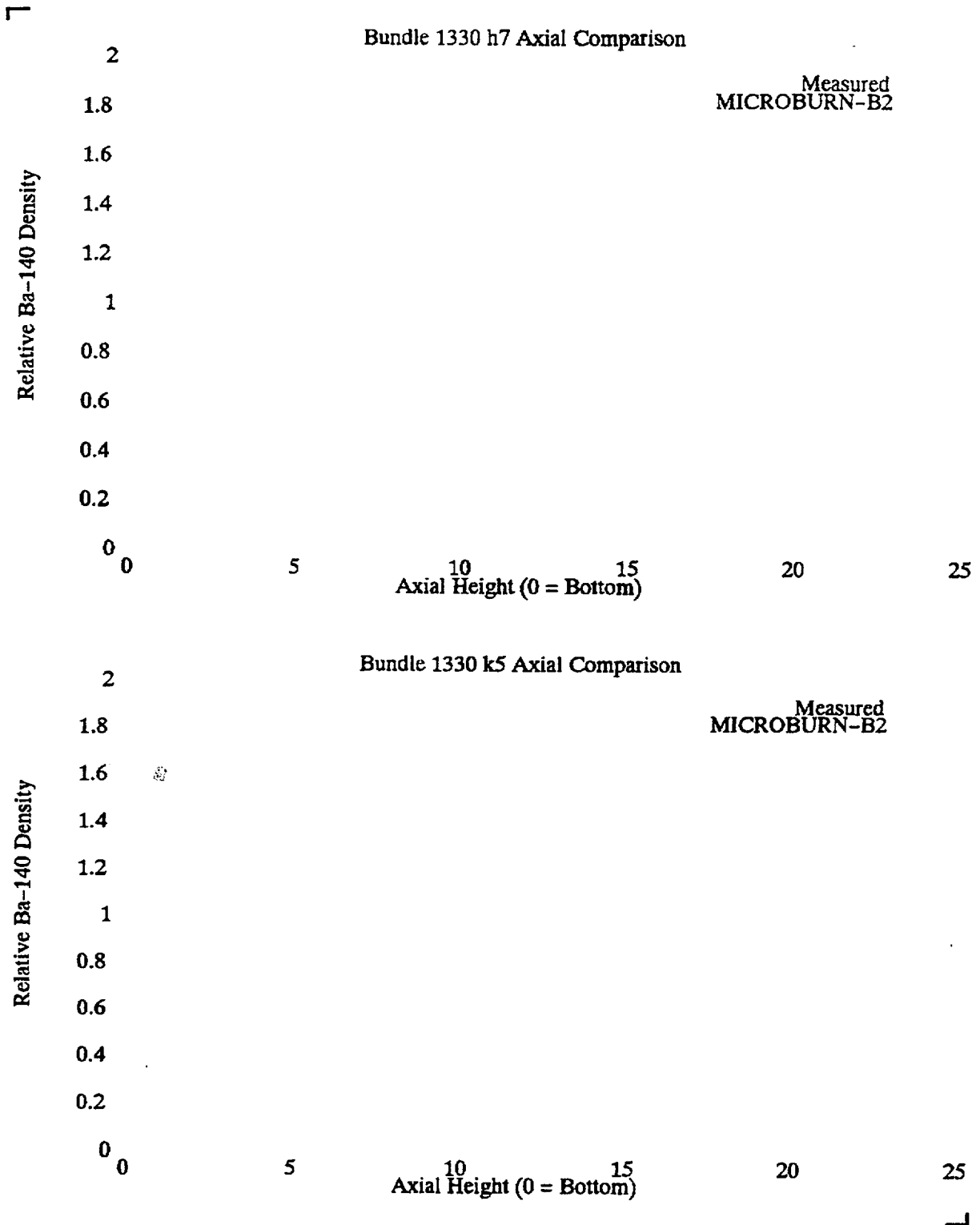


Figure 8.29 KWU-S EOC 13 Bundle B11330 Rod H7 and Rod K5 Axial Ba-140 Distribution Comparison

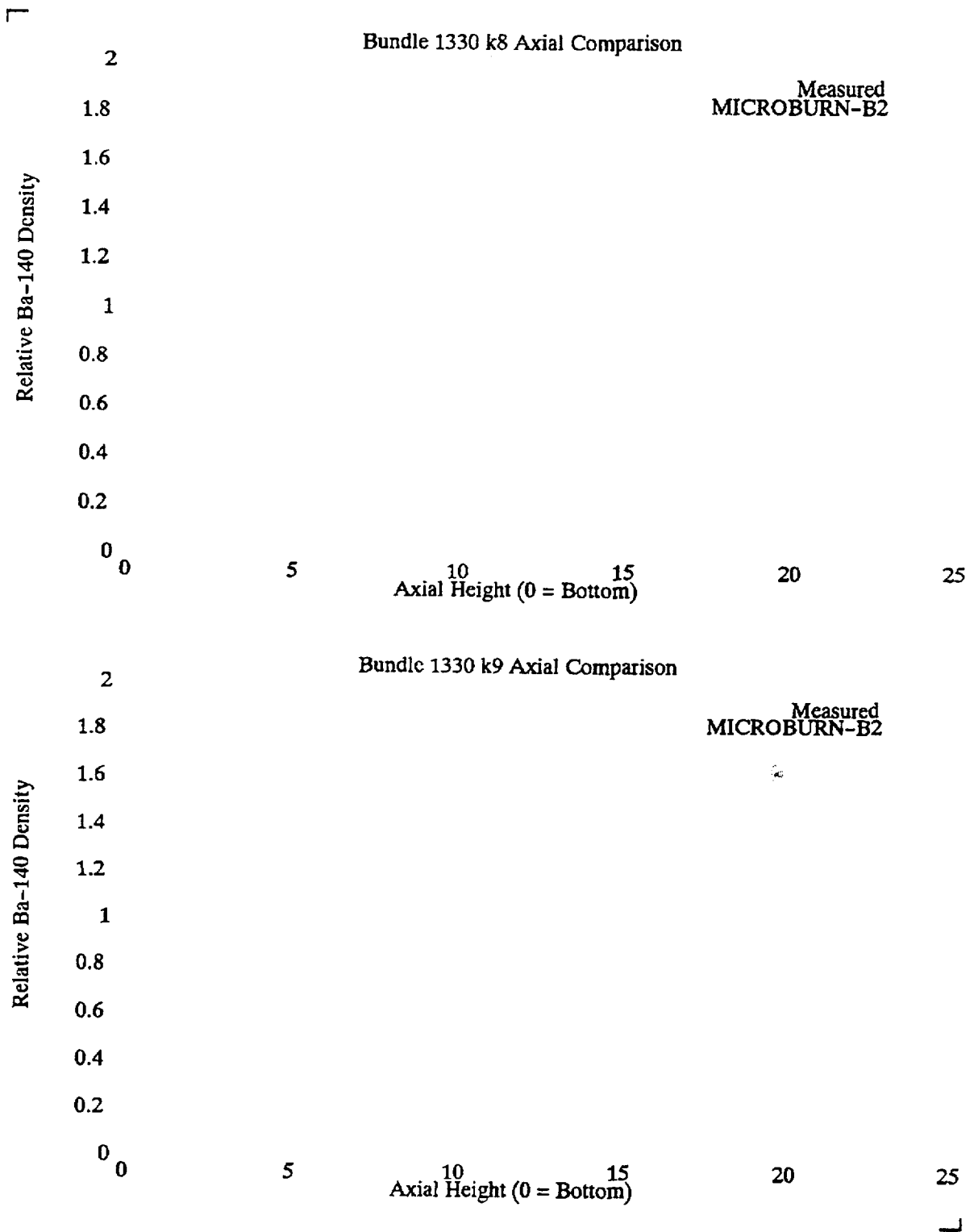


Figure 8.30 KWU-S EOC 13 Bundle B11330 Rod K8 and Rod K9 Axial Ba-140  
 Distribution Comparison

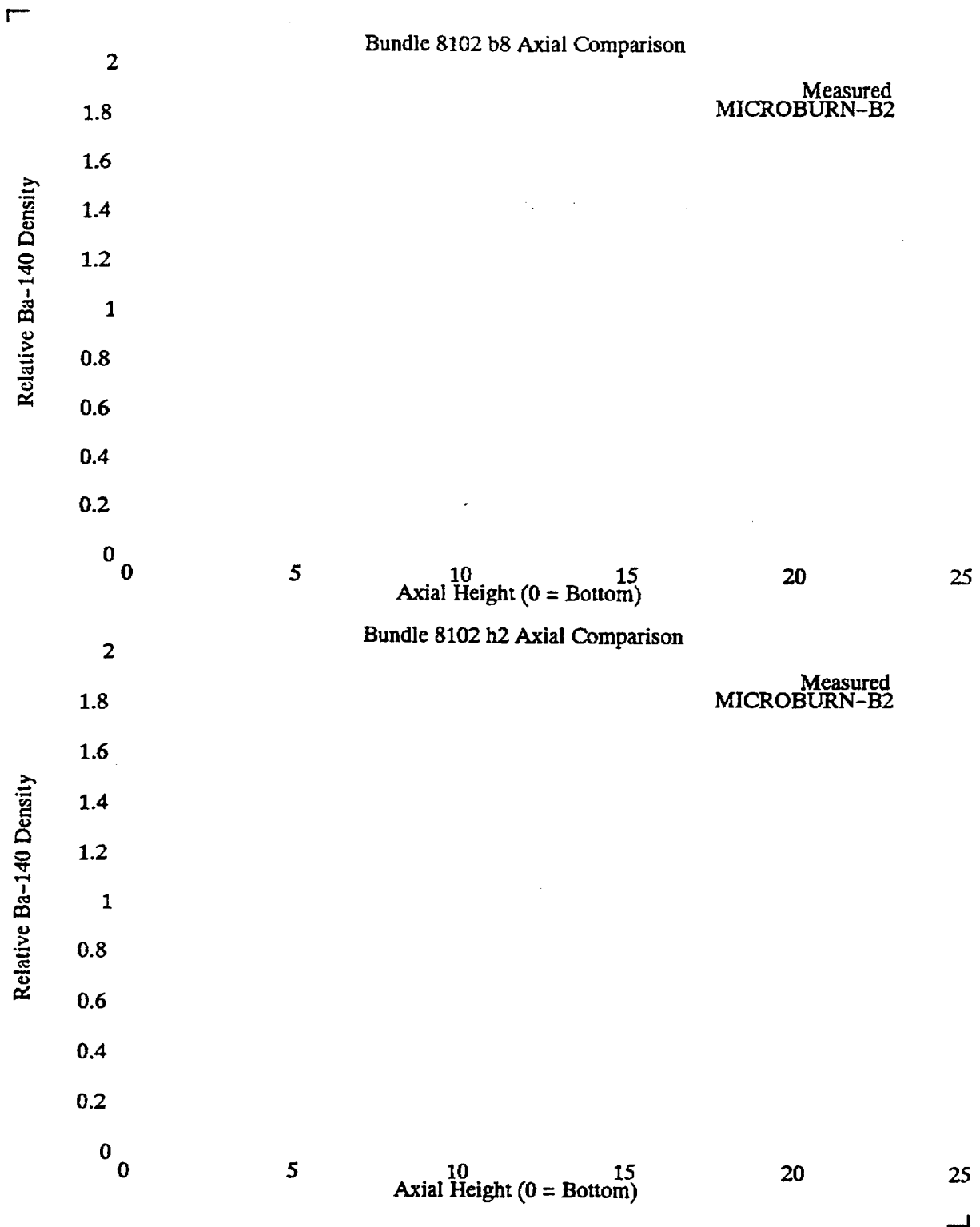


Figure 8.31 KWU-S EOC 13 Bundle B58102 Rod B8 and Rod H2 Axial Ba-140  
 Distribution Comparison

## 9. Verification of CASMO-4/MICROBURN-B2 Measured Power Distribution Uncertainty

### 9.1 Statistical Analysis of Measured Power Distribution Uncertainty

The SPC methodology for measuring the power distribution in a BWR reactor and the procedure by which the uncertainty associated with the measurement of a BWR power distribution would be determined was originally described in Reference 5. The statistical analysis procedure as described in this approved reference is employed to determine the uncertainties in the measured power distribution of the CASMO - 4/MICROBURN - B2 code system.

The accepted procedure for determining measured power distribution is as follows:

1. The gain adjustment factor for each fixed in-core detector LPRM is determined during the periodic TIP measurement (OD-1).
2. Gain on LPRM detectors is adjusted based on gain adjustment factors from a previous TIP measurement (OD-7).
3. LPRM detector response distribution is measured in the fixed instrument locations.
4. A calculated TIP distribution is determined by the core simulator at the core condition corresponding to (3) above.
5. A measured TIP response distribution is determined by synthesizing the calculated TIP response distribution and the measured LPRM response distribution.
6. A measured nodal power distribution is determined by multiplying the calculated nodal power to detector response ratios by the measured TIP response distribution.

The synthesis of the measured LPRM detector response distribution, the calculated TIP distribution, and the calculated nodal power distribution is described by the following equation:

$$\left[ \right. \quad \quad \quad \left. \right] \quad (9 - 1)$$

where

$P_{ijk}^n$  = measured nodal power distribution where i and j indicate the radial location and k denotes the axial elevation

$B_{ijk}$  = calculated nodal relative power distribution





$dx_n, dy_n$  = differences between calculated and measured nodal powers for radially adjacent nodes

The correlation coefficient is determined from the comparison of the calculated power distribution to the available bundle gamma scan measurement. The uncertainty in the calculated bundle power distribution is similarly determined:

┌

(9 - 11)

└

The nodal synthesized TIP uncertainty is determined by a combination of three component uncertainties:

┌

(9 - 12)

where

└

$\delta D_{ijk}$  = relative standard deviation in the synthesized nodal TIP distribution

$\delta T_{ijk}^m$  = relative standard deviation in the nodal TIP measurement

$\delta LPRM$  = relative standard deviation in the measured LPRM response

$\delta S_{ijk}$  = TIP synthesis procedure uncertainty

Similarly, the bundle average synthesized TIP uncertainty is determined by,

┌

(9 - 13)

└

The measured TIP uncertainty is determined by comparing symmetric TIP pairs measured for cores with diagonal core symmetry loading and diagonal core symmetry rod pattern. The measured TIP uncertainty on the nodal basis is thus given by,

┌

(9 - 14)

where

└

$d_{ik}$  = relative difference between a symmetric pair at a radial location  $i$  and axial level  $k$

$IK$  = number of symmetric TIP pairs times the number of axial levels (excluding top two and bottom two nodes)

The measured TIP uncertainty on the 2-dimensional radial basis and that on the planar basis are similarly defined:

┌

(9 - 15)

(9 - 16)

└

The uncertainty in the LPRM detector response was determined to be 3.4 % by General Electric in Reference 21. The uncertainty in the synthesis of the TIP distribution is given by,

┌

(9 - 17)

where

└

$d_{ijk}$  = relative difference between the measured and the synthesized nodal TIP distribution

The uncertainty in the synthesized 2-D TIP distribution is defined in a similar manner:

┌

(9 - 18)

└

The calculated TIP uncertainty on the nodal basis is given by,

┌

(9 - 19)

where

└

$\delta T'_{ijk}$  = relative standard deviation in the calculated nodal TIP distribution including the measurement uncertainty

The calculated TIP uncertainty including the measurement uncertainty is determined by comparing the core simulator predicted TIP distribution to the one measured:

(9-20)

where

$d_{ijk}$  = relative difference between  $T'_{ijk}$  and  $T^m_{ijk}$

Similarly, the 2-dimensional radial calculated TIP uncertainty is determined by comparing the radial distribution of the calculated TIP to that of the measured TIP:

(9-21)

(9-22)

The calculational uncertainty in the bundle maximum pin power is obtained by subtracting the measurement uncertainty from the overall calculation uncertainty:

(9-23)

where

$d_{ij}$  = relative difference between calculated and measured pin power distributions

$\delta_{Lm}$  = uncertainty (relative standard deviation) in the measured pin power distribution

## 9.2 Data Base for Verification of Measured Power Distribution Uncertainty

A data base which is used for verifying the measured power distribution uncertainty of the CASMO-4/MICROBURN-B2 code system is presented in Table 9.1. The data base for



### 9.3 Verification of Predicted Local Pin Power Distribution Uncertainty

The standard deviation of relative differences between calculated pin power and the measured pin power distribution is provided in Table 8.3 and Table 8.4 for the Quad Cities Unit 1 EOC 2 and EOC 3 measurements and in Table 8.5 for the KWU-S EOC 13 measurement. The standard deviation of differences is [ ] for the Quad Cities Unit 1 EOC 2, [ ] for the Quad Cities Unit 1 EOC 3, and [ ] for the KWU-S EOC 13. The measurement uncertainty is [ ] for the Quad Cities Unit 1 measurement and [ ] for the KWU-S measurement. The net calculation uncertainty is computed to be [ ] with [ ] data points for Quad Cities Unit 1 EOC 2 and EOC 3 combined and [ ] for [ ] data points. The combined standard deviation of relative differences is [ ] for a total of [ ] data points.

### 9.4 Verification of Calculated TIP Distribution Uncertainty

MICROBURN-B2 core follow calculations and the comparison of calculated TIP distributions with measurements are described in Section 7. The resulting standard deviations of relative differences between calculated and measured TIP data at each measured exposure point are provided in Table 9.2 through Table 9.7. These tables also provide the TIP measurement uncertainties determined using Eq. (9-14) to Eq. (9-16) and the LPRM synthesized TIP uncertainty determined using Eq. (9-17) and Eq. (9-18). The combined uncertainties for all the reactors are provided as follows:

#### TIP Distribution Calculation

$\delta T'_{ijk}$  (nodal)

[

]

$\delta T'_{ij}$  (radial)

[

]

$\delta T'_{planar}$  (planar)

[

]

#### TIP Distribution Measurement

$\delta T^m_{ijk}$  (nodal)

[

$$\delta T_{ij}^m \text{ (radial)}$$

[

$$\delta T_{planar}^m \text{ (planar)}$$

[

Net Calculated TIP Distribution

$$\delta T_{ijk} \text{ (nodal)}$$

[

$$\delta T_{ij} \text{ (radial)}$$

[

$$\delta T_{planar} \text{ (planar)}$$

[

**9.5 Verification of Synthesized TIP Distribution Uncertainty**

The synthesized TIP distribution uncertainty is determined by Eq. (9-12) for the nodal distribution and by Eq. (9-13) for the 2-dimensional radial distribution. Among the three component uncertainties used in these equations, only the synthesis procedure uncertainty is dependent on the predictive accuracy of the new code system. The synthesis procedure uncertainty determined by using Eq. (9-17) and Eq. (9-18) is as follows:

[

]

[

]

Combining two other component uncertainties, the synthesized TIP distribution uncertainty is determined as follows:

[  
]  
[  
]

### 9.6 *Verification of Calculated Bundle Power Distribution Uncertainty*

The bundle-wise Ba-140 distribution measurements at EOC 2 and EOC 4 of Quad Cities Unit 1 were analyzed using the CASMO-4/MICROBURN-B2 code system. Figure 9.1 and Figure 9.2 present comparisons between the measured and predicted bundle Ba-140 distributions at EOC 2 and EOC 4. The radial standard deviation of relative differences are [ ] at EOC 2 and [ ] at EOC 4. The 3-D planar standard deviation of relative differences are [ ] at EOC 2 and [ ] at EOC 4. The radial bundle power correlation coefficients ( $\rho_{ij}$ ) are [ ] at EOC 2 and [ ] at EOC 4. The 3-D planar power correlation coefficients ( $\rho_{ijk}$ ) are [ ] at EOC 2 and [ ] at EOC 4. The combined overall radial and planar correlation coefficients are respectively [ ] and [ ]. The calculated TIP distribution uncertainties were determined Section 9.5. The calculated power uncertainties,  $\delta B_{ijk}$  and  $\delta B_{ij}$ , are then determined by using Eq. (9-9) and Eq. (9-11):

┌

└

### 9.7 *Verification of Measured Power Uncertainty*

The measured power distribution uncertainty is determined by combining all of the components determined above. Table 9.8 provides a collection of the component

uncertainties. The measured power uncertainties are determined by Eq. (9-5) through Eq. (9-8) using the component uncertainties:

Measured 3-D Nodal Power

[  
]

Measured 2-D Radial Power

[  
]

Measured 3-D Nodal Pin Power

[  
]

Measured 2-D Radial Pin Power

[  
]

The measured power distribution uncertainties for the new code system and the acceptance criteria set forth in Section 5.3 are provided in Table 9.9. It is verified that the new code system produces measured power distribution uncertainties less than the acceptance criteria.

**Table 9.2 BWR – A TIP Standard Deviation of Relative Differences**

┌

└

**Table 9.2 BWR – A TIP Standard Deviation of Relative Differences  
(continued)**

┌

└

Table 9.3 BWR – B TIP Standard Deviation of Relative Differences

┌

└

**Table 9.3 BWR – B TIP Standard Deviation of Relative Differences  
(continued)**

┌

└

**Table 9.3 BWR-B TIP Standard Deviation of Relative Differences  
(continued)**

┌

└

**Table 9.4 BWR – E TIP Standard Deviation of Relative Differences**

┌

└

**Table 9.4 BWR – E TIP Standard Deviation of Relative Differences  
(continued)**

┌

└

Table 9.5 KWU – S TIP Standard Deviation of Relative Differences

┌

└

**Table 9.5 KWU – S TIP Standard Deviation of Relative Differences  
(continued)**

┌

└

**Table 9.6 BWR – C TIP Standard Deviation of Relative Differences**

┌

└

**Table 9.7 BWR – D TIP Standard Deviation of Relative Differences**

┌

└

I

J

**Figure 9.1 Quad Cities Unit 1 EOC2 Assembly Ba – 140 Distribution Comparison**

┌

└

**Figure 9.2 Quad Cities Unit 1 EOC4 Assembly Ba – 140 Distribution Comparison**



**Table 9.8 Measured Power Distribution Uncertainty Components  
(continued)**

<u>Uncertainty Component</u>	<u>Relative Standard Deviation %</u>
----------------------------------	--

┌

└



**Table 9.9 Measured Power Distribution Uncertainty**

Type of Measured Power Distribution	Relative Standard Deviation (%)	
	MICROBURN-B2	Acceptance Criteria

## 10. References

1. D. Knott, B. H. Forssen, and M. Edenius, "CASMO-4. A Fuel Assembly Burnup Program: Methodology", STUDSVIK/ SOA-95/2, Studsvik Proprietary (September 1995).
2. H. Moon, "MICROBURN-B2: Steady State BWR Core Physics Method." EMF-1833(P) Rev. 2, Siemens Power Corporation (September 1998).
3. M. Edenius, A. Ahlin, and H. Haggblom, "CASMO-3. A Fuel Assembly Burnup Program: Methodology", STUDSVIK/ NFA-86/8, Studsvik Proprietary (November 1986).
4. D. H. Timmons, "MICROBURN-B: A Two-Group, Three-Dimensional BWR Nodal Simulator Code." ANF-88-101 (P), Siemens Power Corporation (July 1988).
5. "Exxon Nuclear Methodology for Boiling Water Reactors - Neutronic Methods for Design and Analysis." XN-NF-80-19(A), Vol. 1 (March 1983), Supplement 1 & 2, and "Benchmark Results for the CASMO-3G/MICROBURN-B Calculation Methodology." XN-NF-80-19(P)(A), Vol. 1, Supplement 3 & 4 (November 1990).
6. R. E. MacFarlane, D. W. Muir, and R. M. Boicourt, "The NJOY Nuclear Data Processing System, Volume 1: User's Manual." LA-9303-M (1982).
7. R. Persson, E. Blomsjo, and M. Edenius, "High-temperature critical experiments with H<sub>2</sub>O-moderated fuel assemblies in KRITZ." Tech. Mtg. No. 2/11, NUCLEX 72 (1972).
8. L. W. Newman, "Urania-Gadolinia: Nuclear Model Development and Critical Experiment Benchmark." BAW-1810, B&W Co. (April 1984).
9. R. J. Nodvik et al., "Evaluation of Mass Spectrometric and Radiochemical Analyses of Yankee Core 1 Spent Fuel." WCAP-6068 (1966).
10. J. Briesmeister, "MCNP-A General Monte Carlo Code for Neutron and Photon Transport, Version 3A." LA-7396-M Rev. 2 (1992).
11. General Electric Co., "Quad Cities Nuclear and Fuel Performance Measurements." EPRI NP-3568, Electric Power Research Institute (July 1984).
12. H. Haggblom, "The CASMO-3 Nuclear Data Library." STUDSVIK/ NFA-86/12, Studsvik Proprietary (October, 1986).
13. D. Knott, J. A. Umbarger, and M. Edenius, "CASMO-4 Benchmark Against Critical Experiments." STUDSVIK/ SOA-94/13, Studsvik Proprietary (December 1995).
14. D. Knott, J. A. Umbarger, and M. Edenius, "CASMO-4 Benchmark Against MCNP." STUDSVIK/ SOA-94/12, Studsvik Proprietary (December 1995).
15. Kim Ekberg, "CASMO-4 Benchmark Against Yankee Rowe Isotopic Measurements." STUDSVIK/ SCOAB-96/5, Studsvik Proprietary (December 1996).

16. H. Moon, B. Burdick, and D. H. Timmons, "Recent Improvements in MICROBURN-B Boiling Water Reactor Simulation Method," Proceeds. Int. Conf. Math. & Comp., Reactor Phys. and Env. Anal., Vol.1, P. 39, Portland (May 1995).
17. H. Moon, "Advanced Core Design Using MICROBURN-B2 BWR Core Simulator," Proc. Am. Nucl. Soc. Top. Mtg. - Adv. in Nucl. Fuel Management II, TR-107728-V1, EPRI (March 1997).
18. St. Misu, "Methoden und Qualifikation des Auslegungssystems CASMO-3/MICROBURN-B2." A1C-1301817-0, Siemens Proprietary (December 1996).
19. Bezold, et. al., "Gamma Scan in GUN-B an MOX/Uran 9-1 Brennelementen Durchführung und Auswertubg der Messungen," KWU NT22/98/64, Siemens Proprietary (October 1998).
20. Bezold, et. al., "Gamma Scan in GUN-B an einem Atrium 10 Brennelement Durchführung und Auswertubg der Messungen," KWU NT22/98/65, Siemens Proprietary (October 1998).
21. J. F. Carew, "Process Computer Performance Evaluation Accuracy." NEDO-20340, Generic Electric (June 1974).

## **APPENDIX A Illustration of CASMO-4/MICROBURN-B2 Application to BWR Core Neutronic Designs**

The goal of BWR fuel cycle design is to develop a combination of a fuel loading pattern and a control rod operation scheme that satisfies the plant operator specified fuel cycle energy requirements for the cycle. The cycle energy requirement is satisfied by installing enough reactivity in new fuel assemblies, and by judiciously placing them along with the previously irradiated assemblies such that the core remains operable throughout the cycle. The fuel cycle design must provide for an adequate margin to fuel thermal limits and reactivity margin constraints as specified in the plant technical specifications. The adequacy of operating margin to fuel thermal limits is ensured by accurately modeling the proposed design during the design phase, and subsequently monitoring the actual operational progress throughout the cycle. The currently approved CASMO-3/MICROBURN-B code system has proven to be very reliable for this application. However, as discussed in this report, the CASMO-4/MICROBURN-B2 code system further improves the accuracy of the calculations that are to be utilized both for design of future cycles and monitoring of operating cycles.

To show the relative impact of the new code system as compared to the results obtained from the currently approved code system, a typical BWR fuel cycle is analyzed with both code systems. The results presented below were obtained from modeling the actual operating history of the BWR-A reactor in Cycle 7. This fuel cycle represents a typical sample of BWR operation, and the cycle was originally designed with the currently approved CASMO-3/MICROBURN-B code system. By comparing the thermal margin results calculated for this fuel cycle by the new code system to those obtained from the currently approved system, an indication of the anticipated impact of implementing the new code system is obtained. The results presented in Figure A.1 through Figure A.3 show the following:

- 1.
- 2.
- 3.

These results indicate that the new code system agrees well with the currently approved code system. Further, these results show that implementing the CASMO-4/MICROBURN-B code system with its inherent improved accuracy will not adversely impact the safety of fuel cycle operation and the accuracy of core monitoring analysis.

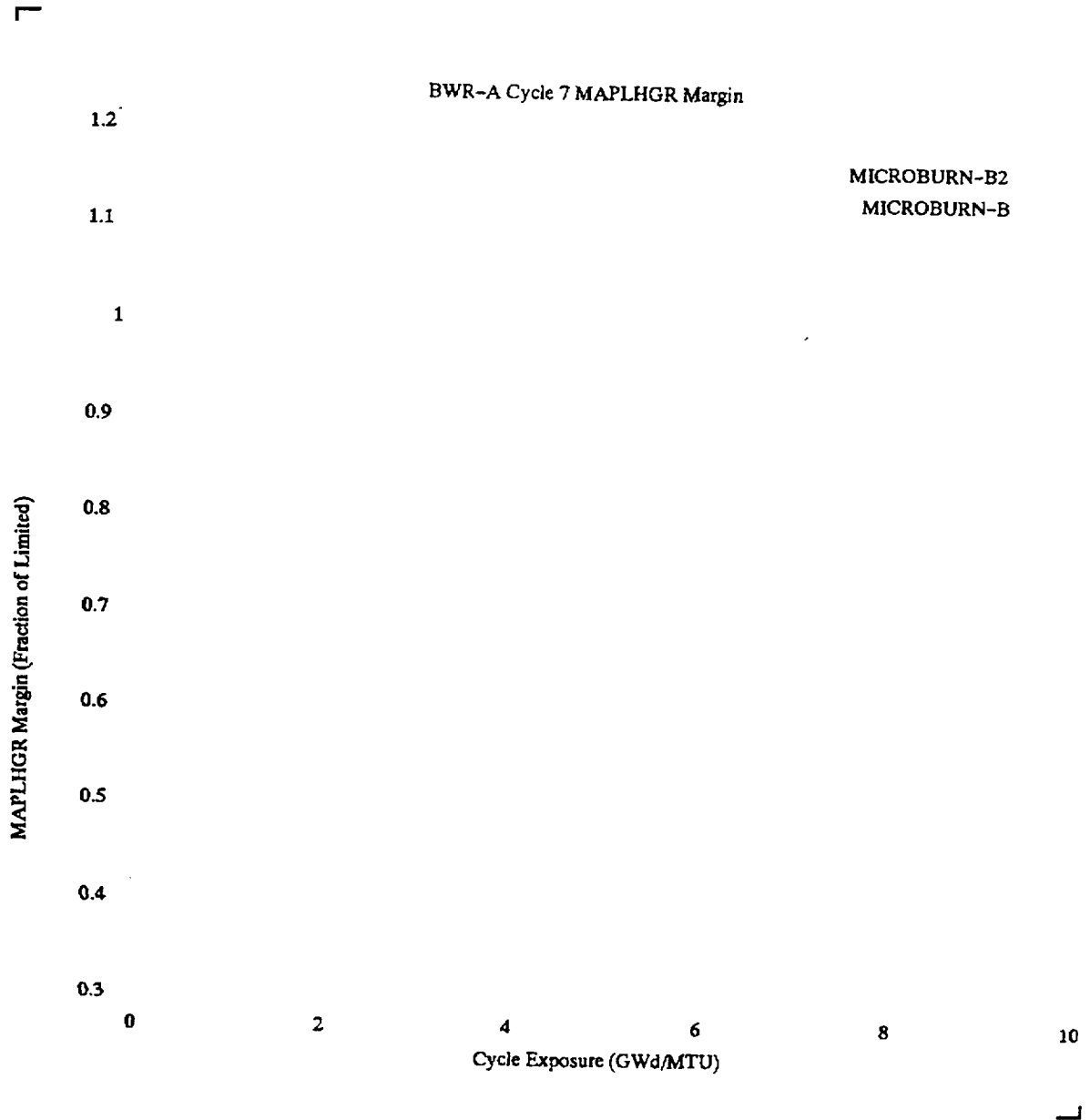
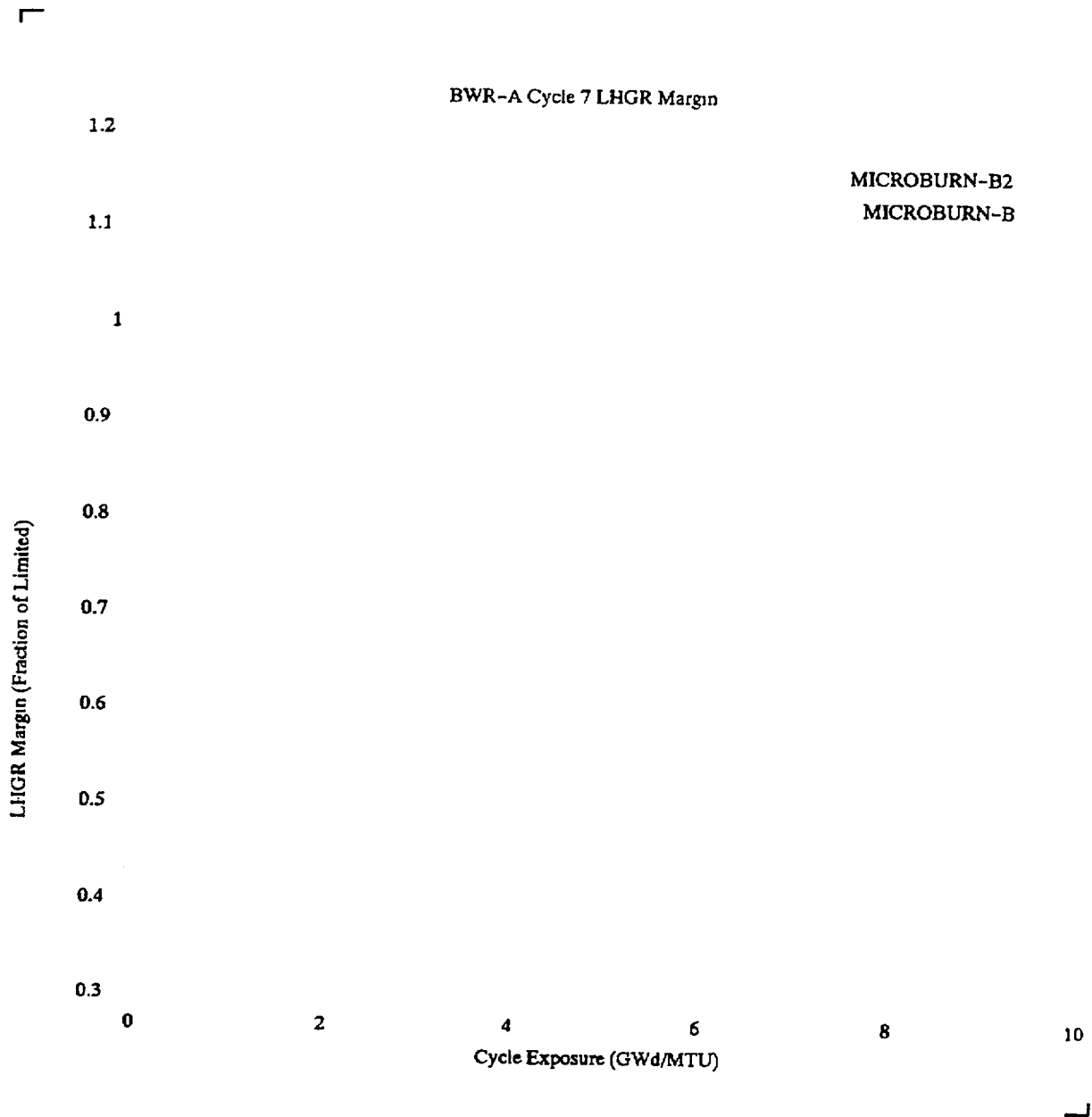
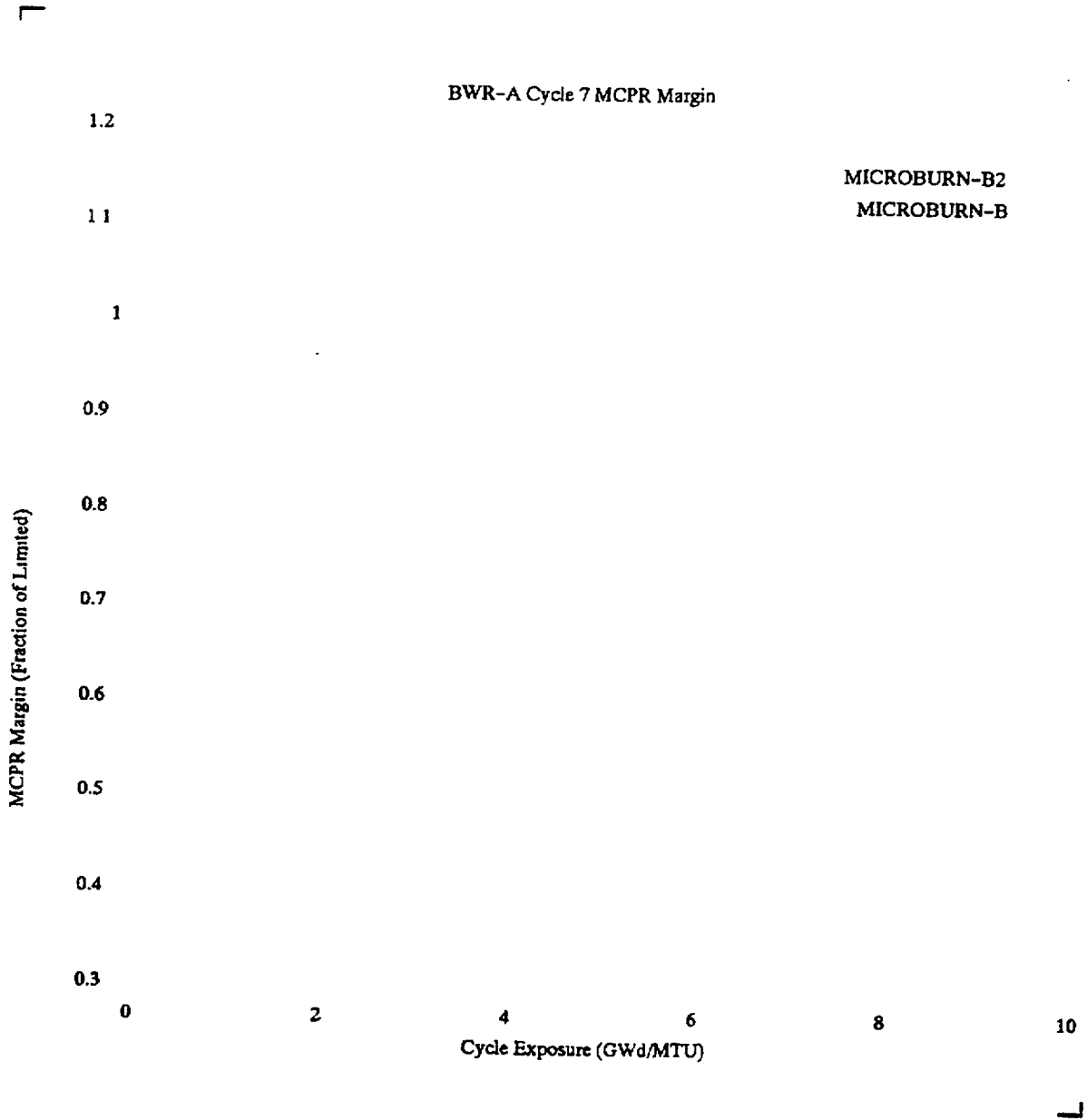


Figure A.1 BWR-A Cycle 7 MAPLHGR Margin Comparison



**Figure A.2 BWR-A Cycle 7 LHGR Margin Comparison**



**Figure A.3 BWR-A Cycle 7 MCPR Margin Comparison**

**Controlled Distribution**

**Siemens Power Corporation Methodology for Boiling Water Reactors: Evaluation and  
Validation of CASMO - 4/MICROBURN - B2**

Richland

H. D. Curet (13)

H. Moon (5)

Document Control (2)